Role of voltage-gated sodium channel β subunit signaling in neuronal development and cancer

by

Jeffrey D Calhoun

A dissertation submitted in partial fulfillment
of the requirements for the degree of
Doctor of Philosophy
(Cellular and Molecular Biology)
in the University of Michigan
2013

Doctoral Committee:

Professor Lori L. Isom, Chair
Professor Mario Delmar, New York University
Professor Sue O'Shea
Professor Jack M. Parent
Associate Professor Eric S. White

“Real DNA is like the sound you hear when you hold a conch shell to your ear. DNA is music.”

— Natalie Angier

Dedication

To my family,

for their unwavering love and support

Acknowledgements

I have been the fortunate beneficiary of excellent training opportunities and mentorship throughout my career. Most of all, I would like to acknowledge my thesis advisor, Dr. Lori Isom. Dr. Isom's lab is like an extension of her family, and I am honored and proud to be a member of the Isom clan. Lori has contributed greatly to my development as a scientist. I could not imagine having any other mentor as a graduate student. Also, Lori donated countless hours of her time in the editing of this thesis, and for that I will be forever grateful. I would like to thank the members of my thesis committee, Dr. Mario Delmar, Dr. Sue O'Shea, Dr. Jack Parent, and Dr. Eric White for providing invaluable guidance and support.

I would like to express my deepest gratitude towards the members of the Isom lab. The support, encouragement, and discussion provided by my labmates were essential throughout my graduate career. I would like to especially thank Dr. Heather O'Malley for providing sage advice, for opening up her home the past year, and for being a true friend. I would like to thank Dr. William Brackenbury for being a mentor and an enthusiastic collaborator. I would like to thank Dr. Gustavo Patino for being a consummate colleague, for always being willing to help me. I would like to thank the members of the Isom lab, especially Dr. Luis Lopez-Santiago, Dr. Raffaella Rusconi, Emily Slat, Dr. Yukun Yuan, Chunling Chen, TJ O'Shea, and Dr. Jim Offord for their support over the years. My classmates in the CMB program have been continual sources of inspiration and encouragement. My deepest thanks to Dr. Jill Haenfler, Dr. Mindy Waite, Dr. Lauren Van Wassenhove, and Dr. Ilea Swineheart for all of their support.

Prior to graduate school, I received an incredible amount of training and support which was essential in preparing me for the rigors of a Ph.D. program. I would like to thank the Merck Ion Channel group, especially Dr. Greg Kaczorowski, Dr. Maria Garcia, and Dr. Birgit Priest for providing me the opportunity to intern with an excellent biotechnology team. I would like to especially thank Dr. Birgit Priest and William Schmalhofer for their guidance and mentorship during my research internship. I was afforded wonderful research and educational opportunities as an undergraduate at the University of Dayton. I would like to extend my sincerest gratitude to Dr. Marie-Claude Hofmann and Dr. Sudhindra Gadagkar for their research mentorship. I would like to thank Dr. Carissa Krane and Dr. Mark Nielsen for inspiring me and providing an example of exemplary teaching. My initial interest in biomedical research was kindled in the classroom of Debra Horger, my high school biology teacher. I am incredibly fortunate to have been exposed to her inspiring teaching at a key moment in my education.

Last, but certainly not least, I would like to thank my family. The love, support, and encouragement provided by my family have been instrumental throughout my education.

Table of Contents

List of Tables

List of Figures

List of Abbreviations

AD, Alzheimer's disease
AF, Atrial fibrillation
AIS, Axon initial segment
APP, Amyloid precursor protein
BCa, breast cancer
CAM, Cell adhesion molecule
CGN, Cerebellar granule neuron
CHL, Chinese hamster lung (cell line)
CHO, Chinese hamster ovary (cell line)
CNS, Central nervous system
CSF, Cerebral spinal fluid
CTF, C-terminal fragment
DRM, Detergent-resistant membrane
DS, Dravet syndrome
EAE, Experimental autoimmune encephalomyelitis
EGL, External germinal layer
EOAE, Early-onset absence epilepsy
GEFS+, Genetic Epilepsy with Febrile Seizures plus
HD, Huntington's disease
HEK, Human embryonic kidney (cell line)
ICD, Intracellular domain
Ig, Immunoglobulin
IGL, Inner granule layer
LQTS, Long QT syndrome
MI, Motility index
ML, Molecular layer
MS, Multiple sclerosis
PCa, prostate cancer
PD, Parkinson's disease
PNS, Peripheral nervous system
SCAMA, single-cell adhesion measuring apparatus
SCLC, small-cell lung cancer
SIDS, Sudden infant death syndrome
SUDEP, Sudden unexplained death in epilepsy
T, Transverse
TLE, Temporal lobe epilepsy
TTX, Tetrodotoxin

VF, Ventricular fibrillation
VGSC, Voltage-gated sodium channel

Chapter I: The role of non-pore-forming β subunits in physiology and pathophysiology of voltage-gated sodium channels

A revised version of this chapter is in press at the Handbook of Experimental Pharmacology (Calhoun and Isom 2013).

Abstract

Voltage-gated sodium channel β1 and β2 subunits were discovered as auxiliary proteins that co-purify with pore-forming α subunits in brain. The other family members, β1B, β3, and β4, were identified by homology and shown to modulate sodium current in heterologous systems. Work over the past two decades, however, has provided strong evidence that these proteins are not simply ancillary ion channel subunits, but are multifunctional signaling proteins in their own right, playing both conducting (channel modulatory) and non-conducting roles in cell signaling. Here, we discuss evidence that sodium channel β subunits not only regulate sodium channel function and localization, but also modulate voltage-gated potassium channels. In their non-conducting roles, voltage-gated sodium channel β subunits function as immunoglobulin superfamily cell adhesion molecules that modulate brain development by influencing cell proliferation and migration, axon outgrowth, axonal fasciculation, and neuronal pathfinding. Mutations in genes encoding β subunits result in paroxysmal diseases including epilepsy, cardiac arrhythmia, and sudden infant death syndrome. Finally, β subunits may be targets for the future development of novel therapeutics.

Roles of Voltage-gated Sodium Channel β Subunits in Normal Physiology

Sodium channel as signaling complex

Voltage-gated sodium channel (VGSC) β subunits are multifunctional molecules with conducting and non-conducting roles. β subunits have conducting roles as ion channel regulatory subunits that form a complex with the pore-forming VGSC α subunit. Within this protein complex, β subunits modulate α subunit gating and cell surface expression as well as provide links to other channelome components. VGSC β subunits are unique among ion channel accessory subunits in that they contain an extracellular immunoglobulin (Ig) domain, thus placing them in the Ig superfamily of cell adhesion molecules (CAMs). Emerging evidence suggests that during brain development, β subunits function in non-conducting roles as CAMs in addition to their channel modulatory roles, and are subsequently involved in both extracellular and intracellular signaling pathways to help guide neuronal patterning (Brackenbury and Isom 2011). β subunits, especially those encoded by *SCN1B*, play important roles in cell proliferation and migration, axon outgrowth, pathfinding, and fasciculation in many central nervous system (CNS) areas including the hippocampus, cerebellum, and corticospinal tract (Brackenbury et al. 2008a; Brackenbury et al. 2013). As multifunctional molecules involved in a diverse set of cellular processes and signaling cascades, β subunits are unique, dynamic proteins which bridge the gap between two distinct signaling paradigms: electrical signaling via action potentials and cell adhesive signaling independent of ion conduction.

There is increasing evidence that β subunits are involved in numerous pathophysiological processes, including but not limited to, epilepsy, cardiac arrhythmia, neuropathic and inflammatory pain, neurodegeneration, and cancer. Mutations in the genes encoding β subunits result in human disease. Of particular note, mutation of *SCN1B*, encoding the β1/β1B subunits, is linked to diseases on the Genetic Epilepsy with

Febrile Seizures plus (GEFS+) spectrum (Patino and Isom 2010). Patients that inherit two loss-of-function mutant alleles of *SCN1B* have Dravet syndrome (DS), a severe pediatric epileptic encephalopathy, while patients who inherit a single mutant copy of *SCN1B* present with the milder GEFS+ or may not exhibit seizures. Genetic deletion of *Scn1b* in mice recapitulates the hallmark phenotypes associated with DS, suggesting that these mice are a DS model (Chen et al. 2004; Patino et al. 2009). Given the diverse role of β subunits in normal physiology and in disease processes, β subunits are potential targets for novel therapeutics.

In this review, the conducting (canonical) and non-conducting (non-canonical) roles of VGSC β subunits will be discussed. The structure, expression profile, and regulation of the β subunits will be described. Finally, the impact of β subunits in pathophysiology and potential for novel therapeutics will be examined.

VGSCs Are αββ Heterotrimers

Heterotrimeric VGSC complexes initiate and propagate action potentials in most electrically excitable mammalian cells including neurons and cardiac myocytes. These heterotrimeric complexes are composed of a single pore-forming α subunit, a non-covalently associated β subunit (β1 or β3), and a covalently associated β subunit (β2 or β4) (**Figure 1.1**). Two distinct gene families encode the 9 α subunit isoforms (*SCN<u>X</u>A*) and the 5 β subunit isoforms (*SCN<u>X</u>B*), respectively (**Table 1.1**). While there is significant evolutionary conservation and functional similarity within each gene family, each individual gene product is distinct in its properties and expression profile. For example, *SCN5A* is the predominant cardiac sodium channel, as its expression is enriched in cardiac tissue relative to other tissues, however, *SCN1A*, *SCN3A*, and *SCN8A* are also expressed in heart, although at lower levels (Westenbroek et al. 2013). Importantly, this diversity allows combinations of α and β isoforms to be expressed at different levels within a specific cell type and even in specific subcellular domains within a cell, based on

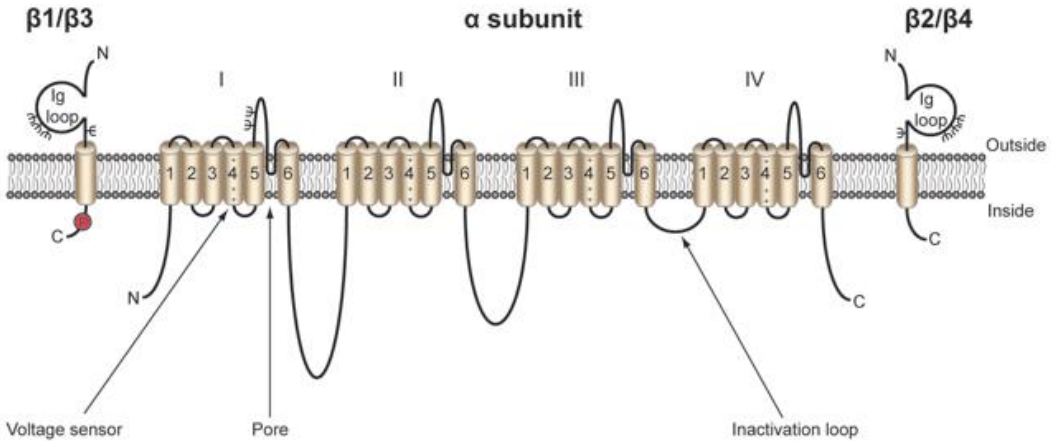

Figure 1.1. Topology of the voltage-gated sodium channel α and β subunits. VGSCs contain a pore-forming α subunit consisting of four homologous domains of six transmembrane segments (1-6). Segment 4 contains the voltage sensor (Catterall 2000). VGSCs also contain one or more β subunits. β1, β2, β3, and β4 contain an extracellular immunoglobulin (Ig) loop, transmembrane domain, and an intracellular C-terminal domain (Isom et al. 1994). β1B also contains an Ig loop, but lacks a transmembrane domain and is therefore a soluble, secreted protein (Patino et al. 2011). β1 contains a tyrosine phosphorylation site in its C-terminus (Malhotra et al. 2004). ψ denotes glycosylation sites. β1 and β3 are non-covalently linked to α, whereas β2 and β4 are covalently linked through disulfide bonds. Figure reproduced from (Brackenbury and Isom 2011).

VGSC α subunits		VGSC β subunits	
Gene	**Protein**	**Gene**	**Protein**
SCN1A	**Nav1.1**	***SCN1B***	**β1**
SCN2A	**Nav1.2**	***SCN1B***	**β1B**
SCN3A	**Nav1.3**	***SCN2B***	**β2**
SCN4A	**Nav1.4**	***SCN3B***	**β3**
SCN5A	**Nav1.5**	***SCN4B***	**β4**
SCN8A	**Nav1.6**		
SCN9A	**Nav1.7**		
SCN10A	**Nav1.8**		
SCN11A	**Nav1.9**		

Table 1.1. *SCNXA* genes encode VGSC α subunits and *SCNXB* genes encode VGSC β subunits.

the cell's specific job within the overall tissue. An important distinguishing feature of VGSCs is whether they are sensitive or resistant to tetrodotoxin (TTX), a sodium channel specific pore-blocking toxin from Fugu, or pufferfish. Most VGSCs (Nav1.1, Nav1.2, Nav1.3, Nav1.4, Nav1.6, and Nav1.7) are blocked by low (nanomolar) concentrations of TTX and are referred to as TTX-sensitive channels (TTX-S) (Catterall 2012). The remainder (Nav1.5, Nav1.8, and Nav1.9) require significantly higher concentrations of TTX (micromolar) for blockade and are referred to as TTX-resistant (TTX-R) (Catterall 2012).

Given that voltage-dependent sodium current is an essential phase of the mammalian action potential, it comes as no surprise that perturbation of sodium channel function due to mutations results in human disease. Additionally, as discussed below, VGSC α subunits are pharmacologic targets for several interventions related to diseases including epilepsy and cardiac arrhythmia.

β Subunit Structure

Four genes in the mammalian genome encode five β subunit proteins (Isom et al. 1992; Kazen-Gillespie et al. 2000; Isom et al. 1995a; Morgan et al. 2000; Qin et al. 2003; Yu et al. 2003). *SCN1B* encodes β1 and the splice variant β1B, *SCN2B* encodes β2, *SCN3B* encodes β3, and *SCN4B* encodes β4. Four of the VGSC β subunits (β1-β4) are transmembrane proteins with type I topology containing an extracellular N-terminus, a single transmembrane segment, and an intracellular C-terminus (Isom 2001). The exception, β1B, contains the same Ig loop domain as β1, but has an alternate C-terminal region that is the product of a retained intron (**Figure 1.2**) that lacks a transmembrane domain, resulting in a secreted, soluble molecule (Patino et al. 2011; Kazen-Gillespie et al. 2000). **Figure 1.3** provides an overview of the functional architecture of β1/β1B. Structural differences underlie whether a β subunit interacts covalently or non-covalently with pore-forming VGSC α subunits. β2 and β4 interact covalently with α subunits via a

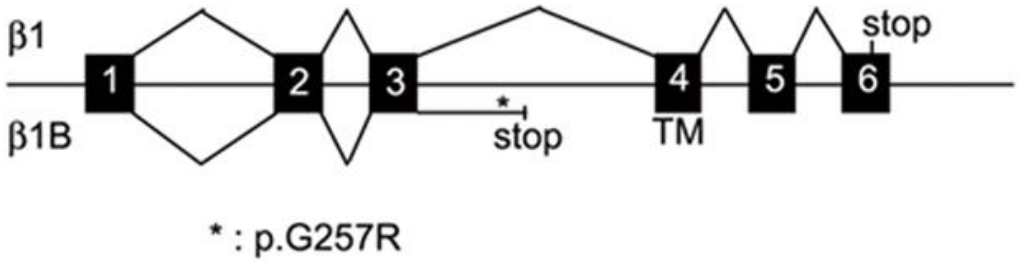

Figure 1.2. The genomic structure of *SCN1B*. Exons 1–6 constitute β1. Extension of exon 3 into intron 3 generates the variant, β1B. The novel 3′ end of β1B does not contain a transmembrane domain (TM). The asterisk (*) indicates the position of the G257R mutation. (This is not drawn to scale.) Figure reproduced from (Patino et al. 2011).

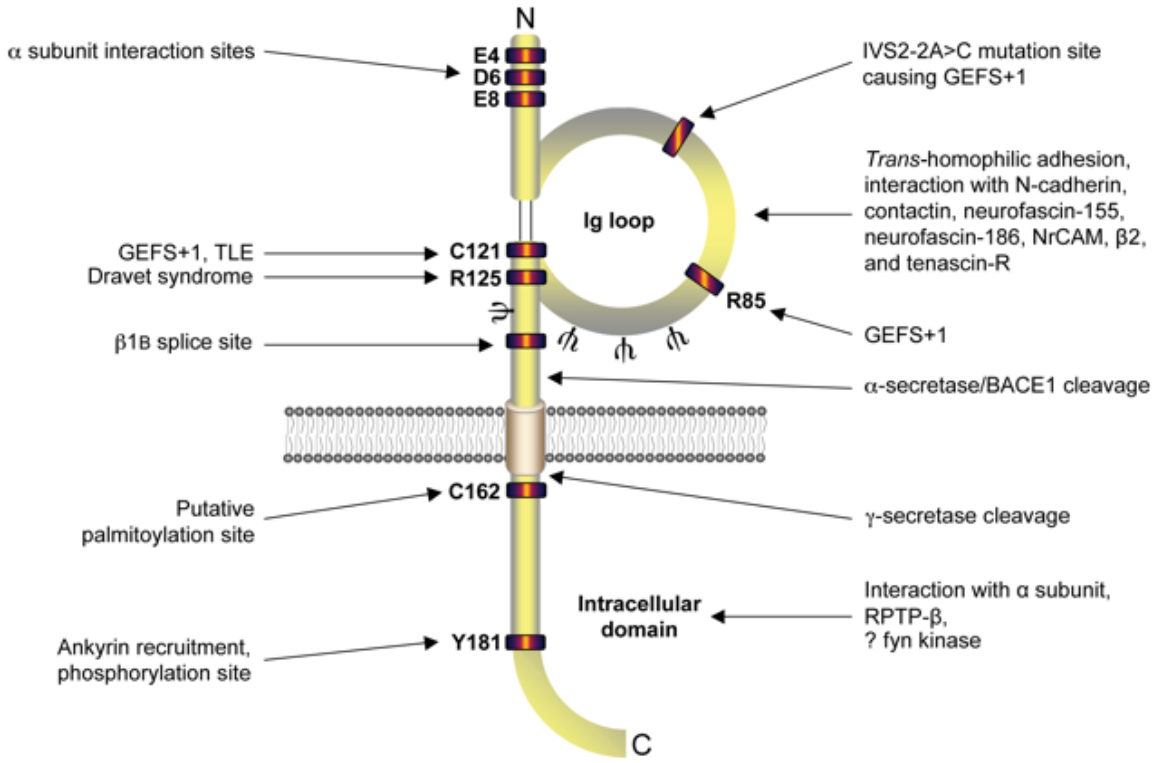

Figure 1.3. Functional architecture of β1/β1B. β1 contains residues responsible for interaction with α subunit in its intracellular and extracellular domains (McCormick et al. 1998; Spampanato et al. 2004). Mutation sites responsible for causing epileptic encephalopathy, including Dravet syndrome, are located in the extracellular immunoglobulin loop (Meadows et al. 2002b; Wallace et al. 2002; Audenaert et al. 2003; Scheffer et al. 2007; Patino et al. 2009). Alternative splicing site for β1B (Kazen-Gillespie et al. 2000; Qin et al. 2003; Patino et al. 2011), putative palmitoylation site (McEwen et al. 2004), ankyrin interaction site (Malhotra et al. 2002), tyrosine phosphorylation site (Malhotra et al. 2004), N-glycosylation sites [ψ] (McCormick et al. 1998), α/β/γ-secretase cleavage sites (Wong et al. 2005), receptor protein tyrosine phosphatase β (RPTPβ) interaction (Ratcliffe et al. 2000), and putative fyn kinase interaction (Brackenbury et al. 2008a) are also marked. Figure reproduced from (Brackenbury and Isom 2011).

single disulfide bond (Messner and Catterall 1985; Chen et al. 2012; Buffington and Rasband 2013; Hartshorne et al. 1982; Hartshorne and Catterall 1984; Yu et al. 2003). Specifically, an N-terminal cysteine at position 26 in the extracellular domain of either β subunit forms a disulfide bond with one of multiple candidate cysteine residues in the S5-S6 loops of the α subunit. β1 and β3 associate non-covalently with VGSC α subunits (Messner and Catterall 1985; Hartshorne et al. 1982; Hartshorne and Catterall 1984). Structure-function analysis of β1 suggests the involvement of both N- and C-terminal residues in non-covalent association with α subunits (McCormick et al. 1998; Meadows et al. 2001; Spampanato et al. 2004). The C-terminal domains of β1 and β2 serve as links to the cytoskeleton via interactions with ankyrinG or ankyrinB (Malhotra et al. 2000; Malhotra et al. 2002). The β1 subunit intracellular domain contains a single tyrosine residue that can be phosphorylated (Malhotra et al. 2002; Malhotra et al. 2004). Finally, β subunits are also targets for sequential proteolytic cleavage (**Figure 1.4**), resulting in release of N-terminal and C-terminal fragments (Wong et al. 2005).

Analysis of genes homologous to mammalian sodium channels has yielded valuable information about the evolution of VGSC α and β subunits. NaChBac, an ancestral gene to mammalian VGSC α subunits, was discovered in bacteria (Ren et al. 2001). Subsequently, additional prokaryotic VGSCs were discovered, including NavAb, NavB1, NavBp, NavPz, NavRd, NavSHp, and NavSIP (Payandeh et al. 2011; Ren et al. 2001; Koishi et al. 2004; Ito et al. 2004; Irie et al. 2010). Interestingly, the genes coding for bacterial VGSCs encode proteins containing only 6 transmembrane domains rather than the 24 transmembrane domains found in mammalian VGSC α subunits (Charalambous and Wallace 2011). In order to form a sodium-conducting channel, bacterial sodium channel proteins must form homotetramers, similar to mammalian voltage-gated potassium channels. Mammalian *SCN<u>X</u>A* genes encode full channels (i.e. four tethered channel domains), suggesting the evolution of VGSC genes from encoding homotetrameric channels to encoding monomeric channels. Genes encoding monomeric

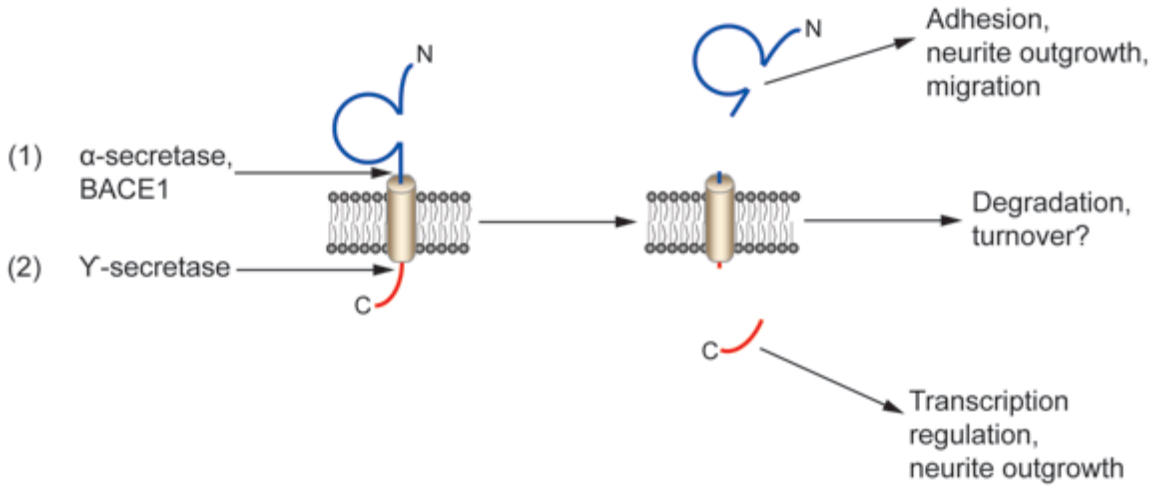

Figure 1.4. Sequential cleavage of β subunits. Cleavage by (1) α -secretase or β -site amyloid precursor protein-cleaving enzyme (BACE1), followed by (2) γ -secretase yields soluble extracellular N-terminal domains and small intracellular C-terminal domains (Wong et al. 2005; Kim et al. 2005). The soluble immunoglobulin domains are responsible for regulation of adhesion and migration (Davis et al. 2004; Kim et al. 2005). β subunit intracellular domains regulate neurite outgrowth and are putative regulators of voltage-gated sodium channel gene transcription (Kim et al. 2007; Miyazaki et al. 2007). Figure reproduced from (Brackenbury and Isom 2008).

(24 transmembrane domains) VGSC α subunits have been identified in a diverse set of species, including *drosophila*, zebrafish, rodents, and humans (Goldin 2002). Genes encoding VGSC β subunits are present in species including zebrafish, rodents, and humans, but are notably absent in invertebrates (Isom et al. 1992; Fein et al. 2007; Chopra et al. 2007; Patino et al. 2009). This suggests that β subunits evolved later relative to pore-forming α subunits. Notably, sodium channels purified from the electroplax (electric organ) of the South American eel *Electrophorus electricus* contain only α subunits and not β subunits, which provides *in vivo* evidence that, similar to results obtained in *Xenopus* oocytes and transfected fibroblasts, α subunits are capable of functioning in the absence of β subunits (Miller et al. 1983; Noda et al. 1986; Goldin et al. 1986; Scheuer et al. 1990; Isom et al. 1995b). Interestingly, while the *drosophila* genome lacks genes encoding VGSC β subunits, it does contain *tipE* which acts as an auxiliary subunit to the pore-forming VGSC α subunit *paralytic* (Li et al. 2011). However, the structure of mammalian VGSC β subunits is distinct from *tipE*.

VGSC β subunits are Ig-CAMs

Each of the mammalian VGSC β subunits contains a single, extracellular Ig domain that is structurally homologous to the V-set of the Ig superfamily of CAMs (Isom et al. 1995a). The Ig loop domain of β1 participates in both homophilic (with itself) and heterophilic (with other CAMs) associations (Malhotra et al. 2000; McEwen and Isom 2004) (**Figure 1.3**). Importantly, the cell adhesive properties of β1 and β2 are independent of α subunit expression *in vitro*, suggesting that β subunits may have channel independent functions *in vivo*. Sequence analysis of the extracellular domains of β1 and β3 show homology to the CAM myelin P_0 (Isom et al. 1995a; McCormick et al. 1998; Morgan et al. 2000), which has provided useful guidance for structure-function predictions. While other members of the family of voltage-gated ion channels contain accessory subunits that modulate channel kinetics, cell surface expression, and voltage-

dependence, only the VGSC β subunits contain extracellular Ig domains. β subunits, particularly β1, function as CAMs. β1 participates in homophilic cell adhesion resulting in cellular aggregation and ankyrin recruitment (Malhotra et al. 2000). Homophilic β1 cell adhesive interactions regulate neurite outgrowth in cerebellar granule neurons (CGNs) (Davis et al. 2004; Brackenbury et al. 2008a). Additionally, β1 interacts heterophilically with the neuronal and glial CAMs contactin, VGSC β2, N-cadherin, neurofascin-155 (NF155), neurofascin-186 (NF186), and NrCAM (McEwen and Isom 2004; Malhotra et al. 2004; Ratcliffe et al. 2001). β1 interactions with contactin and NF186 result in increased α subunit cell surface expression, suggesting a relationship between CAM function and channel modulation (Kazarinova-Noyes et al. 2001). β1 also participates in cell-matrix adhesion, binding to the extracellular matrix protein tenascin-R to influence cell migration (Xiao et al. 1999). β2, like β1, participates in homophilic interactions, in heterophilic interactions with β1, and in cell-matrix interactions with ECM proteins tenascin-R and tenascin-C (Malhotra et al. 2000; Xiao et al. 1999; McEwen and Isom 2004; Srinivasan et al. 1998). While β3 contains an Ig domain, its capacity to engage in CAM interactions is unclear. Unlike β1 and β2, transfection of β3 cDNAs into *Drosophila* S2 cells was not sufficient to induce cell aggregation, suggesting it does not engage in homophilic interactions (McEwen et al. 2009). Using soluble recombinant CAM binding assays, it was observed that heterophilic interactions between β3 and other CAMs are more limited compared to β1 (McEwen and Isom 2004; Ratcliffe et al. 2001). In contrast to (McEwen et al. 2009), Yereddi et al. reported evidence for *trans* β3-β3 homophilic adhesion using co-culture of cells expressing differentially epitope-tagged β3 constructs (Yereddi et al. 2013). Evidence for β4 as a CAM is limited, but it does appear to regulate filopodial morphology in transfected cells, suggesting CAM activity (Miyazaki et al. 2007). However, unlike experiments with β1, plating cerebellar CGNs on β4-expressing monolayers had no effect on neurite outgrowth (Davis et al. 2004). Overall, these observations suggest that VGSC β subunits, particularly β1, are

CAMs that provide a link between electrical excitability and extracellular adhesion or function independently of ion conduction.

Regulation of VGSC β subunits

Glycosylation

Each β subunit Ig domain contains 3 or 4 N-linked glycosylation sites such that glycosylation accounts for approximately one-third of the total molecular weight of the protein (Messner and Catterall 1985; Isom et al. 1992). While the effects of glycosylation on sodium channel α and β subunits *in vivo* are not known, evidence from heterologous expression suggests these modifications may be important for α subunit cell surface expression and may influence the modulatory effects of β subunits on sodium current. In neuroblastoma cells expressing endogenous VGSCs, tunicamycin was used to study the channel under conditions of glycosylation inhibition (Waechter et al. 1983). Reduced glycosylation resulted in a reduction in the level of mature pore-forming α subunits detectable at the cell surface. The role of glycosylation in the interaction between α, β1, and β2 subunits has been studied *in vitro* using Chinese hamster ovary (CHO) cells that are either capable (Pro5) or incapable (Lec2) of sialylation, a type of glycosylation that is prevalent in VGSCs (Johnson et al. 2004; Johnson and Bennett 2006). Sialic acids are necessary for the modulation of α subunit (Nav1.2, Nav1.5, and Nav1.7) gating by β1 (Johnson et al. 2004). However, the impact of sialic acid is context-dependent. β2 had sialic acid-dependent and -independent effects on α subunit gating, depending on which α subunit gene was co-expressed (Johnson and Bennett 2006). While the importance of glycosylation on the CAM function of β1 has not been tested directly, it is possible that glycosylation may be critical for cell adhesive interactions as well. Homophilic interactions of myelin P_0, a CAM which shares homology with β1 and β3 (Isom et al. 1995a), requires glycosylation of the P_0 pair (Filbin and Tennekoon 1993). While more work is needed to fully understand the impact of glycosylation on VGSC α and β

subunits, this post-translational modification is a potential mechanism for fine-tuning of channel function.

Phosphorylation

The β1 C-terminal domain serves as a link between VGSC complexes and the cytoskeleton. This domain contains sites for post-translational modification, including phosphorylation. An intracellular tyrosine residue (β1Y181) is phosphorylated *in vitro* and basal tyrosine phosphorylation of β1 is detectable in rat brain membranes (Malhotra et al. 2002) (**Figure 1.3**). A β1 mutant that mimics phosphorylation (β1Y181E) shows normal β1-mediated cell-cell adhesion in a heterologous system, but disrupted β1-mediated ankyrin recruitment normally observed in response to adhesion (Malhotra et al. 2002). Similar to β1, β1Y181E increases cell surface α subunit expression in heterologous systems, but does not modulate sodium current *in vitro* (McEwen et al. 2004). Finally, tyrosine phosphorylated β1 (pY-β1) has a distinct subcellular localization in cardiac myocytes. Nav1.5 and pY-β1 colocalize at intercalated disks, whereas non-phosphorylated β1 colocalizes with TTX-S channels at the T-tubules (Malhotra et al. 2004). These data suggest that phosphorylation of β1Y181 regulates its interaction with other proteins as well as its subcellular localization. Recently, a β1 peptide phosphorylated on intracellular threonine residues was reported in a screen for phosphorylated proteins in mouse synaptosomes (Trinidad et al. 2012). It will be interesting to determine the functional significance of this modification.

Proteolytic processing

All four VGSC β subunits are targets for sequential proteolytic cleavage, at least *in vitro* (Wong et al. 2005) (**Figure 1.4**). Similar to amyloid precursor protein (APP) (O'Brien and Wong 2011), β subunits are substrates for BACE1 (or β-secretase) and γ-secretase cleavage (Wong et al. 2005). A major gap in our understanding, however, is

how β subunit cleavage is regulated *in vivo*. The initial β-secretase-mediated cleavage results in ectodomain shedding and the release of the Ig-loop containing extracellular domain of the β subunit (Wong et al. 2005). Upon release from the cell surface, the β subunit extracellular domain may function as a soluble CAM similar to the proposed function of an engineered soluble β1 extracellular domain construct, β1Fc, and β1B (Patino et al. 2011; Davis et al. 2004; McEwen and Isom 2004). Following ectodomain shedding, subsequent γ-secretase cleavage results in the release of a β subunit-intracellular domain (ICD) into the cytoplasm (Wong et al. 2005). Interestingly, neurite outgrowth induced by homophilic β1 cell adhesive interactions is abrogated by pharmacological inhibition of γ-secretase, suggesting proteolytic cleavage of the β1 intracellular domain may be critical in this signaling pathway (Brackenbury and Isom 2011). Studies of the role of the β2-ICD suggest that it traffics to the nucleus where it functions to increase *SCN1A* mRNA and subsequent Nav1.1 protein levels without increasing sodium current (Kim et al. 2007). The functions of the other β subunit ICD fragments have not yet been studied. However, *Scn1b* null mice have increased *Scn5a* expression in heart, raising the intriguing possibility that the β1-ICD may normally translocate to the nucleus and negatively regulate *Scn5a* transcription (Lopez-Santiago et al. 2007).

Expression of VGSC β subunits

VGSC β subunits are expressed in excitable cells in the CNS, peripheral nervous system (PNS), skeletal muscle, and the heart (Isom et al. 1992; Isom et al. 1995a; Morgan et al. 2000; Yu et al. 2003; Maier et al. 2004; Lopez-Santiago et al. 2006; Lopez-Santiago et al. 2011; Brackenbury et al. 2010). While particular focus has been given to β subunit expressing neurons and myocytes, β subunits are also expressed in cells traditionally considered to be non-excitable such as astrocytes, radial glia, and Bergmann glia (Aronica et al. 2003; Oh and Waxman 1995; Fein et al. 2008; Davis et al. 2004). For

example, *scn1bb*, a zebrafish ortholog of *SCN1B*, was found to be expressed in zrf-1 positive peripheral Schwann cells, supporting non-neuronal cells within olfactory pits and the inner ear, and myelinating glia surrounding the optic nerve (Fein et al. 2008). In contrast, *scn1ba*, another zebrafish ortholog of *SCN1B*, is largely expressed in excitable cells including neurons and skeletal muscle and may be localized to nodes of Ranvier in optic nerve (Fein et al. 2007). **Table 1.2** summarizes expression data for the β subunits in nervous system and muscle. β subunit expression is developmentally regulated (Sutkowski and Catterall 1990). In general, β1B and β3 are most abundant during fetal development and their expression decreases after birth (Kazen-Gillespie et al. 2000; Patino et al. 2011; Shah et al. 2001). Expression of β1 and β2 increase during the course of postnatal development and dominate during adult life (Kazen-Gillespie et al. 2000; Patino et al. 2011; Isom et al. 1995a). Exceptions to these general rules exist, such as the observation that β1B expression is retained in postnatal and adult heart in contrast to the reduced expression observed in the postnatal brain (Kazen-Gillespie et al. 2000). Additionally, β3 is expressed in adult dorsal root ganglion neurons (DRGs) (Takahashi et al. 2003). β4 is expressed in postnatal tissues, though the developmental time course for β4 expression has not been determined (Yu et al. 2003).

Subcellular localization of β subunits

Electrically excitable cells contain specialized substructures that are critical to normal physiology. Immunolocalization studies demonstrate that β subunits often cluster at specialized, subcellular structures. CNS and PNS neurons develop a specialized subcellular domain at the soma-axon junction called the axon initial segment (AIS). The AIS, devoted to initiating action potentials, contains a high density of a molecular complex (a "channelome") that includes the cytoskeletal adaptor protein ankyrinG and VGSC α and β subunits, including Nav1.1, Nav1.2, Nav1.6, and β1 (Rasband 2010). Importantly, the AIS can be subdivided into two structural units, the proximal segments

Tissue – cell type	**β1**	**β1B**	**β2**	**β3**	**β4**
Central Nervous System					
Hippocampal neurons	+ [a]		+ [l]	+ [b,o]	+ [l]
Cortical neurons		+ [j,k]	+ [l]	+ [b,o]	+ [l]
Basal ganglia	- [b]		+ [l]	+ [b,o]	+ [l]
Retinal ganglion cells	+ [c,d]		+ [d]		
Cerebellar Purkinje cells	+ [h]	+ [j,k]	+ [l]	+ [o]	+ [l]
Cerebellar granule neurons	+ [h]			- [b,o]	
Deep cerebellar nuclei		+ [j]	+ [l]		+ [l]
Ventral horn neurons		+ [j]	+ [l]		+ [l]
Astrocytes	+ [e,f]		+ [m]		
Bergmann glia	+ [i]	- [j]	- [i]	- [i]	+ [i]
Radial glia	+ [g]				
Peripheral nervous					
Dorsal root ganglia	+ [q]	+ [k]	+ [l,n]	+ [p]	+ [l]
Peripheral nerves		+ [k]	+ [n]	+ [p]	
Schwann cells	+ [g]				
Heart					
Ventricular myocytes	+ [r]		+ [r]	+ [r]	+ [r]
Atrial myocytes	+ [s]		+ [s]	+ [s]	+ [s]

Table 1.2. Expression of VGSC β subunits in the CNS, PNS, and heart. + denotes expression of specific β subunit protein or mRNA was detected. - denotes that expression of specific β subunit protein or mRNA was not detected. a: (Chen et al. 2004), b: (Morgan et al. 2000), c: (Fein et al. 2007), d: (Kaplan et al. 2001), e: (Aronica et al. 2003), f: (Oh and Waxman 1995), g: (Fein et al. 2008), h: (Brackenbury et al. 2010), i: (Davis et al. 2004), j: (Kazen-Gillespie et al. 2000), k: (Qin et al. 2003), l: (Yu et al. 2003), m: (Oh et al. 1997), n: (Pertin et al. 2005), o: (Shah et al. 2001), p: (Casula et al. 2004), q: (Lopez-Santiago et al. 2006), r: (Maier et al. 2004), and s: (Kaufmann et al. 2013). This table is adapted from (Patino and Isom 2010).

nearest to the cell soma, and the distal end, which can differ in protein composition (Van Wart et al. 2007). Other CAMs, including the β1 cell adhesive binding partners NrCAM and NF186, are enriched at the AIS (Rasband 2010). β1 may influence channel gating and channel cell surface expression in this domain. Additionally, β1 plays important roles in stabilizing the subcellular localization of Nav1.6 at the AIS, at least in the cerebellum (Brackenbury et al. 2010). Evidence for this comes from the observation that Nav1.6 localization to the AIS of cerebellar Purkinje neurons is reduced in *Scn1b* null mice (Brackenbury et al. 2010). β1 is predicted to function as a CAM at the AIS, although this possibility has not been tested. In addition to β1, β2 and β4 have been demonstrated to be localized to the AIS in specific neuronal subtypes (Chen et al. 2012; Buffington and Rasband 2013).

Myelinated CNS and PNS neurons contain gaps in the myelin sheath called nodes of Ranvier, structures that are critical for saltatory conduction, the mechanism responsible for rapid electrical communication across long distances (Poliak and Peles 2003). Nodes of Ranvier are composed of a high density of ion channels and CAMs arrayed in protein complexes in specific arrangements that differ somewhat between the CNS and PNS. In the CNS, β1 and β2 subunits are found to localize to optic nerve nodes of Ranvier *in vivo* (Patino et al. 2009; Kaplan et al. 2001). β4 localizes to a small subset of optic nerve nodes of Ranvier (Buffington and Rasband 2013). Likewise, in the PNS β1 and β2 subunits localize to nodes of Ranvier in the sciatic nerve *in vivo* (Chen et al. 2004; Chen et al. 2002). β4 localizes to the majority of nodes of Ranvier in dorsal and ventral spinal cord roots (Buffington and Rasband 2013). What is the role of β subunits at the node of Ranvier? β subunits act as channel modulators and influence cell surface levels of pore-forming VGSC α subunits, which are present at high density in nodes (Chen et al. 2004; Chen et al. 2002). Based on the observation that *Scn1b* null mice have reduced numbers of nodes of Ranvier, dysmyelination, and perturbation of axo-glial cell-cell

contacts, β subunits likely have cell adhesive roles in initiating or stabilizing nascent axo-glial cell-cell contacts and developing nodes of Ranvier (Chen et al. 2004).

Another important neuronal subcellular structure is the growth cone, which is located at the tip of developing neurites and is responsible for sensing signaling cues to direct the extension or retraction of the neurite (Lowery and Van Vactor 2009). Proteins involved in neurite outgrowth and pathfinding, including β1, localize to this domain (Brackenbury et al. 2010). Localization to the growth cone may be a requirement for the promotion of neurite outgrowth downstream of β1-β1 *trans* homophilic adhesion (Brackenbury et al. 2008a; Brackenbury et al. 2010).

β2 localizes to the AIS of mature neurons in culture and to nodes of Ranvier formed in myelinating co-cultures. Interestingly, AIS and nodal localization of β2 requires an intact disulfide bond between α and β2 (Chen et al. 2012). A recent report suggests that, like β2, the homologous cysteine residue on β4 allows it to target to the AIS and to nodes (Buffington and Rasband 2013). These data suggest a model whereby the covalently associated VGSC β subunit (β2 or β4) is dependent on its intermolecular disulfide bond to the α subunit for targeting to neuronal subcellular domains. Further experimentation will be needed to study the influence of VGSC β subunits on the subcellular localization of α subunits, however, VGSC α subunits target normally to nodes in *Scn1b* and *Scn2b* null mice (Chen et al. 2002; Chen et al. 2004).

Two functionally important subcellular structures in ventricular cardiomyocytes are the intercalated disks and transverse (T)-tubules. Intercalated disks form at cell-cell junctions and are critical for mechanical and electrical coupling (Delmar 2004). T-tubules electrically link the plasma membrane to the sarcoplasmic reticulum such that an action potential can efficiently lead to calcium-induced calcium-release (Brette and Orchard 2003). β1 localizes to both intercalated disks and T-tubules in the ventricle (Dhar Malhotra et al. 2001; Malhotra et al. 2004; Maier et al. 2004) and to intercalated disks in the atrium (Kaufmann et al. 2013). There is some disagreement in immunostaining

datasets regarding the subcellular localization of β2 subunits. β2 has been reported to localize to the T-tubules or intercalated disks in ventricular myocytes (Dhar Malhotra et al. 2001; Maier et al. 2004) and to the T-tubules in atrial myocardium (Kaufmann et al. 2013). Experiments suggest that β3 localization is limited to T-tubules in ventricular myocytes (Maier et al. 2004) and to intercalated disks and cell surface puncta in atria (Kaufmann et al. 2013). β4 localizes primarily to the intercalated disk in ventricular myocytes (Maier et al. 2004) and to cell surface puncta in atrial myocyardium (Kaufmann et al. 2013). What functional roles are the β subunits playing at these critical cardiac structures? β1 likely functions as a channel modulator at T-tubules, but may act solely as a CAM at the intercalated disk, based on heterologous data showing the absence of channel modulation by β1Y181E (McEwen et al. 2004). In contrast, β1B, which regulates Nav1.5 currents in heterologous cells (Watanabe et al. 2008), may function as a channel modulator in this domain. The intercalated disk contains Nav1.5 α subunits as well as both homophilic and heterophilic adhesion partners, supporting the concept of a multifunctional VGSC complex at cardiomyocyte cell-cell junctions.

Canonical role of VGSC β subunits as modulators of *α* subunit activity and localization

Modulation of sodium current in heterologous systems

Soon after the cloning of the first cDNAs encoding VGSC α and β subunits, heterologous expression systems were used to investigate critical questions like channel subunit topology, electrophysiology, and structure-function relationships. While these systems clearly did not mimic what we now understand to be multi-protein sodium channel signaling complexes in native cells, the resulting data were critical to advancing our understanding of these important molecules. Early work expressing VGSC Nav1.2 α subunits in *Xenopus* oocytes demonstrated non-physiological sodium currents that activated and inactivated much more slowly than sodium currents recorded in neurons

(Auld et al. 1988; Goldin et al. 1986; Joho et al. 1990). Co-injection of α subunit cRNA with low molecular weight mRNA isolated from rat brain into oocytes resulted in increased sodium current density, altered voltage-dependence of inactivation, and rapidly inactivating currents (Auld et al. 1988; Krafte et al. 1990). These results were more representative of physiological sodium currents and suggested that proteins encoded by the low molecular weight brain mRNA fraction are important interacting proteins that modulate pore-forming α subunits. β1 and β2, which were known to associate with VGSC α subunits purified to theoretical homogeneity and predicted to be included in the low molecular weight mRNA fraction, were strong candidates for the functional modulatory proteins in question (Hartshorne et al. 1982; Hartshorne and Catterall 1984). Indeed, after cloning the cDNAs encoding β1 and β2, we found that expression of mRNAs encoding these subunits recapitulated the effects of low molecular weight brain mRNA (Isom et al. 1992; Isom et al. 1995a). Specifically, when co-expressed with Nav1.2, β1 increased peak sodium current density, shifted the voltage-dependence of inactivation to more negative membrane potentials, and accelerated the rate of inactivation (Isom et al. 1992). Co-expression of β2 and Nav1.2 in oocytes led to increased sodium current density and acceleration in the rate of channel inactivation compared to cells injected with Nav1.2 alone (Isom et al. 1995a). β2-expressing oocytes display increased cell surface area, likely due to an increase in fusion of intracellular vesicles with the plasma membrane and predicting its role as a chaperone protein (Isom et al. 1995a). Importantly, the effects of β1 and β2 on Nav1.2 in oocytes were synergistic: Nav1.2, β1, and β2 expressing oocytes have higher sodium current density than oocytes expressing α subunits alone, α and β1 subunits, or α and β2 subunits (Isom et al. 1995a). Unlike sodium currents from oocytes expressing only VGSC α subunits, currents from oocytes expressing α, β1, and β2 subunits were rapidly inactivating and closely representative of currents recorded from mature neurons (Isom et al. 1995a).

In addition to the oocyte system, much of the work done to characterize how β subunits affect pore-forming α subunits has utilized immortalized mammalian cell lines, with human embryonic kidney (HEK), Chinese hamster lung (CHL), and CHO cells being popular tools. Experiments co-expressing Nav1.2 and β1 in CHL cells confirmed the results in oocytes showing that β1 increases peak sodium current density and induces a negative shift in the voltage-dependence of activation and inactivation, although the effects on activation and inactivation were more subtle (Isom et al. 1995b; Patino et al. 2009). In contrast to oocytes, β2 expression in mammalian cells requires co-expression of β1 to exert most of its modulatory effects on α subunits. When β2 is expressed with Nav1.2 α subunits in the absence of β1, sodium current is either unchanged or reduced (Kazarinova-Noyes et al. 2001; McEwen et al. 2004). However, when β2 is expressed with α in the presence of β1, β2 increases cell surface expression of α subunits beyond that observed in the presence of α + β1 (Kazarinova-Noyes et al. 2001).

Work in transfected cell lines identified β1B as a secreted CAM with only subtle effects on sodium current in cells expressing TTX-S channels like Nav1.2 or Nav1.3 (Kazen-Gillespie et al. 2000; Patino et al. 2011). Interestingly, Nav1.5 seems to sequester β1B at the cell surface *in vitro* and this interaction results in increased channel cell surface expression (Watanabe et al. 2008; Patino et al. 2011). These data suggest that β1B may function as a soluble CAM during brain development and as a sodium channel modulator and cell surface CAM in heart and other cell types that express Nav1.5.

Work investigating β3 and β4 suggests that these subunits, like β1 and β2, act as sodium channel modulators in heterologous systems. β3 induces a negative shift in the voltage-dependence of inactivation of Nav1.3 (Meadows et al. 2002a). Modulation of Nav1.3 is likely relevant as neuronal expression of β3 is highest early in development when Nav1.3 expression is also abundant (Shah et al. 2001). β3 also shifts the voltage-dependence of inactivation to more negative membrane potentials when co-expressed with Nav1.5 (Ko et al. 2005). When β4 was originally identified, its co-expression with

Nav1.2 or Nav1.4 resulted in negative shifts in the voltage-dependence of activation (Yu et al. 2003). Studies on Nav1.1 suggested that, in addition to shifting the voltage-dependence of activation to more negative membrane potentials, β4 increased the amount of non-inactivating current *in vitro* (Aman et al. 2009). β4 appears to affect Nav1.5 channels differently by inducing a negative shift in the voltage-dependence of inactivation (Medeiros-Domingo et al. 2007). Finally, β4 modulates resurgent sodium current, as discussed below.

While oocytes and immortalized mammalian cell lines are obviously very different from neurons or myocytes and cannot replicate the situation in native cells, data collected from heterologous overexpression of VGSC α and β subunits made important predictions regarding the roles of β subunits in primary cells and tissues (Ragsdale 2008; Escayg and Goldin 2010). Cell background impacts the effects of β subunits in cell culture, along with the particular VGSC α subunit and specific channel interacting proteins that are co-expressed (Dib-Hajj and Waxman 2010; Abriel and Kass 2005), accurately predicting that β subunits have context-dependent effects *in vivo*. Factors contributing to these differences include specific combinations of VGSC α and β subunits expressed, relative expression levels of each VGSC gene product, molecular composition of the VGSC macromolecular complex including non-channel binding partners, subcellular distribution of VGSC complexes, and developmental maturity (e.g. immature vs. mature neurons).

Modulation of sodium current and excitability in vivo

The use of genetically engineered mouse models and viral-mediated gene transfer has allowed for the investigation of VGSC α and β subunit function in the whole animal, in acutely isolated primary cells, and in tissue slices. Observations using these methods suggest that β subunit modulation of sodium current *in vivo*, while cell-type specific and

subtler in nature than observed in heterologous systems, is critical for normal electrical excitability in the nervous system and heart.

Sodium current and action potential recordings from *Scn1b* null mice have provided important insights into the role of β1/β1B in modulating electrical excitability *in vivo*. Recordings from acutely isolated hippocampal pyramidal or bipolar neuronal soma found no measurable differences in sodium current properties in P10-18 *Scn1b* null neurons relative to wildtype (Chen et al. 2004; Patino et al. 2009). However, recordings from *Scn1b* null brain slices from the same age range demonstrated hyperexcitability in the CA3 region of the hippocampus as well as epileptiform activity in the hippocampus and cortex (Patino et al. 2009; Brackenbury et al. 2013), suggesting that β1/β1B subunits in neuronal processes may be critical in regulating excitability. These excitability changes are proposed to contribute to the severe seizures observed in *Scn1b* null mice, that are a model of DS (Chen et al. 2004; Patino et al. 2009). The observation of altered sodium current and impaired excitability in *Scn1b* null CGNs suggests a role for *Scn1b* in regulating the excitability of the cerebellum (Brackenbury et al. 2010) that may contribute to the ataxic phenotype of *Scn1b* null mice (Chen et al. 2004). In contrast to reduced excitability observed in *Scn1b* null CGNs, *Scn1b* null DRG neurons are hyperexcitable, suggesting that these animals may have allodynia (Lopez-Santiago et al. 2011). Recordings from *Scn1b* null ventricular myocytes demonstrated increased transient and persistent sodium current relative to wildtype cells, with prolonged QT and RR internals on the electrocardiogram (ECG) (Lopez-Santiago et al. 2007). Clearly, β1/β1B subunits have cell type specific context-dependent effects on electrical excitability *in vivo*.

In addition to modulation of sodium current in primary cells, *Scn1b* gene products (β1 or β1B) regulate the expression and subcellular distribution of VGSC α subunit proteins in a cell-type specific manner. *Scn1b* null CA3 hippocampal neurons have decreased levels of Nav1.1 and increased levels of Nav1.3 protein compared to wildtype,

as assessed by immunofluorescence, which may correspond to the overall developmental delay exhibited by these mice (Chen et al. 2004). *Scn1b* is required for localization of Nav1.6 to the AIS in a subpopulation of CGNs and a subpopulation of *Scn1b* null CGNs display increased levels of Nav1.1 channels at the AIS compared to wildtype (Brackenbury et al. 2010).

Other members of the VGSC β subunit gene family are involved in modulation of electrical excitability *in vivo*. Sodium current recordings in *Scn2b* null hippocampal neurons demonstrate a negative shift in the voltage-dependence of inactivation relative to cells from WT littermates, resulting in increased channel availability (Chen et al. 2002). In contrast, *Scn2b* null small-fast DRG neurons display decreased TTX-S (Nav1.7) sodium current density and slowed rates of TTX-S sodium current activation and inactivation, with no measurable changes in TTX-R currents (Lopez-Santiago et al. 2006), again demonstrating that β subunit effects *in vivo* are cell type specific. Experiments using transfection to knockdown or express β4 in primary neurons suggest that this subunit promotes persistent sodium current (Aman et al. 2009; Bant and Raman 2010). Interestingly, β1 and β4 are proposed to play opposite roles in hippocampal neurons, such that β1 promotes channel inactivation, acting as a "brake" on excitability, whereas β4 promotes channel activation, acting as the "accelerator" (Aman et al. 2009). This is consistent with findings that *Scn1b* null mice are spontaneously epileptic (Chen et al. 2004; Brackenbury et al. 2013).

In addition to their roles in the nervous system, β subunits are regulators of electrical excitability in the heart *in vivo*. Sodium current recordings from *Scn1b* null ventricular cardiomyocytes demonstrated increases in both transient and persistent sodium current density, resulting in prolongation of action potential repolarization and extension of the heart rate-corrected QT interval (Lopez-Santiago et al. 2007). Here, *Scn5a* mRNA, Nav1.5 protein, and ^{3}H-saxitoxin (a potent sodium channel blocker also used as a research tool to assess cell surface VGSC expression) binding were all

increased compared to wildtype, suggesting increases in both TTX-R and TTX-S VGSC expression in these cells. Mutations in *SCN2B* have been linked to atrial fibrillation (AF) and Brugada syndrome, suggesting a role for β2 in cardiac excitability (Watanabe et al. 2009; Riuro et al. 2013). Cardiac excitability is also abnormal in *Scn3b* null mice, suggesting a role for β3 in the heart (Hakim et al. 2008; Hakim et al. 2010). Upon programmed electrical stimulation, ventricular tachycardia occurs in *Scn3b* null, but not wildtype, Langendorff-perfused hearts (Hakim et al. 2008). *Scn3b* null hearts display atrial tachycardia during atrial burst pacing (Hakim et al. 2010). *Scn4b* has been identified as a modifier gene for Long QT Syndrome (LQTS) resulting from a mutant *Scn5a* gene (Remme et al. 2009). While the 129P2/OlaHsd mice used in this study are cardiac *Scn4b* hypomorphs, expression in the brain is unaffected (Calhoun and Isom, unpublished observation), suggesting 129P2/OlaHsd mice harbor a mutation that abolishes a cardiac-specific *cis* regulatory element.

Role of VGSC β subunits in resurgent sodium current

Resurgent sodium current, defined as the influx of sodium through VGSC α subunits during repolarization (Bean 2005), is an important adaptation for high-frequency firing neurons such as cerebellar Purkinje neurons (Burgess et al. 1995; Raman et al. 1997). The intracellular domain of β4 was proposed to serve as the open-channel blocking particle that allows for resurgent sodium current in neurons (Grieco et al. 2005). Here, a β4 C-terminal peptide was shown to prevent the fast inactivation gate from closing, thus allowing for more rapid channel recovery. Subsequent knockdown of β4 expression using siRNA in CGNs resulted in reduced resurgent sodium current and decreased repetitive firing, providing further evidence for β4 as the open-channel blocking particle (Bant and Raman 2010). A peptide corresponding to β4 was sufficient to invoke resurgent sodium current in HEK 293 cells (Theile and Cummins 2011), again strongly suggesting a role for β4 in the generation of resurgent sodium current *in vivo*.

Importantly, however, co-expression of full length β4 and Nav1.6 subunits was not sufficient to generate resurgent current (Chen et al. 2008), suggesting that key cellular processes, possibly including post-translational modification, that allow β4 subunits to participate as the open-channel blocking particle may be specific to neurons. In addition to β4, β1 or β1B play roles in regulating resurgent current, at least in the cerebellum. *Scn1b* null CGNs have normal transient sodium current but reduced resurgent sodium current and, importantly, β4 protein levels are not reduced (Brackenbury et al. 2010). These observations strongly argue that VGSC β subunits, in particular β4, play a role in regulating resurgent sodium current *in vivo*.

VGSC β subunits modulate cell surface expression of α subunits

In heterologous systems, β subunits increase the cell surface expression of α subunits. The final step in VGSC biosynthesis *in vivo* is concomitant α-β2 association and cell surface insertion (Schmidt et al. 1985; Schmidt and Catterall 1986). *In vivo* observations support this conclusion. Primary *Scn2b* null hippocampal neurons display reduced sodium current density compared to wildtype (Chen et al. 2002). In support of this, ^{3}H-saxitoxin binding to cell surface VGSCs is reduced in whole brain neurons isolated from *Scn2b* null mice while total ^{3}H-saxitoxin binding (intracellular plus cell surface) is unchanged (Chen et al. 2002). Interestingly, this is not the case for all brain areas. Neurons acutely dissociated from wildtype and *Scn2b* null dentate gyrus exhibit similar sodium current densities (Uebachs et al. 2010). This result suggests that, similar to β1, the effect of β2 on cell surface α subunit expression may be cell-type specific. In addition to being cell-type specific, β2 has VGSC-specific effects based on TTX sensitivity. For example, *Scn2b* null small-fast DRG neurons have reduced TTX-S sodium current, but unchanged TTX-R sodium current (Lopez-Santiago et al. 2006).

Novel role for VGSC β subunits in modulation of potassium channels

β1 was originally discovered as a subunit of rat brain VGSCs purified to theoretical homogeneity (Hartshorne et al. 1982; Hartshorne and Catterall 1984). In spite of this, β1 is promiscuous in its ability to modify ion channels. For example, when co-expressed with Kv4.3 in *Xenopus* oocytes, β1 modulates potassium current (Deschenes and Tomaselli 2002). Subsequent experiments by this group using siRNA to knock down *Scn1b* expression in neonatal rat ventricular cardiomyocytes resulted in reduced sodium current ***and*** transient outward potassium current, demonstrating that *Scn1b* modulates multiple channel types *in vivo* (Deschenes et al. 2008). More recently, β1 has been shown to modulate potassium currents expressed by Kv1.1, Kv1.2, Kv1.3, Kv1.6, or Kv7.2 (but interestingly not Kv3.1) in oocytes (Nguyen et al. 2012). Importantly, immunoprecipitation from mouse brain revealed that β1 subunits associate with Kv4.2 (Marionneau et al. 2012). This provides critical *in vivo* evidence for association of potassium channels and β1 in a neuronal protein complex. In this same study, shRNA-mediated knockdown of *Scn1b* resulted in a reduction of Kv4-mediated current in neurons (Marionneau et al. 2012). *Scn1b* null mice show prolonged action potentials and increased repetitive firing in cortical pyramidal neurons, supporting not only changes in sodium current, as shown in (Brackenbury et al. 2013) but also a link between VGSC β1/β1B subunits and potassium channel activity (Marionneau et al. 2012). These observations suggest a novel role for VGSC β1/β1B subunits in interacting with and modulating potassium channels, suggesting, perhaps, that these multifunctional proteins should be re-classified independently from the VGSC family.

Non-canonical roles of VGSC β subunits in brain development and cell signaling

Neurite outgrowth

VGSC β subunits are multifunctional molecules that do more than modulate channel expression and ionic currents. As CAMs, β subunits, especially β1, participate in neuronal proliferation and migration, neurite outgrowth (**Figure 1.5**), and axonal

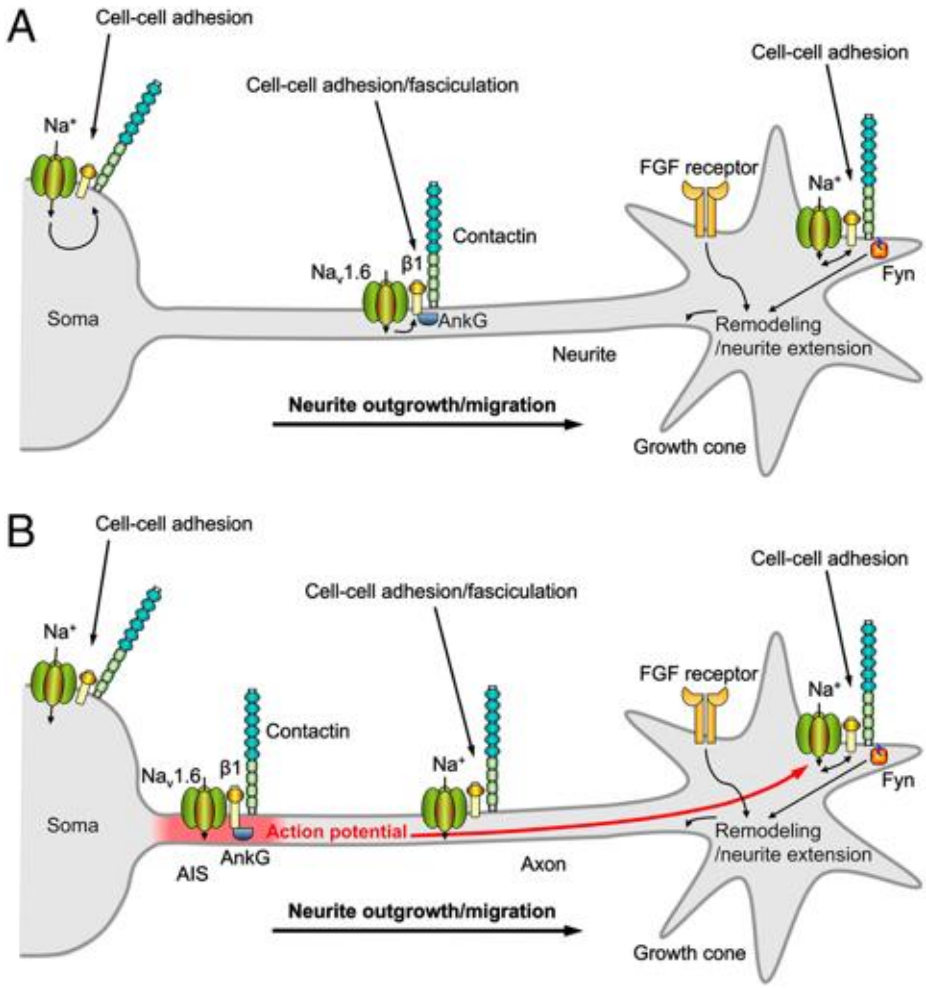

Figure 1.5. A model for β1-mediated neurite outgrowth. (A) In immature CGNs lacking AIS, complexes containing Nav1.6, β1, and contactin are present throughout the neuronal membrane in the soma, neurite, and growth cone. Localized sodium influx is necessary for β1-mediated neurite extension and migration (Brackenbury et al. 2010). VGSC complexes along the neurite are proposed to participate in cell–cell adhesion and fasciculation (Davis et al. 2004; Brackenbury et al. 2008a). (B) In 14 DIV CGNs, β1 is also required for Nav1.6 expression at the AIS (Brackenbury et al. 2010), and subsequent high-frequency AP firing through modulation of resurgent sodium current (Van Wart and Matthews 2006; Raman et al. 1997; Raman and Bean 1997). Electrical activity may further promote β1-mediated neurite outgrowth at or near the growth cone in vivo (Van Wart and Matthews 2006; Raman et al. 1997; Raman and Bean 1997). Thus, the developmental functions of β1 and Nav1.6 are complementary, such that sodium influx carried by Nav1.6 is required for β1-mediated neurite outgrowth and β1 is required for normal expression/activity of Nav1.6 at the AIS. Fyn kinase and AnkG also are likely present in all complexes, but they are only shown once in each panel for clarity. The FGF-mediated, β1-independent neurite outgrowth pathway is shown as well. Other CAMs that regulate neurite outgrowth and also may interact with β1 in this system, have been omitted for clarity. Figure reproduced from (Brackenbury et al. 2010).

fasciculation. The first evidence of involvement of β1 in neurite outgrowth came from the observation that CGNs develop longer neurites on β1-expressing fibroblast monolayers compared to mock transfected monolayers (Davis et al. 2004). To test the effects of other β subunits, CGNs were also plated on β2- or β4-expressing monolayers (Davis et al. 2004). β4-expressing monolayers had no effect, whereas β2-expressing monolayers reduced, neurite length. Comparing CGNs isolated from *Scn1b* null mice with those from wildtype littermates demonstrated that β1-mediated neurite outgrowth required *trans* homophilic adhesion (Davis et al. 2004). This suggests a model where β1-β1 *trans* homophilic adhesion acts as the initiating event for a signaling cascade that results in neurite outgrowth. β1-mediated neurite outgrowth is abrogated in *Fyn* and *Cntn1* null CGNs, implying that these molecules are key, (Brackenbury et al. 2008a). *Cntn1* null mice are β1 hypomorphs, suggesting that *Cntn1* and *Scn1b* are linked in some fashion (Brackenbury et al. 2008a). β1 expression levels are unchanged in *Fyn* null mice, suggesting that this member of the src family of tyrosine kinases may participate in a signaling cascade downstream of β1-β1 mediated cell-cell adhesion (Brackenbury et al. 2008a). A portion of β1 and fyn co-localize in detergent resistant membrane (DRM) fractions in brain (Brackenbury et al. 2008a) and contactin has been identified in this fraction as well (Kramer et al. 1999). These results suggest that β1-mediated neurite outgrowth may occur through a lipid raft signaling mechanism that requires the presence of both fyn and contactin (Brackenbury and Isom 2011). β1-mediated neurite outgrowth in CGNs requires the expression of Nav1.6 and is inhibited by TTX, suggesting that TTX-S sodium current modulates β1-mediated neurite outgrowth (Brackenbury et al. 2010). However, the location of these signaling events in the neuron may differ. It is proposed that sodium current initiated at the AIS (where β1 is also located) signals to β1 subunits at the growth cone which may or may not be associated with α subunits (Brackenbury et al. 2010). Importantly, while TTX inhibits β1-mediated neurite outgrowth, it does not affect FGF-mediated neurite outgrowth (Brackenbury et al. 2010).

Conversely, neither FGF nor EGF receptor kinase inhibitors affect β1-mediated neurite extension (Brackenbury et al. 2008a). Thus, these signaling cascades appear to involve different players.

Brain Development

The gene products of *Scn1b* are important for neuronal patterning during brain development. Immunohistological examination of wildtype and *Scn1b* null cerebellae demonstrated cerebellar microorganization defects in the null brain (Brackenbury et al. 2008a). Specifically, in the cerebellum of *Scn1b* null mice, parallel fiber fascicles were less compact than in wildtype. In addition, the external germinal layer (EGL) was expanded in size in null mice relative to wildtype, suggesting that a defect in migration may have trapped granule precursors in the EGL, preventing them from migrating to the inner granule layer (IGL). In wildtype cerebellar sections, axon fibers traversing the molecular layer (ML) ran perpendicular to the parallel fibers. However, in *Scn1b* null cerebellar sections, some of the axons traversing the ML deviated from this perpendicular trajectory, suggesting axon outgrowth and pathfinding deficits. In the developing hippocampus, *Scn1b* null mice display a series of developmental defects, including elevated levels of cellular proliferation in the hilus, ectopic *Prox1*-expressing dentate granule neurons in the hilus, decreased neuronal density in the dentate gyrus granule cell layer, increased thickness of the dentate gyrus granule cell layer, and abnormal axon outgrowth and pathfinding (Brackenbury et al. 2013). Spontaneous seizures begin at approximately postnatal day 10 in *Scn1b* null mice (Chen et al. 2004). Importantly, developmental defects in the *Scn1b* null cerebellum and hippocampus precede the onset of seizures and are detectable at P5 (Brackenbury et al. 2013). Taken together, these observations suggest that β1 or β1B function as CAMs in the developing CNS and that perturbation of *Scn1b* results in patterning defects which may set up a substrate for altered excitability.

Roles of Voltage-gated Sodium Channel β Subunits in Pathophysiology

Epilepsy

Epilepsy is a common neurological disorder defined by recurrent, unprovoked seizures due to abnormal surges of electrical activity in the brain. While epilepsy can be caused by injury or other disease, as many as 40% of epilepsy cases are idiopathic and presumed to stem from genetic anomalies. Not surprisingly, mutations in ion channels ('channelopathies') cause epilepsy. Of particular interest is the GEFS+ spectrum of epilepsy disorders which includes GEFS+ and DS. The GEFS+ epilepsy spectrum is a continuum of disease severity and includes pediatric epilepsies wherein febrile seizures persist beyond six years of age and are associated with generalized or partial epilepsy (Escayg and Goldin 2010). DS patients exhibit frequent febrile seizures which precede the development of other seizure types and are at risk for status epilepticus, developmental delay, and ataxia. DS patients are also at elevated risk of death, or Sudden Unexplained Death due to EPilespsy (SUDEP). While multiple mechanisms have been proposed for SUDEP, lethal cardiac arrhythmia is an interesting candidate as ion channel-driven cellular excitability is a shared trait between the brain and the heart (Surges and Sander 2012). Mutations in the VGSC α subunits *SCN1A* and *SCN2A* are linked to GEFS+ and DS, with mutations in *SCN1A* causing haploinsufficiency being the predominant cause of DS (Meisler and Kearney 2005; Escayg et al. 2000; Claes et al. 2001; Sugawara et al. 2001; Shi et al. 2009).

Human *SCN1B* mutations are also linked to epilepsies on the GEFS+ spectrum, including GEFS+ and DS (Wallace et al. 1998; Wallace et al. 2002; Patino et al. 2009; Audenaert et al. 2003; Ogiwara et al. 2012). In addition to the GEFS+ spectrum, *SCN1B* mutations are also linked to temporal lobe epilepsy (TLE) and early onset absence

epilepsy (EOAE) (Audenaert et al. 2003; Scheffer et al. 2007). To date, most known disease-related *SCN1B* mutations cluster in the Ig loop region of β1/β1B (Brackenbury and Isom 2011). Probands in a number of GEFS+ pedigrees carry rare heterozygous *SCN1B* mutations (Wallace et al. 1998; Wallace et al. 2002; Audenaert et al. 2003; Scheffer et al. 2007; Fendri-Kriaa et al. 2011). A homozygous DS mutation in *SCN1B* was identified by screening candidate genes after the patient was found to lack mutations in *SCN1A* (Patino et al. 2009). Recently, another homozygous *SCN1B* mutation was discovered in a DS patient (Ogiwara et al. 2012). While the majority of human mutations map to the Ig loop region that is shared by both β1 and β1B splice variants, a β1B-specific mutation was recently identified in two unrelated pedigrees with idiopathic epilepsy (Patino et al. 2011).

Mouse models support the link between *Scn1b* and epilepsy. *Scn1b* null mice display spontaneous generalized seizures and ataxia (a co-morbidity of DS), die by P21 (Chen et al. 2004), and are proposed to be a model of DS (Patino et al. 2009). Characterization of *Scn1b* null mice has demonstrated defects in excitability and neuronal development (Patino et al. 2009; Brackenbury et al. 2008a; Brackenbury et al. 2013). Importantly, defects in neuronal patterning are observed at P5, prior to seizure onset, suggesting that this may be a cause, rather than an effect, of neuronal hyperexcitability (Brackenbury et al. 2013). A mouse model of *SCN1B*-related GEFS+, a knock-in of the β1 p.C121W mutation, recapitulates a number of aspects of the human disease (Wimmer et al. 2010). Both p.C121W heterozygous and homozygous mice are more susceptible to febrile seizures relative to wildtype littermates (Wimmer et al. 2010). Action potential recordings from subicular pyramidal neurons suggest p.C121W knock-in neurons are hyperexcitable (Wimmer et al. 2010). Immunoblots with an anti-β1 antibody suggest no change in β1 expression in C121W knock-in heterozygous or homozygous brains (Wimmer et al. 2010), however, the authors make note of a number of nonspecific immunoreactive bands when performing Western blot analysis with this particular anti-β1

antibody (Wimmer et al. 2010). Data suggest that heterozygous p.C121W knock-in mice, expressing a single mutant copy of *Scn1b*, display a GEFS+-like phenotype. At the cellular level, the p.C121W mutation results in a hyperexcitable phenotype in subicular pyramidal neurons, which may provide evidence toward the mechanism of febrile seizures resulting from this mutation.

Studies of *SCN1B* mutants have yielded insight into the molecular mechanisms underlying the perturbed functionality of these alleles. β1 p.R125C is a trafficking deficient mutation which is retained intracellularly, resulting in a functional null phenotype (Patino et al. 2009). Importantly, the β1 p.R125C trafficking defect can be rescued by incubating cells at lowered temperature, opening the possibility of future development of novel therapeutics similar to those for CFTR and muscular dystrophy (Eckford et al. 2012; Cirak et al. 2011). β1 p.C121W disrupts a conserved intramolecular disulfide bond, a critical feature of the Ig loop structure. β1 p.C121W traffics normally to the cell surface and promotes VGSC α subunit expression in transfected cell lines, however, it does not participate in *trans* homophilic adhesion and does not modulate sodium current *in vitro* (Meadows et al. 2002b). The trafficking of β1 p.C121W was studied by viral expression of wildtype or mutant β1-eGFP fusion constructs in neurons. Under these conditions β1 p.C121W was excluded from the AIS, suggesting that the mutation affects β1 trafficking *in vivo* (Wimmer et al. 2010). Studies of the *SCN1B* GEFS+ mutations p.R85C and p.R85H in heterologous systems showed that these mutant β1 subunits fail to modulate VGSC α subunits due to reduced membrane and intracellular β1 expression (Xu et al. 2007). In contrast, we were able to detect p.R85H at the cell surface in transfected CHL cells (Patino et al. 2011). These results present a complex picture of *SCN1B* mutations with differential effects in different expression systems that may include defects in trafficking or sodium channel modulation. Importantly, a gap in the literature is in understanding the role of these *SCN1B* mutations *in vivo*, including their effects on neuronal patterning or potassium channel modulation.

Thus far, data on *SCN1B* epilepsy mutations suggest a model in which gene dosage may determine the severity of disease presentation. For example, a single mutant *SCN1B* allele may result in the development of the milder disease GEFS+. In contrast, expression of two non-functional *SCN1B* alleles may result in the very severe disease DS. As more *SCN1B* mutant alleles associated with epilepsy are identified and studied, the picture will become clearer. The future identification of *SCN1B* modifier genes and gain-of-function or dominant-negative *SCN1B* mutations will certainly revise this model.

Ataxia

Ataxia, or altered gait, largely resulting from abnormal electrical excitability in the cerebellum, is a comorbidity of DS. *Scn1b* null mice display ataxia (Chen et al. 2004) and the patient carrying two DS mutant *SCN1B* alleles (p.R125C), predicted to be a functional null, displayed psychomotor deterioration after 5 months of age (Patino et al. 2009). Evidence from studying cerebellar microorganization of *Scn1b* null mice has yielded important information for the understanding of ataxia related to *SCN1B.* As described above, *Scn1b* null CGNs display reduced resurgent sodium current and impaired excitability (Brackenbury et al. 2010). Additionally, the developing *Scn1b* null cerebellum has defasciculated parallel fibers, abnormal migration of CGN precursors, and aberrant axon outgrowth and pathfinding of developing CGNs (Brackenbury et al. 2008a). Finally, the expression of β1 subunits in Bergmann glia in the cerebellum raises the possibility that *SCN1B* mutations may result in altered axo-glial interations (Davis et al. 2004). Thus, the ataxic phenotype of *Scn1b* null mice and possibly of *SCN1B*-linked epilepsy patients likely results from a combination of developmental defects compounded by altered excitability.

Cardiac arrhythmia

Channelopathies increase the risk of abnormal heart rhythms, or cardiac arrhythmias, which can be life-threatening in the case of ventricular fibrillation (VF). For

example, mutations in the predominant cardiac sodium channel gene *SCN5A* are associated with LQTS, Brugada syndrome, and VF (Remme and Bezzina 2010). Mutations in VGSC β subunits *SCN1B, SCN2B*, and *SCN3B* are linked to Brugada syndrome, which confers increased risk of sudden cardiac death due to VF (Watanabe et al. 2008; Riuro et al. 2013; Ishikawa et al. 2013). Mutations in *SCN1B*, *SCN2B*, *SCN3B*, and *SCN4B* are linked to AF (Watanabe et al. 2009; Olesen et al. 2011; Li et al. 2013). A mutation in *SCN4B* has been linked to LQTS, in which impaired repolarization of the myocardium provides a substrate for arrhythmia that can result in heart palpitations, syncope, or sudden death due to VF (Medeiros-Domingo et al. 2007).

Evidence in transgenic mice suggests an important role for VGSC β subunits in the heart. *Scn1b* null mice have abnormal cardiac action potentials evidenced by an elongated heart rate-corrected QT interval (Lopez-Santiago et al. 2007). Acutely dissociated ventricular cardiomyocytes from *Scn1b* null mice have increased peak and persistent sodium current relative to wildtype cells. Ventricular tachycardia is observed following programmed electrical stimulation in *Scn3b* null, but not wildtype, Langendorff-perfused hearts (Hakim et al. 2008). In hearts paced using atrial burst pacing, *Scn3b* null hearts were susceptible to atrial tachycardia (Hakim et al. 2010). A genetic modifier screen identified *SCN4B* as a genetic modifier for phenotype severity in a mouse model of an *SCN5A* allele which results in conduction disease and Brugada syndrome with variable severity in patients (Remme et al. 2009).

These results suggest VGSC β subunits are involved in normal cardiac function and that perturbation of these genes by mutation can result in disease. Given that β subunit mutations are linked to both brain and cardiac disease, one cannot help but consider the possibility of a link between these syndromes. Elucidation of this putative relationship may be an important step towards understanding and preventing SUDEP in the future.

Sudden Infant Death Syndrome (SIDS)

SIDS is characterized by the sudden death of an infant with no obvious trauma or identifiable underlying medical condition. Arrhythmia is emerging as one of the potential causes of SIDS (Towbin 2010). In addition to mutations of the predominant cardiac sodium channel gene *SCN5A* in SIDS, rare mutations have been identified in *SCN3B* and *SCN4B* in 3 cases (Tan et al. 2010; Wang et al. 2007; Arnestad et al. 2007). Biochemical characterization of the resulting β3 and β4 mutant proteins suggested that the mutations perturbed the normal function of the proteins. When co-expressed with Nav1.5, the β3 mutant (p.V36M) decreased peak sodium current while wildtype β3 had no effect (Tan et al. 2010). In contrast, neither wildtype β4 nor the β4 mutant (p.S206L) had an effect on peak current (Tan et al. 2010). Importantly, the β3 and β4 mutants both resulted in increased persistent sodium current (Tan et al. 2010). Expression of β4 p.S206L in adult rat ventricular cardiomyocytes also led to increased persistent sodium current, suggesting the presence of substrates for lethal arrhythmias in these SIDS patients (Tan et al. 2010). These results suggest the possibility of common molecular mechanisms between epilepsy, SUDEP, cardiac arrhythmia, and SIDS, and provide further evidence that treatment of arrhythmia may be a potential avenue for preventing both SUDEP and SIDS.

Neuropathic Pain

Neuropathic pain can be caused by genetic mutation or nerve injury, resulting in elevated pain sensation, or allodynia, in individuals due to disruptions in nociception, the normal neuronal pathways involved in the sensation of noxious stimuli. VGSC β subunits are expressed in multiple cell types involved in nociception, including DRG neurons and peripheral nerves, and animal studies suggest the involvement of β subunits in nociception. Specifically, *Scn1b* null DRG neurons are hyperexcitable (Lopez-Santiago et al. 2011). While the early postnatal lethality of *Scn1b* null mice has complicated behavioral pain testing, hyperexcitable DRG neurons in these mice may increase their

sensitivity to stimulation and result in allodynia. The role of *Scn2b* in nociception has also been explored. As described above, β2 modulates TTX-S but not TTX-R VGSC α subunits and currents in small-fast DRG neurons. *Scn2b* null mice are less sensitive than wildtype mice in the late phase of the formalin test, suggesting a role for β2 in inflammatory pain (Lopez-Santiago et al. 2006). β2 protein expression increases with nerve injury and this expression is required for the development of mechanical allodynia in a rodent model (Pertin et al. 2005). Finally, β3 is expressed in small-diameter c-fiber DRG neurons and the expression of β3 is upregulated in a chronic constriction rat neuropathic pain model (Shah et al. 2000). These results suggest β subunits play important roles in nociception and are potential therapeutic targets in neuropathic pain.

Neurodegenerative disease

Neurodegenerative diseases, including Alzheimer's disease (AD), Parkinson's disease (PD), Multiple sclerosis (MS), and Huntington's disease (HD), are characterized by a progressive loss of neuron function over time and often involve neuronal cell death. Accumulation of intra-axonal sodium ions resulting in calcium overload is an emerging mechanism for axonal loss and cell death in neurodegenerative disease, suggesting a potential link between VGSCs and neurodegeneration (Waxman 2006). Importantly, pharmacological inhibition of VGSCs is neuroprotective in experimental autoimmune encephalomyelitis (EAE), a model of MS (Lo et al. 2002; Lo et al. 2003). This result suggested that a reduction in sodium current might be a general mechanism for neuroprotection. *Scn2b* null mice (lacking β2) display reduced sodium current density in CNS and PNS neurons. Thus, it was hypothesized that these mice display protection from neurodegeneration (Chen et al. 2002; Lopez-Santiago et al. 2006). Using the EAE model, it was demonstrated that *Scn2b* null mice have higher rates of survival and lower rates of symptomatic progression relative to wildtype mice (O'Malley et al. 2009). This finding

raised the possibility that in, addition to VGSC α subunits, β2, and possibly other β subunits, may be targets for therapeutic intervention in neurodegenerative disease.

β4 is down-regulated in the striatum of HD patients (Oyama et al. 2006). However, whether loss of β4 expression is relevant to the HD disease process or a secondary effect of the disease is unknown. Given the role of β4 in sodium current modulation, resurgent sodium current generation, and potentially as a CAM, it seems plausible that down-regulation of β4 could have a significant impact on brain function. A recent report investigating PD identified glycosylated β4 in patient cerebral spinal fluid (CSF) (Zhou et al. 2012), suggesting that the ectodomain of β4 may be released into the CNS during the disease process. However, additional evidence is needed to implicate β4 in the pathogenesis of neurodegenerative disease. At this time, the possibility that altered proteolytic cleavage of β4 is a secondary byproduct of disease progression cannot be excluded. Even if β4 is not directly involved in the disease mechanism, it may be useful as a biomarker.

Potential role of VGSC β subunits in cancer

Increasing evidence implicates ion channels, including VGSCs, in carcinogenesis (Prevarskaya et al. 2010). Much of the research on the role of VGSCs in cancer has focused on α subunits as molecules which promote metastatic potential, the ability of a cancer cell to release from the primary tumor and form secondary tumors (Brackenbury 2012). Importantly, pharmacologic inhibition of sodium current inhibits cancer cell invasion *in vitro*, raising the possibility that VGSCs may be novel targets for treating metastatic cancer (Brackenbury et al. 2007; Yang et al. 2012). Less is known about VGSC β subunits in cancer, though a few studies have been performed which suggest context-specific roles for these molecules. *SCN1B* mRNA transcripts have been detected in prostate cancer and may correlate with high metastatic potential (Diss et al. 2008). In contrast, studies in breast cancer cell lines suggest that β1 expression is high in weakly

metastatic cells and low in strongly metastatic cells (Chioni et al. 2009). In cell culture models, β1 acts to limit metastatic potential, suggesting it may be a novel therapeutic target (Chioni et al. 2009). These results suggest a cell type-specific function for *SCN1B* in cancer, however, they must be interpreted with caution until *in vivo* evidence emerges. In addition, *SCN3B* may play a novel role as a p53-inducible proapoptotic gene that may partially mediate the tumor suppressor function of p53 (Adachi et al. 2004). However, a putative molecular mechanism for how *SCN3B* functions in apoptosis remains elusive.

Therapeutic potential of VGSC β subunits

As discussed above, VGSC β subunits may be drug targets for a variety of diseases including epilepsy, cardiac arrhythmia, neuropathic pain, migraine, multiple sclerosis, and cancer. How to target these molecules remains unknown, although emerging clues, as discussed below, may provide important insights.

β subunits alter VGSC pharmacology

Perhaps the observation with most immediate ramifications for therapeutics is the finding that β subunits affect VGSC pharmacology. In *Xenopus* oocytes, co-expression of β1or β3 with Nav1.3 abrogates the inhibitory effect of lidocaine, a sodium channel blocker utilized as an antiarrhythmic and local anesthetic (Lenkowski et al. 2003). In addition, in a heterologous system the β1 p.C121W GEFS+ mutation diminishes tonic and use-dependent channel block induced by phenytoin, a sodium channel blocker used as an anticonvulsant (Lucas et al. 2005). The efficacy of the anticonvulsant carbamazepine, a sodium channel blocker, relies on the expression of *Scn1b in vivo* (Uebachs et al. 2010). In contrast, the anticonvulsant lacosamide functions normally in this model (Uebachs et al. 2012). These studies emphasize the importance of understanding how drugs interact not only with the pore-forming α subunits in isolation, but with relevant VGSC α/β protein complexes. Also, since the expression of VGSC β

subunits can be altered by pathophysiology, understanding how sodium channel compounds work in the absence and presence of β subunits is clinically relevant (Ellerkmann et al. 2003).

Rescuing trafficking deficient α subunits

Some *SCN1A* epilepsy mutations result in trafficking deficient Nav1.1 channels that can be rescued by modulatory proteins, including VGSC β subunits, or by a number of VGSC targeting compounds (Rusconi et al. 2007; Rusconi et al. 2009; Thompson et al. 2012). In addition to providing a model for heterogeneity of disease severity in which genetic background may influence the level of mutant Nav1.1 channel proteins trafficked to the cell surface, this suggests a novel treatment strategy. Utilizing VGSC targeting drugs or gene therapy to deliver modulatory β subunits may correct channel trafficking in this patient cohort and provide a viable therapeutic intervention. A potential caveat here is that forcing channels with gain-of-function mutations to the neuronal cell surface may exacerbate, rather than ameliorate, disease (Thompson et al. 2012).

Modulation of SCN2B expression in neurodegenerative disorders and neuropathic pain

Scn2b deletion is neuroprotective in EAE, a model of MS (O'Malley et al. 2009). It is interesting to consider the possibility that reducing the expression of β2 in patients, through small molecules or gene therapy, may be neuroprotective and a potential therapeutic approach to neurodegeneration in MS. Because *Scn2b* null mice are healthy and live normal lifespans, the safety risks of targeting β2 in limited brain areas may be acceptable. In addition, β2 may be a potential therapeutic target in the treatment of neuropathic pain. As discussed above, global *Scn2b* deletion modulates TTX-S VGSC α subunit expression and function in small-fast DRG neurons as well as the animal's response to an inflammatory pain model (although these mice are more sensitive to acute noxious thermal stimuli than wildtype) (Lopez-Santiago et al. 2006). In addition, the

expression of β2 increases with nerve injury and β2 upregulation is necessary for the development of mechanical allodynia (Pertin et al. 2005). A small molecule or gene therapy approach to reduce the expression of β2 in neurons within the nociceptive pathway may be a viable strategy to treat neuropathic pain.

Concluding Remarks

SCN1B: A tale of two splice variants

SCN1B encodes both the transmembrane protein β1 and the secreted protein β1B (Patino et al. 2011). Importantly, both splice variants are CAMs (Malhotra et al. 2000; Patino et al. 2011). A critical gap in our knowledge is how each splice variant contributes to normal development and thus how mutations in only one of the gene products but not the other might contribute to pathophysiology. Most of the disease-related *SCN1B* mutations cluster in or near the extracellular Ig loop, which is common to both β1 and β1B (Brackenbury and Isom 2011). *Scn1b* null mice, which exhibit spontaneous seizures and premature lethality and are a DS model, lack expression of both splice variants and thus imply the importance of both in establishing and maintaining normal physiology (Chen et al. 2004). Further, mutations that affect β1B and not β1 have been identified in a case of Brugada syndrome and two pedigrees of idiopathic epilepsy (Watanabe et al. 2008; Patino et al. 2011), suggesting that both splice variants of *SCN1B* play important roles in normal physiology.

Characterization of *Scn1b* null mice suggests that β1 or β1B subunits are critical for normal brain development. But what about adult brain function? It has been demonstrated that proteins involved in tissue development can be co-opted and utilized for adult tissue maintenance. While much of the focus on studying β subunits has focused on early postnatal development, it will be interesting to ask whether β subunit function is

critical in later adulthood. If the β1/β1B subunits play important roles at later time points, this may open up a new avenue to investigate the potential involvement of these proteins in aging, dementia, or neurodegeneration, as has been suggested for β2 and β4.

Functional redundancy – a putative model for disease severity

Perturbation of β1/β1B function, either in inherited human disease or by genetic deletion of *Scn1b* in mice, may be more harmful to the organism than perturbation of other VGSC β subunits. While *Scn1b* null mice model DS and SUDEP, *Scn2b* null mice and *Scn3b* null mice do not have seizures and live normal life spans. Thus, *SCN1B* is essential for life while *SCN2B* and *SCN3B* are not. Currently, the lack of a *Scn4b* null mouse model prevents us from understanding the role of β4 *in vivo* and represents a major gap in our knowledge. A theory that might explain the apparent discrepancy in functional importance of the β subunits, at least in brain, is functional redundancy. It is possible that compensation is poorly achieved with altered *SCN1B* function since β3, the other transmembrane VGSC β subunit that non-covalently associates with α, has a different developmental expression profile and may have altered CAM functions in developing brain compared to β1/β1B. Also, because a secreted splice variant of β3 has not been identified, the loss of secreted β1B, especially during brain development, may be an important factor. *Scn3b* null mice are relatively healthy, thus *Scn1b* may be compensatory in this model. In *Scn2b* null mice, which are also generally healthy, *Scn4b* (encoding the other disulfide-liked β subunit, β4) may provide functional redundancy, for example, serving as a chaperone for the remaining (~50% of control levels) VGSCs detected at the cell surface of *Scn2b* null neurons. If so, then a double null mouse (*Scn2b/Scn4b*) is predicted to have little to no cell surface VGSCs, and result in a lethal phenotype. Interestingly, *Scn2b* may not reciprocally compensate for *Scn4b*, considering the role of β4 as a key player in the generation of resurgent sodium current in high-frequency firing neurons. Loss-of-function *Scn4b* mutations may thus be especially

deleterious to neuronal circuits that rely on resurgent sodium current for which *Scn2b* cannot compensate. Development of a *Scn4b* null mouse model will be essential to addressing these questions. Additionally, characterizing mice with multiple null *Scnxb* alleles will shed important light on this ongoing area of investigation. For example *Scn1b*/*Scn2b* null mice (Aman et al. 2009) have a more severe phenotype and die at a younger age than *Scn1b* null mice (Chen and Isom, unpublished observations). While anecdotal due to a limited sample size, this observation illustrates the potential utility of using such genetic approaches to answer questions about β subunit functional redundancy.

Modifier genes – a model for disease heterogeneity

The existence of modifier genes may explain heterogeneity in disease severity within epilepsy, cardiac arrhythmia, and other channelopathies between families and even within the same family. Based on the topics reviewed here about the multifunctional VGSC β subunits, it seems reasonable to predict that β subunit gene variants/mutations may be disease modifying in addition to disease causing. For example, *SCN4B* has been identified as a modifier gene in a mouse model of *SCN5A*-linked LQTS (Remme et al. 2009). Conversely, it is likely that other genes may modify the severity of disease-causing VGSC β subunit gene mutations, for example, genes encoding some of the key β subunit interacting proteins discussed here. Future discovery of these genetic relationships will not only shed light on disease mechanisms but will provide critical new information regarding the biology of VGSC β subunit-containing protein complexes in normal development and physiology.

Anything but Auxiliary: The future of VGSC β subunits

While originally discovered as ancillary proteins that co-purify with pore-forming VGSC α subunits, there is growing evidence that the β subunits are multifunctional signaling proteins that play VGSC-dependent and –independent roles, including

homophilic and heterophilic cell adhesion, regulation of gene transcription, and modulation of potassium currents. Importantly, *SCN1B*-linked channelopathies may be diseases of brain or heart development, resulting from impaired β1/β1B-mediated cell adhesion leading to altered neuronal circuitry or cardiac cell-cell junctions. This fascinating VGSC β subunit field now looks forward to the use of tissue- and developmental time-specific null mouse models, knockin mouse models of human mutations, the identification of modifier genes, the development of novel therapeutics, and the use of patient-specific human induced pluripotent stem cell models to investigate genetic background issues in personalized medicine.

Acknowledgments

I thank Dr. Lori L. Isom for important contributions to this chapter including valuable discussion and help with editing.

Thesis Goals

The overall goal of my thesis work was to improve our understanding of how VGSC β subunits regulate important cell processes such as cell motility. In addition, I endeavored to improve our knowledge regarding how β subunits, in turn, are regulated by other proteins.

Specifically, for the work described in Chapter II, our objective was to determine the role of VGSC β subunits, in particular β1, in human breast cancer cell motility and metastatic potential *in vitro*. In addition to studying the expression of β subunit mRNA and β1 protein expression, we used complementary approaches to examine the effects of β1 knockdown and β1 expression in human breast cancer cell lines *in vitro*. We observed that β1 is endogenously expressed in weakly metastatic MCF-7 cells, and knockdown of

β1 expression resulted in increased cell motility. Conversely, β1 is weakly expressed in highly metastatic MDA-MB-231 cells, and stable transfection of β1 increases cell-cell adhesion and reduces cell motility.

For the study described in Chapter III, we used CGNs as a model system to investigate the role of β1 tyrosine phosphorylation in β1-mediated neurite outgrowth. We postulated that tyrosine phosphorylation of β1 may act as a molecular switch for downstream signal transduction in response to β1-β1 *trans* homophilic adhesion. In this study, a BacMam baculovirus system was used to express β1 WT or β1Y181E (a phosphomimetic substitution) in *Scn1b* null CGNs to ask if the tyrosine phosphomimetic mutation affected neurite outgrowth in the absence of β1-β1 *trans* homophilic adhesion. We observed that expression of β1Y181E resulted in significantly increased neurite length relative to the expression of β1 WT. In addition, we found that cells grown as aggregates displayed increased levels of tyrosine phosphorylated β1 compared to cells grown as monolayers. Importantly, we observed tyrosine phosphorylation of a β1 peptide in a cell-free fyn kinase assay, suggesting that β1 is a putative substrate for fyn.

For the project discussed in Chapter IV, the goal was to determine the cysteine residue(s) of β2 involved in covalent linkage with α subunits and ask whether this linkage affected protein trafficking. Using a mutagenesis based approach, we were able to identify cysteine residue 26 (β2C26) as the cysteine residue that covalently links to the α subunit. Interestingly, we observed that α-β2 disulfide-linkage is important for the proper subcellular localization of β2 to nodes of Ranvier and the AIS.

Chapter II: A novel adhesion molecule in human breast cancer cells: Voltage-gated sodium channel β1 subunit

Chapter II was published in The International Journal of Biochemistry & Cell Biology (Chioni et al. 2009). My primary contributions to this study include: (1) generation of the MDA-MB-231 cell lines stably expressing GFP or β1-GFP and (2) characterization of *in vitro* cell behaviors of MDA-MB-231 stable cell lines including cell motility, cell-cell adhesion, morphology, and proliferation.

Abstract

Voltage-gated sodium channels (VGSCs), predominantly the 'neonatal' splice form of Nav1.5 (nNav1.5), are upregulated in metastatic breast cancer (BCa) and potentiate metastatic cell behaviors. VGSCs comprise one pore-forming α subunit and one or more β subunits. The latter modulate VGSC expression and gating, and can function as cell adhesion molecules of the immunoglobulin superfamily. The aims of this study were (1) to determine which β subunits were expressed in weakly metastatic MCF-7 and strongly metastatic MDA-MB-231 human BCa cells, and (2) to investigate the possible role of β subunits in adhesion and migration. In both cell lines, the β subunit mRNA expression profile was *SCN1B* (encoding β1) » *SCN4B* (encoding β4) > *SCN2B* (encoding β2); *SCN3B* (encoding β3) was not detected. MCF-7 cells had much higher levels of all β subunit mRNAs than MDA-MB-231 cells, and β1 mRNA was the most abundant. Similarly, β1 protein was strongly expressed in MCF-7 and barely detectable in MDA-MB-231 cells. In MCF-7 cells transfected with siRNA targeting β1, adhesion

was reduced by 35%, while migration was increased by 121%. The increase in migration was reversed by tetrodotoxin (TTX). In addition, levels of nNav1.5 mRNA and protein were increased following β1 down-regulation. Stable expression of β1 in MDA-MB-231 cells increased functional VGSC activity, process length and adhesion, and reduced lateral motility and proliferation. We conclude that β1 is a novel cell adhesion molecule in BCa cells and can control VGSC (nNav1.5) expression and, concomitantly, cellular migration.

Introduction

Voltage-gated sodium channels (VGSCs) are classically responsible for action potential generation and conduction in excitable cells (Catterall 2000). VGSCs contain one pore-forming α subunit and one or more β subunits (Catterall 1992). VGSCs are also widely expressed in cells from a range of human cancers, including breast cancer (BCa) (Fraser et al. 2005; Roger et al. 2003), prostate cancer (PCa) (Laniado et al. 1997), lymphoma (Fraser et al. 2004), lung cancer (Onganer and Djamgoz 2005; Roger et al. 2007), mesothelioma (Fulgenzi et al. 2006), neuroblastoma (Ou et al. 2005), melanoma (Allen et al. 1997), and cervical cancer (Diaz et al. 2007). In addition, VGSCs are upregulated in line with metastasis in BCa, PCa, and small-cell lung cancer (SCLC) *in vivo* (Onganer et al. 2005; Fraser et al. 2005; Diss et al. 2005).

In human and rodent cell models of BCa, PCa and lung cancer, the specific VGSC blocker tetrodotoxin (TTX) suppresses a variety of in vitro metastatic cell behaviors including invasion (Grimes et al. 1995; Bennett et al. 2004; Laniado et al. 1997; Roger et al. 2003), migration (Brackenbury and Djamgoz 2006), galvanotaxis (Djamgoz et al. 2001), morphological development and process extension (Fraser et al. 1999), endocytic membrane activity (Onganer and Djamgoz 2005), lateral motility (Fraser et al. 2003), adhesion (Palmer et al. 2008), and gene expression (Brackenbury and Djamgoz 2006).

Strongly metastatic MDA-MB-231 human BCa cells express a TTX-resistant (IC_{50} in μM range) VGSC current that is absent in weakly metastatic MCF-7 cells (Fraser et al. 2005; Roger et al. 2003). In MDA-MB-231 cells, the predominant α subunit (Nav1.5; gene: *SCN5A*) is expressed primarily in its 'neonatal' D1:S3 5'-splice form (nNav1.5) (Chioni et al. 2005; Fraser et al. 2005). nNav1.5 is primarily responsible for the VGSC-dependent enhancement of migration and invasion of MDA-MB-231 cells (Brackenbury et al. 2007). However, the possible functional involvement of β subunits in potentiation of metastatic cell behaviors is not yet known.

So far, four VGSC β subunits (β1–β4; genes: *SCN1B–SCN4B*) have been identified. β1 and β3 are non-covalently associated with the α subunit (Morgan et al. 2000; Isom et al. 1992), whereas β2 and β4 are disulfide linked (Isom et al. 1995a; Yu et al. 2003). VGSC β subunits are multifunctional molecules (Brackenbury and Isom 2008). These are unique among ion channel auxiliary subunits in that they are homologous to the immunoglobulin superfamily of cell adhesion molecules (CAMs) (Isom 2001; Isom et al. 1994). β subunits also direct α subunit insertion into the plasma membrane and permit interaction of the channel with other signaling proteins. For example, β1 and β2 interact with the extracellular matrix proteins tenascin-C and tenascin-R, influencing migration (Xiao et al. 1999; Srinivasan et al. 1998). In addition, β1 and β2 participate in homophilic cell adhesion, resulting in cellular aggregation and ankyrin recruitment (Malhotra et al. 2000; Malhotra et al. 2002). Furthermore, β1 interacts heterophilically with N-cadherin, contactin, neurofascin-155, neurofascin-186, NrCAM, and β2 (Malhotra et al. 2004; Kazarinova-Noyes et al. 2001). β1 promotes process extension, migration and pathfinding in neurons (Brackenbury et al. 2008a; Davis et al. 2004). β1 can also influence intracellular mechanisms, e.g. a site within the cytoplasmic domain of β1 interacts with receptor tyrosine phosphatase β (Ratcliffe et al. 2000). At least some of these functional roles may be independent of α subunits; in fact, it has been suggested that independent β subunit functioning may be equally important (Malhotra et al. 2002;

Fein et al. 2008). β subunits may have direct involvement in pathophysiologies, e.g. cardiac arrhythmia, epilepsy and pain (Brackenbury and Isom 2008) and indirect involvement, via interacting partners, e.g. contactin, as in metastasis (Su et al. 2006). A recent study on human prostate cancer found (i) that the β subunit mRNA level *in vitro* was positively correlated with metastatic potential and (ii) that *SCN1B* was most abundant of the β subunits (Diss et al. 2008). β subunit expression in human BCa has not previously been studied.

The main aims of the present study were 2-fold: (1) to investigate β subunit expression in two human BCa cell lines of contrasting metastatic potential: MCF-7 (non/weakly metastatic) and MDA-MB-231 (strongly metastatic) in a comparative approach; and (2) to explore the involvement of the β subunit(s), mainly β1, in cellular adhesion and migration.

Methods

Cell culture

MDA-MB-231 and MCF-7 cells were cultured in Dulbecco's modified Eagle's medium supplemented with 5–10% fetal bovine serum (FBS) and 4mM l-glutamine, as described previously (Fraser et al. 2005).

Real-time PCR

RNA extraction, cDNA synthesis and real-time PCR were performed as described previously (Brackenbury et al. 2007). Primers for Cytb5R and nNav1.5 were as described previously (Diss et al. 2001; Brackenbury et al. 2007). The following primer pairs and annealing temperatures were also used:

1. *SCN1B*: 5'-AGAAGGGCACTGAGGAGTTT-3' and 5'-GCAGCGATCTTCT-TGTAGCA- 3' (60 ◦C).

2. *SCN2B*: 5’-GAGATGTTCCTCCAGTTCCG-3’ and 5’-TGACCACCATCAG-CACCAAG-3’ (62 ◦C).

3. *SCN3B*: 5’-CTGGCTTCTCTCGTGCTTAT-3’ and 5’-TCAAACTCCCGGGA-CACATT-3’ (60 ◦C).

4. *SCN4B*: 5’-TAACCCTGTCGCTGGAGGTG-3’ and 5’-TGAGGATGAGGAG-CCCGATG-3’ (60 ◦C).

Threshold amplification cycles were determined using the Opticon Monitor 2 software (MJ Research,Waltham, MA) and analysed by the $2^{-\Delta\Delta Ct}$ method (Livak and Schmittgen 2001).

RNA interference

RNA interference was performed with a pool of siRNAs (Genome smart pool for human SCN1B NM 001037; Dharmacon, Lafayettte, CO), as described previously (Brackenbury et al. 2007). mRNA and protein levels were measured 4–12 days after transfection, and compared with two controls:

1. ‘Mock’. Transfection without siRNA.

2. ‘siControl’. Transfection with siControl non-targeting siRNA pool (Dharmacon).

Transfection efficiency was assessed independently using a positive control siRNA targeting Lamin A/C (Dharmacon), which significantly reduced the lamin A/C protein level by ≥70% after 4 days, compared to siControl non-targeting siRNA.

Creation of a stable MDA-MB-231 line expressing β1

Cells (50% confluent) were transfected overnight with cDNA (2 μg) using Fugene6 reagent (Roche, Nutley, NJ, USA). cDNA encoding eGFP was subcloned from pEGFPN1 into pcDNA3.1+ (Invitrogen). β1-GFP was generated by inserting β1 cDNA lacking the stop codon into pEGFPN1 to create a C-terminal fusion protein. The β1-eGFP cDNA was then subcloned into pcDNA3.1/Hygro+. eGFP-transfected cells were selected

with 400 µg/ml geneticin. One clone was derived and maintained in 200 µg/ml geneticin. β1-eGFP-transfected cells were selected with 200 µg/ml hygromycin B. One clone was derived and maintained in 100 µg/ml hygromycin B.

Western blotting

Total cell lysate preparation, cell membrane preparation, SDS polyacrylamide gel electrophoresis, transfer to nitrocellulose and chemiluminescent detection were performed as described previously (Lopez-Santiago et al. 2006; McEwen et al. 2004; Laniado et al. 1997; Chioni et al. 2005; Fraser et al. 2005). The following primary antibodies were used:

1. Pan-VGSC α subunit antibody (1 µg/ml; Millipore, Watford, UK).
2. NESO-pAb antibody (1 µl/ml) (Chioni et al. 2005).
3. Anti-β1ex antibody (1:500) (Malhotra et al. 2002).
4. Anti-actin antibody (1:700; Sigma, Dorset, UK).
5. Anti-actinin antibody (1 µl/ml; Sigma).
6. Anti-GFP A-11121 (1:1000; Invitrogen).

Densitometric analysis was performed using the Image-Pro Plus software (Media Cybernetics, Bethesda, MD, USA). Signal density was normalized to anti-actinin or anti-actin antibody as a loading control/reference, for at least three separate experiments. For each antibody, linearity of signal intensity with respect to increasing protein loading in the range 20–80 µg was ensured using a standard dilution of MDA-MB-231 cell extract.

Immunocytochemistry and confocal microscopy and image analysis

Cells (2×10^4) grown on poly-l-lysine-coated glass coverslips were fixed in paraformaldehyde (2%) and labelled with fluorescein isothiocyanate (FITC)-conjugated concanavalin A (conA; Sigma) as plasma membrane marker (Brackenbury and Djamgoz 2006). Nonspecific binding sites were blocked with 5% FBS prior to incubation with NESO-pAb. The secondary antibody was Alexa567- conjugated goat anti-rabbit IgG

(Dako). Cells were mounted in Vectashield (Vector Laboratories, Peterborough, UK). Fluorescence was detected using a Leica (Wetzlar, Germany) DM IRBE microscope with TCS-NT confocal laser scanner. GFP was detected using an Olympus (Tokyo, Japan) Fluoview 500 confocal laser-scanning microscope. Densitometric analysis was performed as described previously (Brackenbury and Djamgoz 2006). Measurements were taken from at least 50 cells per condition, for three repeat treatments.

Electrophysiology

Whole-cell recording of sodium currents from cells grown on glass coverslips was performed as described previously, with some modifications (Brackenbury et al. 2007). Patch pipettes (TW150F-3, WPI, Sarasota, FL, USA) were pulled using a Model P-97 puller (Sutter Instruments, Novato, CA, USA) and fire-polished to give resistances of 2–3MΩ when filled with internal solution. Voltage-clamp recordings were performed using a Multiclamp 700B amplifier (Molecular Devices, Union City, CA, USA) compensating for series resistance by 60%. Currents were digitized using a Digidata 1320 interface (Molecular Devices), low-pass filtered at 10 kHz, sampled at 50 kHz and analyzed using pClamp 9.2 software (Molecular Devices). Linear components of leak were subtracted using a standard P/6 protocol (Armstrong and Bezanilla, 1977). Data manipulation and curve fitting were performed as described previously (Ding and Djamgoz 2004).

Morphometric analysis

Transfected cells were viewed under a Zeiss Axioplan fluorescent microscope at The University of Michigan Microscopy and Image Analysis Laboratory. Images captured at 40× were exported into the NIH ImageJ software for analysis. The following measurements were taken for both monopolar and bipolar cells, as described previously (Fraser et al. 1999):

1. Process length.
2. Process thickness.

3. Cell body diameter.

Measurements were recorded from 40 cells from each class, for each cell line.

Single-cell adhesion

Measurements were performed on cells 48 h after plating into 35 mm dishes at a density of 2.5×104 cells/ml, using the single-cell adhesion measuring apparatus (SCAMA), as described previously (Palmer et al. 2008). The peak detachment negative pressure (DNP), measured digitally for each cell, was converted to kPa.

Cell–cell adhesion

The cell–cell adhesion assay was performed as described previously, with some modifications (Wong and Filbin 1996). Suspensions of single cells (2×10^6 cells/ml) were allowed to aggregate at 37 °C with gentle rocking (25 rpm). The particle number of aliquots was determined with a Coulter counter (ZBI; Beckman Coulter, Fullerton, CA, USA) every 30 min for 2 h. Duplicate samples were counted three times, for three repeat experiments.

Proliferation

Cells (1×10^4 cells/ml) were seeded in triplicate wells of a 12-well plate for 24 h. The number of cells per well after 24 h was determined using the thiazolyl blue tetrazolium bromide (MTT) assay, as described previously (Grimes et al. 1995). Results were compiled as the mean of three repeats.

Transwell migration

Cells (2×10^5 cells/ml) were plated onto 12 μm-pore Transwell migration filters in 12-well plates (Corning, NY, USA). siRNA-treated or control cells were incubated with or without TTX (10 μM, applied once at the beginning of the assay), in a 1–10% chemotactic FBS gradient overnight (12 h). The number of cells migrating was

determined using the MTT method (Grimes et al. 1995). Results were compiled as the mean of ≥ four repeats.

Lateral motility

Wound-heal assays were performed as described previously (Fraser et al. 2003). Measurements of wound width (15 per wound) were made at wound formation (W_0) and 24 h later (W_t). The motility index (MI) was calculated as $MI = 1-(W_t/W_0)$. Means were compiled from three repeat experiments.

Data analysis

All quantitative data are presented as means ± standard errors, unless stated otherwise. Statistical significance was determined with Student's t-test, Mann–Whitney rank sum test, one-way analysis of variance (ANOVA) followed by Newman–Keuls test, or two-way ANOVA, as appropriate. Results were considered significant at $P < 0.05$ (*).

Results

We evaluated the expression of VGSC β subunits in weakly metastatic MCF-7 and strongly metastatic MDA-MB-231 cells in a comparative approach. β1 was then downregulated in MCF-7 cells, and stably expressed in MDA-MB-231 cells in order to elucidate its functional involvement in the cells' adhesion and migration.

Expression of VGSC *α* and β subunits in human BCa cell lines

Both MCF-7 and MDA-MB-231 cell lines expressed *SCN1B* (encoding β1), *SCN2B* (encoding β2) and *SCN4B* (encoding β4) mRNAs; *SCN3B* mRNA (encoding β3) was not detected in either line but could be detected in human prostate cancer PC-3M cells (**Figure 2.1A**). Two products were amplified using the *SCN4B* primers: the full-length product (459 nt), and a shorter form (310 nt; **Figure 2.1A**). Real-time PCR

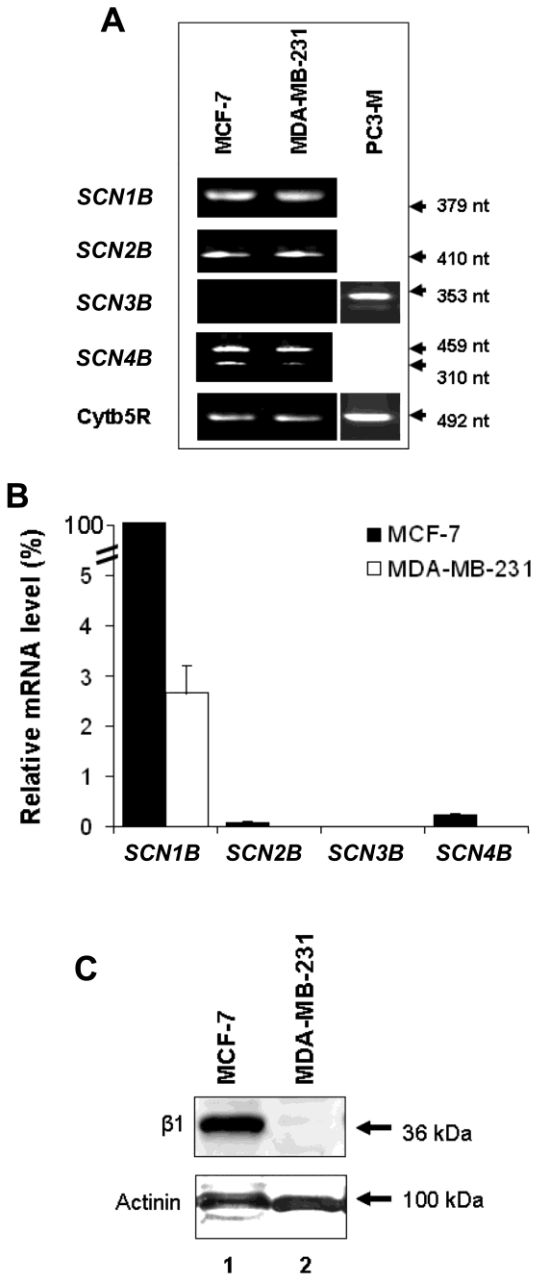

Figure 2.1. β subunit expression in MCF-7 and MDA-MB-231 cells. (A) Typical gel images of PCR products, taken at the end of the PCR, for *SCN1B*, *SCN2B*, *SCN3B*, *SCN4B* and cytochrome b5-reductase (Cytb5R) from MCF-7, MDA-MB-231 and PC-3M cells. The PC-3M cell line was used as a positive control for *SCN3B* expression (Diss et al., 2008). (B) Relative mRNA levels of *SCN1B*, *SCN2B*, *SCN3B* and *SCN4B*, normalized to Cytb5R by the $2^{-\Delta\Delta Ct}$ method, and expressed as a percentage of the *SCN1B* mRNA level inMCF-7 cells (fixed as 100%). Each histobar indicates mean + error propagated

through the $2^{-\Delta\Delta Ct}$ analysis (n = 3). Significance is shown in **Table 2.1**. (C) Western blot with 70 µg of total protein per lane from MCF-7 and MDA-MB-231 cells, using β1ex and an actinin antibody as a control for loading. The same membrane was stripped and re-blotted.

revealed that MCF-7 cells had 40–50-fold higher levels of all β subunit mRNAs than MDA-MB-231 cells (**Table 2.1A; Figure 2.1B**). In both cell lines, *SCN1B* was expressed at the highest level of any β subunit (**Figure 2.1B**). The relative levels of mRNA in both cell lines were *SCN1B* » *SCN4B* > *SCN2B* (**Table 2.1B**). Western blot analysis using anti-β1ex antibody confirmed that β1 polypeptides were highly expressed in MCF-7 and barely detectable in MDA-MB-231 cells (**Figure 2.1C**).

The mRNA level of nNav1.5, the predominant α subunit in MDA-MB-231 cells (Fraser et al. 2005), was ~4200-fold higher than in MCF-7 cells ($P < 0.05$, n=4; **Figure 2.2A**). Both the total α subunit and nNav1.5 protein levels were ~4-fold higher in MDA-MB-231 than MCF-7 cells ($P < 0.01$, n=6; **Figure 2.2B**).

In conclusion, β1, the most highly expressed VGSC β subunit in both MDA-MB-231 and MCF-7 cells, was significantly more abundant in the latter, non/weakly metastatic line, especially at the protein level.

Silencing of β1 expression in weakly metastatic MCF-7 cells by RNAi

Cells were transfected with a pool of siRNAs targeting *SCN1B*. In siRNA-treated cells, the *SCN1B* mRNA level was reduced by 76% after 4 days ($P < 0.01$, n=3; **Figure 2.3A and B**). β1 protein was reduced by 18% after 5 days and 40% after 8 days ($P < 0.05$, $n = 6$ and $P < 0.05$, $n = 8$, respectively; **Figure 2.3C and D**). In contrast, after 4 days, mRNA levels of *SCN2B* and *SCN4B* were unaffected ($P = 0.71$ and $P = 0.97$, respectively; n=3; **Figure 2.3B**).

Five days after transfection with siRNA targeting *SCN1B*, the nNav1.5 mRNA level increased by 280% ($P < 0.05$, n=3; **Figure 2.3B**). However, there was no change in either the total VGSC α subunit or nNav1.5 protein levels ($P = 0.93$ and $P = 0.42$, respectively, n=4; **Figure 2.4A and B**). In contrast, 8 days after transfection, when the β1 protein level was lowest, both the total VGSC α subunit and nNav1.5 protein levels were increased by 256% and 147%, respectively ($P < 0.05$, $n \geq 3$; **Figure 2.4A and B**).

A. Fold differences in expression compared between cell lines

β subunit mRNA	Fold difference (MCF-7 vs. MDA-MB-231)	P
SCN1B	40	< 0.001
SCN2B	20	< 0.01
SCN4B	50	< 0.001

B. Fold differences within given cell lines.

Cell line	*SCN1B* >> *SCN2B*	*SCN4B* > *SCN2B*	*SCN1B* >> *SCN4B*
MCF-7	1500-fold	4-fold	450-fold
MDA-MB-231	800-fold	2-fold	500-fold

Table 2.1. VGSC β subunit mRNA expression in MCF-7 and MDA-MB-231 human breast cancer cell lines.

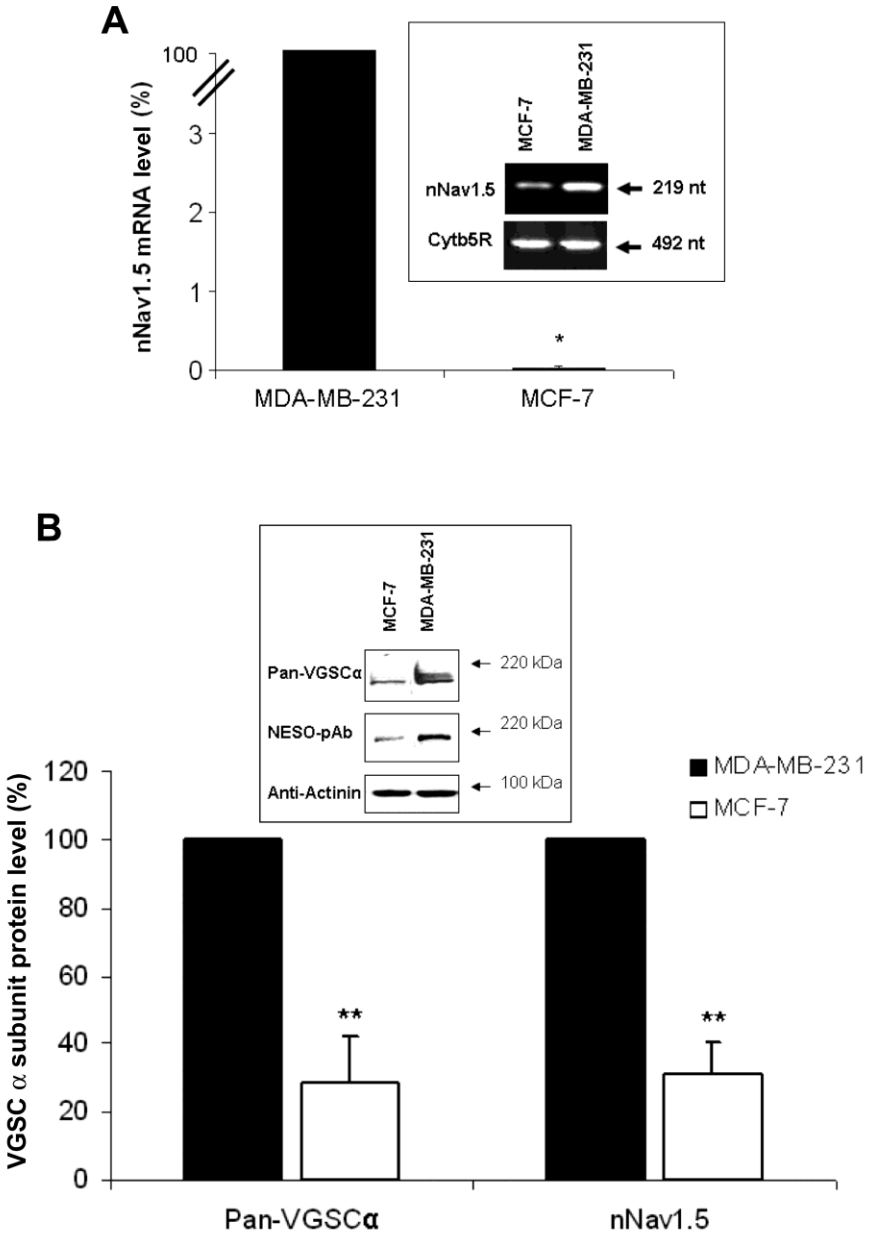

Figure 2.2. Expression of nNav1.5 mRNA and protein in MCF-7 and MDA-MB-231 cells. (A) Relative mRNA levels of nNav1.5, normalized to cytochrome b5-reductase (Cytb5R) by the $2^{-\Delta\Delta Ct}$ method, and expressed as a percentage of the level in MDA-MB-231 cells (fixed as 100%). Errors are propagated through the $2^{-\Delta\Delta Ct}$ analysis (n = 4). Inset, typical gel images of nNav1.5 and Cytb5R real-time PCR products, taken at the end of the PCR. (B) Relative nNav1.5 and total VGSC α subunit protein levels in MDA-MB-231 and MCF-7 cells. For each antigen, the expression level in MDA-MB-231 cells was fixed as 100%. The signal from NESO-pAb or pan-α subunit antibodies was normalized

to the actinin control. Inset, Western blot with 60 µg of total protein per lane from MCF-7 and MDA-MB-231 cells, using NESO-pAb, pan-VGSC α subunit antibody, and actinin antibody as a control for loading. The same membrane was stripped and re-blotted. Each histobar indicates mean + S.E.M. (n = 6). Significance: (*) $P < 0.05$, (**) $P < 0.01$; Mann–Whitney Rank Sum test.

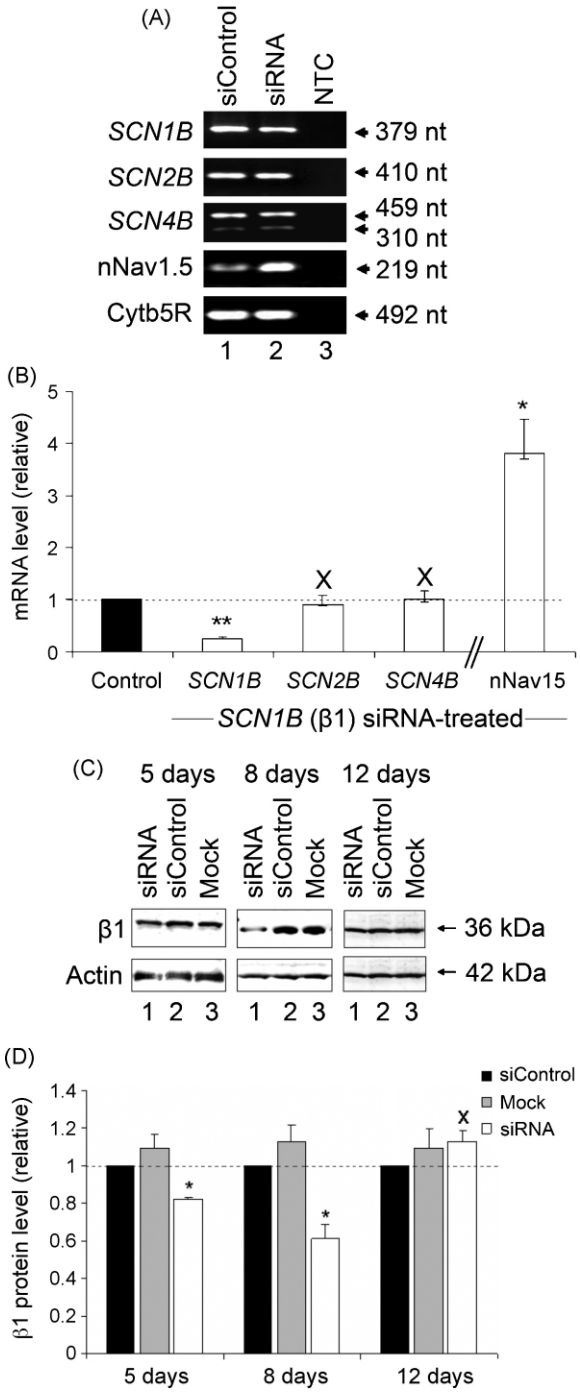

Figure 2.3. Effects of silencing *SCN1B* on VGSC expression in MCF-7 cells. (A) Typical gel images of PCR products, taken at the end of the PCR, for *SCN1B*, *SCN2B*, *SCN4B*, nNav1.5 and cytochrome-b5 reductase (Cytb5R) from MCF-7 cells 4 days after transfection with siControl (lane 1), or siRNA targeting *SCN1B* (lane 2). NTC (lane 3), no-template controls for PCR amplification. (B) Relative (%) mRNA levels of *SCN1B*, *SCN2B*, *SCN4B* and nNav1.5. Control (black bar – 100%): MCF-7 cells treated with siControl non-targeting RNAi; white bars: MCF-7 cells treated with siRNA targeting

SCN1B. β subunit and nNav1.5 mRNA levels were normalized to Cytb5R by the $2^{-\Delta\Delta Ct}$ method. Errors are propagated through the $2^{-\Delta\Delta Ct}$ analysis (n = 3). (C) Western blots with 70 µg of total protein per lane from cells 5, 8 and 12 days after treatment. For each case, lane 1, treatment with 'mock' control (no siRNA); lane 2, treatment with non-targeting siControl siRNA; and lane 3, treatment with siRNA targeting *SCN1B*. The β1ex antibody and an anti-actin antibody were used for β1 and for loading control, respectively (the same membrane was stripped and re-blotted). (D) Quantification of the data shown in (C). Relative total β1 protein levels were normalized to the actin control. Data are presented as mean and S.E.M. ($n \geq 4$). Significance: (×) $P > 0.05$; (*) $P < 0.05$; (**) $P < 0.01$; ANOVA with Newman Keuls (B), Student's paired t-test (D).

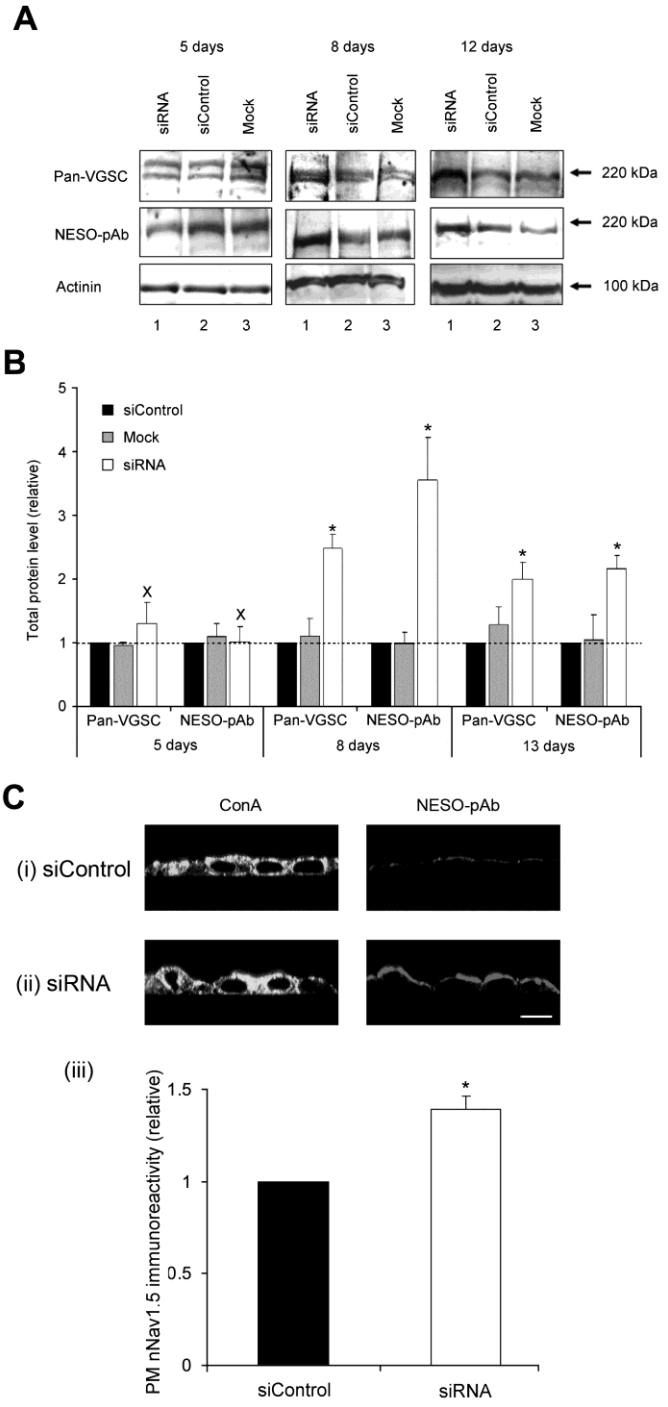

Figure 2.4. Effect of RNAi targeting *SCN1B* on the nNav1.5 protein level in MCF-7 cells. (A) Western blots with 80 µg of total protein per lane from cells 5, 8 and 12 days after treatment. For each case, lane 1, treatment with 'mock' control (no siRNA); lane 2, treatment with non-targeting siControl siRNA; and lane 3, treatment with siRNA targeting *SCN1B*. Antibodies used were pan-VGSC (for total VGSC), NESO-pAb for

nNav1.5 and an actinin antibody for loading control. The same membrane was stripped and re-blotted. (B) Quantification of the data shown in (A). Relative total VGSC α subunit and nNav1.5 protein levels normalized to the actinin control. (C) Typical confocal XZY images of non-permeabilised MCF-7 cells 8 days after transfection with (i) non-targeting siControl siRNA or (ii) siRNA targeting SCN1B double-immunolabelled with conA plasma membrane marker (left) and NESO-pAb (right); (iii), Relative peripheral nNav1.5 level, measured from the confocal XZY images. Data are presented as mean and SEM [(B) n = 4; (C) n = 3]. Significance: (*) $P < 0.05$; (B) ANOVA with Newman–Keuls; (C) Student's paired t-test.

Furthermore, 12 days post-transfection, when *SCN1B* mRNA had returned to normal, total VGSC α subunit and nNav1.5 protein levels remained elevated by 99% and 117%, respectively ($P < 0.05$, $n \geq 3$; **Figure 2.4A and B**). Confocal microscopy revealed a 39% increase in nNav1.5 immunoreactivity towards the cell periphery defined by conA labelling, 8 days after RNAi treatment ($P < 0.05$, n=3; **Figure 2.4C**).

In conclusion, the RNAi reduced *SCN1B* mRNA and β1 protein levels in MCF-7 cells, but increased nNav1.5 mRNA and protein levels.

Effects of β1 silencing on metastatic cell behaviors of MCF-7 cells

MCF-7 cells are significantly more adhesive to substrate than MDA-MB-231 cells (Palmer et al. 2008), consistent with the relatively higher level of *SCN1B* in the former (**Figure 2.1**) and the role of β1 as a CAM (Davis et al. 2004; Malhotra et al. 2000; Malhotra et al. 2002). Measurements of single-cell adhesion of *SCN1B* siRNA-treated MCF-7 cells revealed a significant reduction in adhesion of 25% ($P < 0.05$, n=3) and 35% ($P < 0.001$, n = 6) after 5 and 8 days, respectively (**Figure 2.5A**). However, by 12 days post-transfection, when levels of *SCN1B* mRNA had returned to normal, the cells' adhesive capability had recovered such that there was no significant difference (P=0.13, n=3; **Figure 2.5A**), consistent with the interpretation that β1 normally functions as a CAM in these cells. Pre-treatment of cells for 48 h with TTX (10 μM, continued during the assay) increased the adhesion of control cells by 16% ($P < 0.01$, n=4; **Figure 2.5B**, bars 1 vs. 3). Similarly, TTX increased the adhesion of *SCN1B* siRNA-treated cells by 28% ($P < 0.05$, n=4; **Figure 2.5B**, bars 2 vs. 4). In conclusion, downregulation of β1 reduced adhesion of MCF-7 cells, and this effect was partially reversed by TTX.

Eight days following transfection with siRNA targeting *SCN1B*, the number of migrating MCF-7 cells increased by 121% ($P < 0.05$, n=8; **Figure 2.5C**, bars 1 vs. 2), again suggesting that β1 normally functions as a CAM in these cells. Pre-treatment with TTX for 48 h (continued during the assay) reduced migration of siControl treated cells by

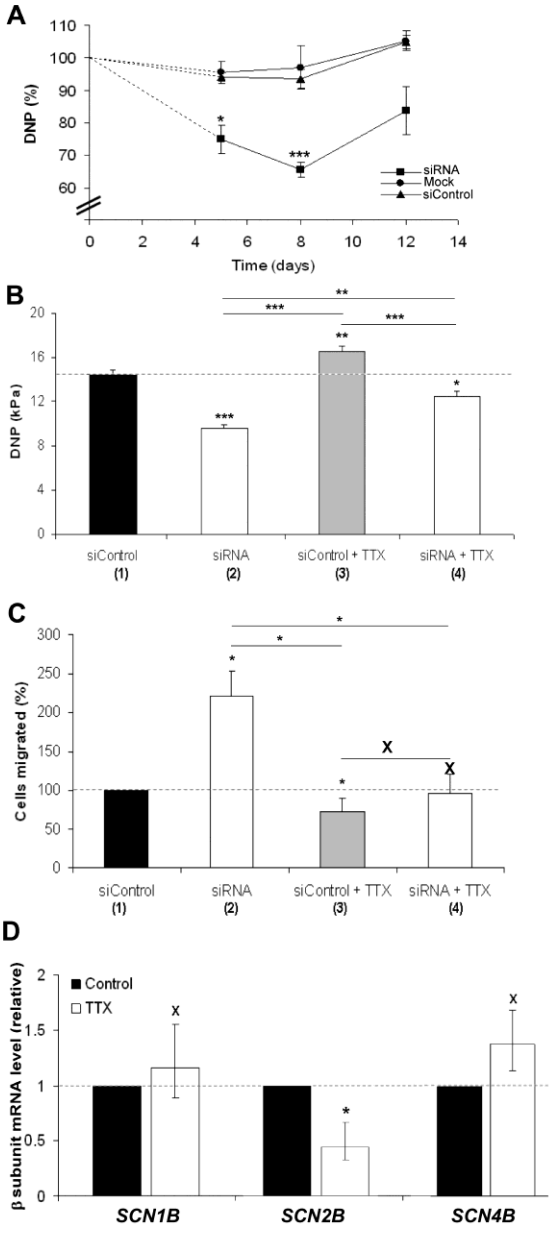

Figure 2.5. Effects of β1 downregulation on adhesion and migration of MCF-7 cells. (A) Time-course of reduction in relative detachment negative pressure (DNP) of MCF-7 cells following transfection with siRNA targeting *SCN1B*. Circles, 'mock' control (without siRNA); triangles, siControl non-targeting siRNA; squares, siRNA targeting *SCN1B*. (B) Absolute DNP values (in kPa) of MCF-7 cells 8 days after transfection with siControl non-targeting siRNA (bar 1) or siRNA targeting *SCN1B* (bar 2). In a separate experiment, cells were pre-treated with TTX (10 μM for 48 h), continued during the assay for cells transfected with siControl non-targeting siRNA (bar 3) or siRNA targeting β1 (bar 4). (C) Relative number of cells migrating through a transwell chamber over 12 h, 8 days after transfection with siControl non-targeting siRNA (bar 1) or siRNA targeting

SCN1B (bar 2). In a separate experiment, cells were pre-treated with TTX (10 µM for 48 h), continued during the assay for cells transfected with siControl non-targeting siRNA (bar 3) or siRNA targeting *SCN1B* (bar 4). (D) Relative mRNA levels of *SCN1B*, *SCN2B*, and *SCN4B* in MCF-7 cells after 48 h treatment with/without TTX (10 µM), normalized to cytochrome b5-reductase (Cytb5R) by the $2^{-\Delta\Delta Ct}$ method. Errors are propagated through the $2^{-\Delta\Delta Ct}$ analysis (n = 3). Data in (A)–(C) are presented as mean ± S.E.M. (n≥3). Significance: (×) $P > 0.05$; (*) $P < 0.05$, (**) $P < 0.01$, (***) $P < 0.001$; (A)–(C) ANOVA with Newman–Keuls; (D) Student's paired t-test.

27% ($P < 0.05$, n=8; **Figure 2.5C**, bars 1 vs. 3). Similarly, TTX also reduced migration of siRNA-treated cells by 43% ($P < 0.05$, n=8; **Figure 2.5C**, bars 2 vs. 4). Importantly, there was no difference in migration between TTX-pretreated siControl or siRNA-treated cells ($P > 0.05$, n=8; **Figure 2.5C**, bars 3 vs. 4). TTX had no effect on *SCN1B* or *SCN4B* mRNA levels ($P = 0.85$ and $P = 0.70$, respectively, n=3; **Figure 2.5D**), although *SCN2B* mRNA was reduced by 55% ($P < 0.05$, n=3; **Figure 2.5D**).

In conclusion, downregulation of β1 reduced adhesion but increased migration of MCF-7 cells. Both effects were sensitive to TTX, consistent with involvement of VGSC activity.

Effects of stably expressing β1 in MDA-MB-231 cells

β1 protein is detectable in MCF-7 cells, but not MDA-MB-231 cells (**Figure 2.1**). Further, MCF-7 cells exhibit enhanced adhesion and reduced migration compared to MDA-MB-231 cells, suggesting that β1 expression influences these properties (**Figure 2.5**). Thus, we next investigated whether overexpression of β1 in MDA-MB-231 cells might increase their adhesion and reduce cellular migration. β1-eGFP was transfected into MDA-MB-231 cells and stable expression was monitored by epifluorescence (**Figure 2.6A**). For all experiments, the effects of β1 were compared with control cells expressing eGFP alone. Western blot analysis confirmed expression of eGFP protein (30 kDa) in the control cell line, and revealed the expected increase of 37 kDa in molecular weight of eGFP in cells expressing the β1-eGFP fusion protein (**Figure 2.6B**).

Expression of β1 protein in MDA-MB-231 cells increased peak sodium current density by 34%, from−34.5±4.2 mV, to−46.4±4.1mV ($P < 0.05$, n = 20; **Figure 2.7A and B; Table 2.2**). In addition, β1 accelerated the kinetics of activation, reducing the time to reach peak current (T_p), from 0.73±0.03ms to 0.65±0.02ms ($P < 0.05$, n = 20; **Table 2.2**). In contrast, the whole-cell capacitance, persistent current, voltage-dependence of activation and steady-state inactivation, time constants of inactivation, recovery from

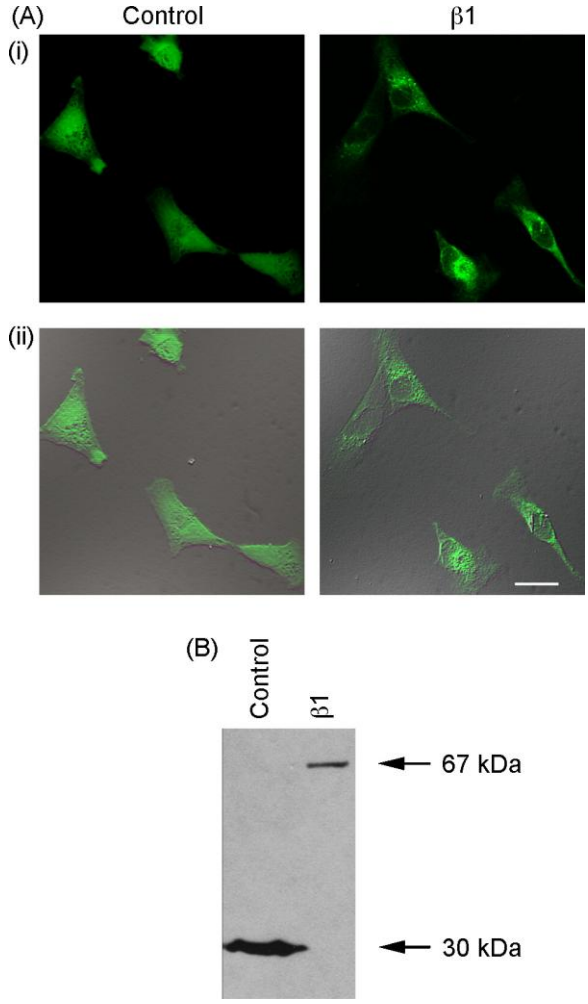

Figure 2.6. Stable expression of β1 in MDA-MB-231 cell lines. (A) Typical confocal XY (i) and merged bright-field images (ii) of MDA-MB-231 cells stably transfected with eGFP ('Control') and β1 with an eGFP C-terminal fusion ('β1'). (B) Western blot of protein from MDA-MB-231 cells stably transfected with eGFP ('Control'; total cell lysate) and β1 with an eGFP C-terminal fusion ('β1'; membrane preparation) using an anti-GFP antibody. eGFP, 30 kDa; β1-eGFP, 67 kDa.

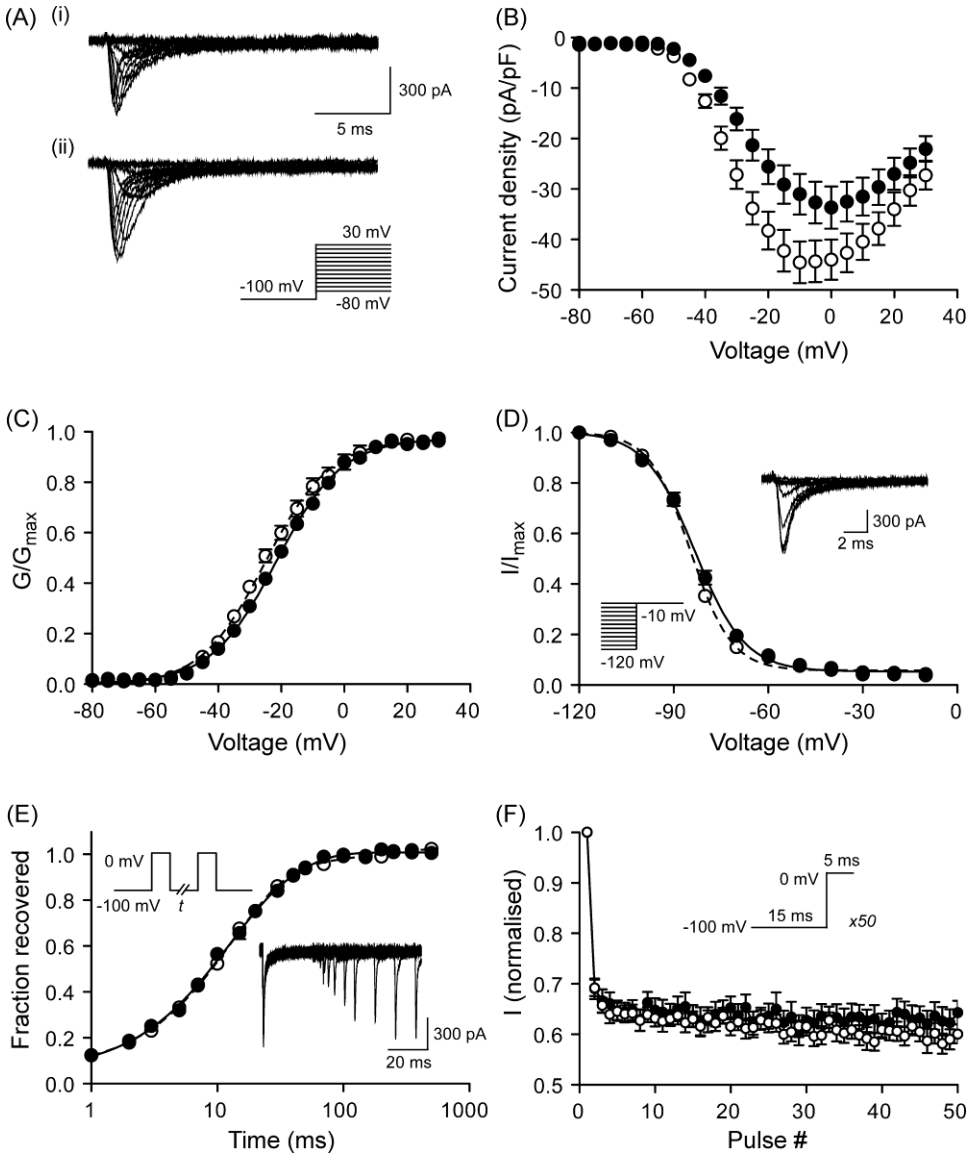

Figure 2.7. Effects of β1 over expression on VGSC activity in MDA-MB-231 cells. (A) Typical whole-cell sodium currents elicited by 60ms depolarizing voltage pulses between −80mV and +30mV applied from a holding potential of −100mV: (i) a control cell expressing eGFP; (ii) a cell expressing β1-eGFP. (B) Current -voltage relationship. Peak sodium current density was plotted as a function of voltage for control cells expressing eGFP (filled circles) and cells expressing β1-eGFP (open circles). (C) Activation. Normalized conductance (G/G_{max}), calculated from the current data, plotted as a function of voltage for control cells expressing eGFP (filled circles) and cells expressing β1-eGFP (open circles). (D) Steady-state inactivation. Normalized current (I/I_{max}), elicited by 60ms test pulses at −10mV following 1 s conditioning voltage pulses between −120 and −10 mV, applied from a holding potential of −100mV, plotted as a function of the prepulse voltage for control cells expressing eGFP (filled circles) and cells expressing β1-eGFP (open circles). Inset, typical recording from a control cell. (E)

Recovery from inactivation. The fraction recovered (I_t/I_0) was determined by a 25ms pulse to 0mV (I_0), followed by a recovery pulse to −100mV for 1–500ms, and a subsequent 25ms test pulse to 0mV (I_t), applied from a holding potential of −100 mV, and plotted as a function of the recovery interval for control cells expressing eGFP (filled circles) and cells expressing β1-eGFP (open circles). Inset, typical recording from a control cell. (F) Use-dependent rundown. Current (*I*), elicited by 50 Hz pulse trains to 0mV, applied from a holding potential of −100mV, normalised to the current evoked by the first pulse plotted as a function of the pulse number for control cells expressing eGFP (filled circles) and cells expressing β1-eGFP (open circles). Control (solid lines) and β1-eGFP (dashed lines) data are fitted with Boltzmann functions (C) and (D); and double exponential functions (E). Data are presented as mean ± S.E.M. (n = 20).

Parameter	Control	β1
C_m (pF)	22.4 ± 1.8	19.8 ± 0.9
I_p (pA/pF)	34.5 ± 4.2	46.4 ± 4.1*
I_{per} at 35 mV (pA/pF)	1.6 ± 0.4	2.2 ± 0.3
V_a (mV)	54.0 ± 0.8	54.5 ± 0.9
V_p (mV)	1.0 ± 1.2	4.5 ± 1.5
Activation, $V_{1/2}$ (mV)	21.3 ± 0.9	23.3 ± 2.6
Activation, k (mV)	10.2 ± 0.5	10.0 ± 0.7
Inactivation, $V_{1/2}$ (mV)	83.6 ± 0.8	84.8 ± 0.6
Inactivation, k (mV)	7.9 ± 0.8	6.5 ± 0.3
T_p at 0 mV (ms)	0.73 ± 0.03	0.65 ± 0.02*
τ_f at 0 mV (ms)	0.51 ± 0.03	0.50 ± 0.03
τ_s at 0 mV (ms)	3.7 ± 0.4	3.7 ± 0.4

Table 2.2. Effect of β1 overexpression on sodium current characteristics in MDA-MB-231 cells. Abbreviations: C_m, membrane capacitance; I_p, peak current density; I_{per}, persistent current density; V_a, activation voltage; V_p voltage at current peak; $V_{1/2}$, half (in)activation voltage; k, slope factor; T_p time to peak; $\tau_{f/s}$, fast/slow time constant of inactivation. Data are expressed as mean ± S.E.M. Significance: *P < 0.05 (n = 20).

inactivation, and use-dependent rundown at 50 Hz were unchanged (**Figure 2.7C–F; Table 2.2**). In summary, β1 increased peak VGSC current density and reduced T_p, without affecting other sodium current characteristics.

The distribution of β1-eGFP fusion protein in transfected cells was detected throughout the cell body and processes, with high expression observed in perinuclear clusters (**Figure 2.6A**). β1-eGFP transfected cells had significantly increased process length and this was observed in cells with both monopolar and biopolar morphologies ($P < 0.01$ for both, n = 40; **Figure 2.8A**). The thickness of processes on β1-eGFP-expressing monopolar cells was significantly reduced compared to cells expressing eGFP alone ($P < 0.01$, n = 40; **Figure 2.8B**). In contrast, the process thickness on bipolar cells was unchanged ($P = 0.46$, n = 40; **Figure 2.8B**). The cell body diameter of β1-eGFP-transfected cells was unchanged in both monopolar and bipolar cells compared to eGFP alone ($P = 0.26$ and 0.91, respectively, n = 40; **Figure 2.8C**). In conclusion, β1 overexpression appeared to increase process extension in MDA-MB-231 cells. While the mechanism of this effect is not clear for BCa cells, we have shown previously that β1–β1 cell adhesive interactions result in increased process length in neurons (Brackenbury et al. 2008a; Davis et al. 2004).

Cell–cell adhesion was measured using a cellular aggregation assay. β1-eGFP overexpression increased cell–cell adhesion of MDA-MB-231 cells compared to cells expressing eGFP alone following 30 min of shaking, and this effect persisted for 2 h ($P < 0.05$, n=3; **Figure 2.8D**). This result is consistent with the proposed role for β1 in *trans*-homophilic cell adhesion, described previously (Malhotra et al. 2000).

The lateral motility of MDA-MB-231 cells was measured using a wound-healing assay. β1-eGFP expression reduced the motility index by 21% from 0.68±0.01 to 0.53±0.01 compared to cells expressing eGFP alone ($P < 0.001$, n > 320; **Figure 2.8E**). In addition, the proliferation of cells expressing β1-eGFP was reduced by 19% compared to control ($P < 0.05$, n=3; **Figure 2.8F**). These findings suggest that β1 expression may

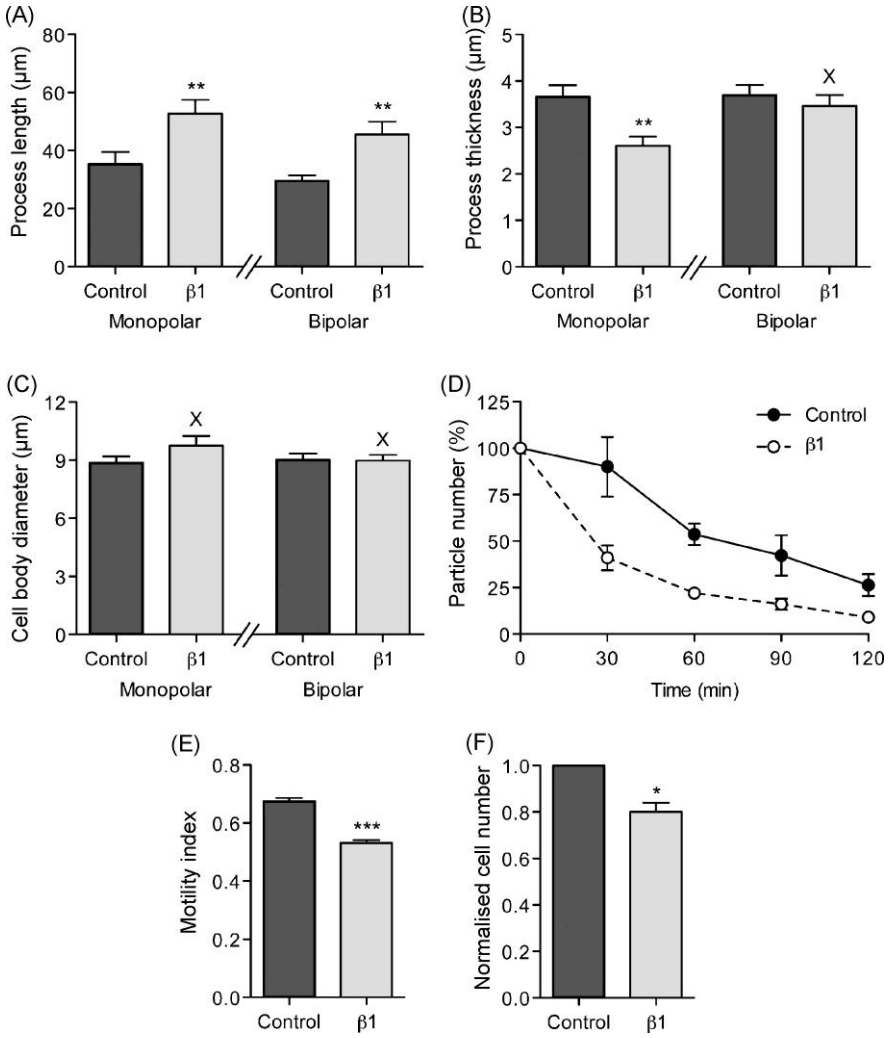

Figure 2.8. Effects of β1 over expression on morphology, adhesion, migration and proliferation of MDA-MB-231 cells. (A) Process length of MDA-MB-231 cells stably transfected with eGFP ('Control') and β1 with eGFP C-terminal fusion ('β1'). (B) Process thickness of MDA-MB-231 cells stably transfected with eGFP ('Control') and β1 with eGFP C-terminal fusion ('β1'). (C) Cell body diameter of MDA-MB-231 cells stably transfected with eGFP ('Control') and β1 with eGFP C-terminal fusion ('β1'). In (A)–(C), cells were defined as having monopolar or bipolar morphologies and analyzed separately (n = 40). (D) Cell–cell adhesion. Single MDA-MB-231 cells stably transfected with eGFP ('Control') and β1 with eGFP C-terminal fusion ('β1') were incubated with gentle agitation for 2 h. The number of particles was monitored every 30 min and expressed as a percentage of the starting value. As cells adhered to one-another and formed aggregates, the particle number decreased (n = 3 repeat experiments). (E) Motility index (MI) of MDA-MB-231 cells stably transfected with eGFP ('Control') and β1 with eGFP C-terminal fusion ('β1') in a wound-heal assay. Wound width was measured at 0 h (W_0) and 24 h (W_t). MI was calculated as $1-(W_t/W_0)$ (n = 135). (F) Proliferation of MDA-MB-231 cells stably transfected with eGFP ('Control') and β1 with eGFP C-terminal fusion ('β1'), normalized relative to control. Cells were grown for 24 h and counted using

the MTT assay (n = 3 repeat experiments). Data are presented as mean ± S.E.M. Significance: (×) $P > 0.05$; (*) $P < 0.05$, (**) $P < 0.01$, (***) $P < 0.001$; (A)–(C), (E) Student's t-test; (F) Student's paired t-test.

reduce wound closure by enhancing cell–cell or cell–matrix adhesion. However, the reduced proliferation of these cells may also have contributed to this effect.

Discussion

This study is the first investigation of the role of VGSC β subunits in BCa cells and provides new insights into the potential role of these multifunctional molecules in cancer metastasis. The main findings of this study are as follows: (i) Weakly metastatic MCF-7 cells expressed considerably higher levels of *SCN1B*, *SCN2B*, and *SCN4B* mRNAs than metastatic MDA-MB-231 cells. (ii) *SCN1B* was the most abundant VGSC β subunit mRNA expressed in both MCF-7 and MDA-MB-231 cell lines. (iii) β1 silencing experiments suggested that β1 normally increases adhesion and attenuates transwell migration of MCF-7 cells. (iv) β1 silencing positively regulated nNav1.5 mRNA and plasma membrane protein levels in MCF-7 cells. (v) TTX partially reversed the effects of β1-silencing on adhesion and migration in MCF-7 cells, suggesting that VGSC expression and resulting changes in electrical activity may influence metastasis. A potential caveat to this interpretation is the observation that TTX reduced *SCN2B* mRNA expression. β2 has also been shown to play roles in cell adhesion *in vitro*, including attenuating neurite outgrowth and thus may also contribute to the observed changes in adhesion and migration. (vi) Overexpression of β1 inMDA-MB-231 cells increased sodium current density, cell process length, and cell–cell adhesion, and reduced cellular lateral motility and proliferation. Taken together, these results suggest that β1 expression enhances adhesiveness and attenuates migration of BCa cells. The cell adhesive effects of β1 overexpression in MDA-MB-231 cells were observed concomitantly with β1-mediated upregulation of sodium current density, suggesting that the cell adhesive effects of β1 may be independent of changes in excitability and supporting the notion that β1 may have autonomous functional roles independent of the ion-conducting pore

(Brackenbury and Isom 2008; Brackenbury et al. 2007). The regulation of nNav1.5 expression/activity by β1 silencing in MCF-7 cells further suggests that β1 may control VGSC-dependent electrical signal transduction in BCa.

Expression of β subunits in human BCa cell lines

We used RNAi to downregulate *SCN1B* in MCF-7 cells. The siRNAs reduced *SCN1B* mRNA by 75% after 4 days, without affecting *SCN2B* or *SCN4B*. β1 protein levels were reduced to a lesser extent, by 40% after 8 days. The reduced and delayed protein reduction could be due to incomplete downregulation of the target gene (Jackson et al. 2003). Although dynamics of α and β subunit mRNA/protein expression in cancer cells are not known, it is possible that large intracellular protein stores or slow turnover may also contribute to the difference in time course (Brackenbury et al. 2007; Li et al. 2004). Also, increasing evidence suggests that VGSC mRNA and protein levels do not correlate (Lopez-Santiago et al. 2006; Brackenbury and Djamgoz 2006). Nonetheless, a small reduction in protein level can still result in significant functional changes. For example, 40–60% silencing of nNav1.5 was enough to critically disrupt cancer cell migration (Brackenbury et al. 2007).

SCN4B mRNA was present in both MCF-7 and MDA-MB-231 cells in a longer and a shorter form. A similar situation has been found in a human prostate cancer cell line (LNCaP) (Diss et al. 2008). In addition, we found that *SCN3B* mRNA was not detectable in either MCF-7 or MDA-MB-231 cells. Given that the *SCN3B* gene contains two p53 response elements and may be involved in p53-dependent apoptosis (Adachi et al. 2004), the absence of *SCN3B* in BCa cells may promote oncogenesis. This is an interesting possibility that would be worthy of further investigation.

Effect of VGSC activity on β subunit expression

TTX had no effect on *SCN1B* or *SCN4B* mRNA levels in MCF-7 cells. However, *SCN2B* mRNA expression was reduced by 55%. Thus, β subunit expression appears

dynamic and, in the case of *SCN2B*, may be controlled by β subunit activity. In agreement with this, electrical activity affects L1 CAM expression in mouse sensory neurons (Itoh et al. 1995). In addition, α subunit activity regulates *SCN9A* mRNA levels in metastatic PCa cells (Brackenbury and Djamgoz 2006). Interestingly, VGSC α subunit mRNA levels are regulated by a cleavage product of β2 protein in neurons (Kim et al. 2007). Thus, VGSC α and β2 transcription and translation may be tightly and reciprocally regulated.

Regulation of metastatic cell behaviors by β1

Downregulation of β1 in MCF-7 cells reduced single-cell adhesion, while overexpression of β1 in MDA-MB-231 cells increased cell–cell adhesion and process length. These results are consistent with the hypothesis that β1 functions as a CAM in BCa cells. β1 participates in homophilic adhesion *in vitro* and *in vivo*, resulting in cellular aggregation, ankyrin recruitment, neurite outgrowth, fasciculation, and migration (Davis et al. 2004; Malhotra et al. 2000; Malhotra et al. 2002; Brackenbury et al. 2008a). In addition, given that β1 can interact with other CAMs, as well as the extracellular matrix protein tenascin-R (Malhotra et al. 2004; Kazarinova-Noyes et al. 2001; Xiao et al. 1999), it is likely that β1 could play a significant adhesive role in BCa. For example, contactin, known to interact with β1, is involved in invasion and metastasis of lung adenocarcinoma cells (McEwen et al. 2004; Brackenbury et al. 2008a; Su et al. 2006). *SCN1B* siRNA increased the transwell migration of MCF-7 cells. We propose that downregulation of β1 reduced the cells' adhesion, and in doing so, rendered them more capable of migration. Consistent with this result, overexpression of β1 in MDA-MB-231 cells reduced their lateral motility. As with the MCF-7 cells, β1 may reduce MDA-MB-231 motility via enhanced adhesion. However, β1 also reduced the proliferation ofMDA-MB-231 cells, which could also contribute to the reduced MI. Thus, β1 may also regulate survival or proliferation of MDA-MB-231 cells by as yet, unidentified mechanism(s).

Interestingly, TTX partially reversed the effects of *SCN1B* silencing on the adhesion and migration of MCF-7 cells. Thus, the reduction in adhesion, and increase in migration in the absence of β1 is, at least in part, dependent on α subunit activity. TTX has been shown to inhibit a variety of behaviors associated with the metastatic cascade (Brackenbury et al. 2008b). It is possible that metastatic cell behaviors dependent on VGSC α subunit activity may also require concomitant downregulation of β1.

Regulation of nNav1.5 functional expression by β1

Overexpression of β1 in MDA-MB-231 cells increased sodium current density and reduced T_p. The effects of β1 on Nav1.5, the predominant α subunit expressed in MDA-MB-231 cells (Fraser et al. 2005), appear to be controversial, and dependent on the cell type studied. Consistent with the present findings, some studies report that β1 increases Nav1.5 current density without affecting gating (Nuss et al. 1995; Qu et al. 1995). However, other reports suggest that β1 does not affect Nav1.5 function (Makita et al. 1994; Yang et al. 1993), or shifts voltage-dependence of steady-state inactivation (An et al. 1998; Dhar Malhotra et al. 2001), or affects recovery from inactivation (Fahmi et al. 2001). In contrast to these previous studies, Nav1.5 is primarily expressed in MDA-MB-231 cells as the D1:S3 nNav1.5 splice variant (Brackenbury et al. 2007; Fraser et al. 2005). Given that nNav1.5 exhibits subtly different gating and kinetics compared to the 'adult' splice variant (Onkal et al. 2008), it is possible that β1 may modulate nNav1.5 in a different manner.

Downregulation of β1 in MCF-7 cells resulted in upregulation of nNav1.5 mRNA and protein. *Scn1b* null mice have increased *Scn5a* mRNA and Nav1.5 protein in cardiomyocytes (Lopez-Santiago et al. 2007). Therefore, β1 may be a novel regulator of *Scn5a*/Nav1.5 expression in multiple tissues. Emerging evidence suggests that β subunits may function as transcription factors. For example, β subunits can be cleaved by secretases, yielding functional intracellular domains (ICDs) (Wong et al. 2005; Kim et al.

2005). In the case of β2, the ICD increases *Scn1a* mRNA and Nav1.1 protein levels (Kim et al. 2007). The β1-ICD may normally participate in repression of *SCN5A* transcription, such that the *SCN1B* null mutation results in *SCN5A* overexpression. In an alternative scenario, β1 in MCF-7 cells may serve to negatively regulate nNav1.5 expression indirectly, via adhesion. Downregulation of β1 would reduce the cells' adhesion, in turn enhancing metastatic behaviors including migration, concomitant with nNav1.5 upregulation. nNav1.5 is primarily responsible for the VGSC-dependent enhancement of invasive behavior in metastatic MDA-MB-231 cells (Brackenbury et al. 2007). The mechanism(s) underlying VGSC α subunit upregulation in metastatic cancer cells is not understood, although serum and growth factors are important (Pan and Djamgoz 2008; Uysal-Onganer and Djamgoz 2007; Ding et al. 2008; Ding and Djamgoz 2004; Brackenbury and Djamgoz 2007). Given that β1 increased sodium current density in MDA-MB-231 cells, but reduced lateral motility, this would suggest that the steady-state contribution of basal α subunit activity to enhancing motility in MDA-MB-231 cells is maximal. However, it is not yet clear whether nNav1.5 expression is required for the acquisition of metastatic capability, or whether it is upregulated once the BCa cells have become highly metastatic.

Concluding remarks

This work further supports the proposed role of VGSCs in the cancer process and may have important clinical implications. Loss of β1 expression in line with acquisition of metastatic capability may provide a novel prognostic marker for BCa progression (Brackenbury and Isom 2008). Furthermore, β1 may provide a target for gene therapy, whereby its overexpression could enhance adhesion, resulting in reduction of metastatic cell behavior in BCa.

Acknowledgments

The work described in Chapter II was done in collaboration with a postdoctoral fellow, Dr. William J Brackenbury, in Dr. Lori Isom's laboratory. Dr. Athina-Myrto Chioni, a collaborator in the lab of Dr. Mustafa Djamgoz, was an essential contributor to Chapter II. Dr. William J. Brackenbury performed the electrophysiological experiments described in Chapter II. Dr. Athina-Myrto Chioni performed experiments to assess β subunit expression in MCF-7 and MDA-MB-231 cells and to test the effects of siRNA knockdown of β1 expression in MCF-7 cells.

Chapter III: Tyrosine phosphorylation of sodium channel β1 regulates neurite outgrowth

The work described within this chapter is entirely my own.

Abstract

The voltage-gated sodium channel (VGSC) β1 subunit is critical for neuronal migration, axon outgrowth, and axonal pathfinding in the cerebellum during postnatal development. *Scn1b* null mice, which lack β1 subunits, exhibit ataxia as a result of cerebellar dysfunction. β1-β1 *trans* homophilic adhesion initiates a signaling cascade in cerebellar granule neurons (CGNs) that results in neurite outgrowth. A number of critical cofactors for β1-mediated neurite outgrowth, including fyn kinase, contactin, γ-secretase activity, sodium current, and $Na_v1.6$ expression, have been previously identified. Here we used biochemical techniques and functional neurite outgrowth assays to demonstrate that tyrosine phosphorylation is a critical component of the β1-mediated neurite outgrowth signaling cascade.

Introduction

Voltage-gated sodium channels (VGSCs) are responsible for action potential initiation and propagation in excitable cells. Mammalian VGSCs are heterotrimers containing a single pore-forming α subunit, a non-covalently linked β subunit (β1 or β3), and a disulfide-linked β subunit (β2 or β4) (Isom 2001). VGSCs are unique with respect to other voltage- and ligand-gated ion channels in that they contain non-pore-forming β

subunits that not only modulate channel kinetics, but also function as cell adhesion molecules (CAMs) that direct channel insertion into the plasma membrane and channel interaction with other signaling proteins (Isom 2001). VGSC β subunits are type 1 membrane proteins and are immunoglobulin (Ig)-superfamily CAMs that participate in homophilic and heterophilic interactions (Malhotra et al. 2000; McEwen and Isom 2004). As multifunctional molecules which play important roles in electrical conduction and adhesion, VGSC β subunits provide an important link between these processes during brain development.

SCN1B, encoding the β1 and β1B subunits, plays important roles in brain development. Perturbation of *SCN1B* function or expression can result in pathologies in human patients that include epilepsy and ataxia (Patino et al. 2009). In mice, genetic deletion of *Scn1b* results in multiple forms of seizures, ataxia, growth retardation, neuronal pathfinding abnormalities, and early death (Chen et al. 2004; Brackenbury et al. 2013). Inherited homozygous mutations in *SCN1B* have been linked to Dravet Syndrome (DS), an intractable pediatric epileptic encephalopathy that involves comorbidities including mental retardation, developmental delay, and ataxia, in two independent pedigrees (Patino et al. 2009; Ogiwara et al. 2012). The severe epileptic and ataxic phenotype of *Scn1b* null mice demonstrates that these mice are a model of DS.

β1 and β1B polypeptides are expressed in neurons and glia during postnatal development through adulthood in mammals (**Table 1.2**). Defects in cerebellar, corticospinal tract, and hippocampal microorganization in *Scn1b* null mice suggest a role for these β subunits in neuronal migration, axon outgrowth, and axonal pathfinding (Davis et al. 2004; Brackenbury et al. 2008a; Brackenbury et al. 2013). β1 and β1B promote neurite outgrowth of isolated cerebellar granule neurons (CGNs) *in vitro* through *trans* homophilic cell-cell adhesion (Davis et al. 2004; Patino et al. 2011). Work focusing on the β1 subunit signaling cascade has shown that this mechanism requires contactin, fyn kinase, sodium current (particularly, the expression of *Scn8a*), and γ-secretase

activity (Davis et al. 2004; Brackenbury et al. 2008a; Brackenbury et al. 2010; Brackenbury and Isom 2011). We have suggested that β1 subunits expressed in cerebellar Bergmann glia adhere in *trans* to β1 subunits expressed in CGNs, resulting in a signal transduction mechanism to promote neurite extension (Davis et al. 2004). Similarly, we have proposed that secreted β1B subunits bind to transmembrane β1 subunits on adjacent cells or on the same cell, through paracrine or autocrine actions, respectively (Patino et al. 2011).

The work in this chapter focuses on the β1-mediated signaling cascade. β1 is known to be subject to post-translational modification, including tyrosine phosphorylation (Malhotra et al. 2002). An intracellular tyrosine residue in the β1 polypeptide (Y181) is phosphorylated *in vitro* and *in vivo* (Malhotra et al. 2002). A β1 mutant construct that mimics phosphorylation (β1Y181E) shows normal β1-mediated cell-cell adhesion *in vitro*, but disrupted β1-mediated ankyrin recruitment that is normally observed in response to adhesion (Malhotra et al. 2002). Similar to β1, β1Y181E increases cell surface VGSC expression in heterologous systems, but does not modulate sodium current *in vitro* (McEwen et al. 2004). Tyrosine phosphorylated β1 (pYβ1) has a distinct subcellular localization from β1 in highly polarized cardiac ventricular myocytes (Malhotra et al. 2004).

We postulated that tyrosine phosphorylation of β1 may act as a molecular switch for downstream signal transduction in response to β1-β1 *trans* homophilic adhesion leading to neurite outgrowth. To test this, we used CGNs as a model system to investigate the role of β1 tyrosine phosphorylation in β1-mediated neurite outgrowth. We demonstrate that expression of a construct mimicking the tyrosine phosphorylated form of β1 drives neurite outgrowth independent of *trans* homophilic cell-cell adhesion. In a heterologous system, cellular aggregation resulted in elevated levels of β1 tyrosine phosphorylation. A peptide representing the intracellular domain of β1, including residue Y181, was identified as a fyn kinase substrate. Taken together, our results suggest a

model where β1 tyrosine phosphorylation is a critical step in signal transduction from *trans* homophilic cell-cell adhesion to neurite outgrowth.

Methods

Antibodies and Reagents

For immunoprecipitation, primary antibodies used included mouse monoclonal anti-GFP obtained from Invitrogen (A-11120; 2 to 10 µg per IP) and mouse monoclonal anti-PY20 antibody obtained from Invitrogen (AHO0681; 10 µg per IP). For Western blot studies, primary antibodies included rabbit GFP antiserum obtained from Invitrogen (A6455; 1:500 dilution). For immunofluorescence studies, primary antibodies used included mouse monocolonal anti-Tuj1 obtained from Covance (MMS-435P; 1:1000 dilution) and rabbit anti-β1 (kind gift from Dr. Nobuyuki Nukina; 1:1000 dilution). Protease inhibitors were Complete EDTA free obtained from Roche (11873580001).

BacMam 2.0 virus

BacMam 2.0 baculovirus preparations encoding GFP, human WT β1, or human β1Y181E were obtained through a collaboration with Life Technologies. We performed the cloning steps for each viral construct. These plasmids were then sent to Life Technologies for viral preparation. To infect mammalian cell lines, virus was added at 10% v/v at cell plating. To infect CGNs, virus was added at 3% v/v at cell plating. Cells were subsequently incubated for 10 min at RT in the dark and then transferred to a cell culture incubator (37°C, 5% CO_2) for 24 or 48 h prior to experimentation for mammalian cells and CGNs, respectively.

Neuronal culture

To obtain CGNs, cerebella from *Scn1b* null mice (P14 to P16) were dissected and minced in HibernateA (BrainBits) containing B27 (Life Technologies). Tissue was trypsinized in dissociation buffer (6 mL of HibernateA/B27 and 5 mL of 0.25% trypsin) for 30 min at 37°C. Tissue was transferred to fresh HibernateA/B27 and triturated 9 times. After allowing tissue to settle for 2 min, the cell suspension was collected and pelleted at 150 x g for 5 min. Cells were resuspended in NeurobasalA (Life Technologies) containing B27 and plated onto poly-D lysine coated glass coverslips.

Neurite Outgrowth

Virally transduced *Scn1b* null CGNs were cultured for 48 hr and fixed for 20 min with 4% paraformaldehyde. Neurons were processed for immunofluorescence to label Tuj1-positive neurons and for β1 expression using a previously described protocol (Davis et al. 2004). Images were captured using Nikon Elements software and a Nikon A1R confocal microscope using a 20x objective and 2x digital zoom (40x final) in the Department of Pharmacology at the University of Michigan. At least 10 neurites were measured per experiment and at least three independent experiments were performed. Statistical significance was determined using the Mann-Whitney rank sum test.

Cell Culture and Protein Sample Preparation

MDA-MB-231 β1GFP cells were described previously in Chapter 2 (Chioni et al. 2009). Cells were cultured in Dulbecco's modified Eagle's medium supplemented with 5% fetal bovine serum (FBS) and 4 mM L-glutamine, as described previously (Fraser et al. 2005). The media was also supplemented with 100 µg/ml hygromycin to maintain β1GFP expression. Cultured cells were washed with cold PBS and detached from the culture dishes using a cell scraper in ice-cold homogenization buffer (HB: 50 mM Tris, 10 mM EGTA, pH 8) containing protease inhibitors and 1 mM sodium orthovanadate. Cells were lysed by homogenization in a cold room with 25 strokes at 5,000 rpm. Nuclei

were pelleted by a 3500 rpm centrifugation in a microfuge for 10 min. The supernatant was collected and membranes were pelleted at 16,000 x g in a microfuge for 20 min. Membrane proteins were solubilized for 30 min in dilution buffer (DB: 50 mM Tris/HCl pH 8.0, 180 mM NaCl, 1% Triton X-100, 10 mM EGTA containing protease inhibitors and 1 mM sodium orthovanadate). After solubilization, a 20 min centrifugation at 16,000 x g in a microfuge was performed to remove insoluble material. For both membrane proteins and total cell lysates, protein yield was determined using a BCA assay (Pierce). All centrifugation steps were performed at 4°C.

Immunoprecipitation

Protein G-Sepharose beads (Sigma) were washed with PBS and resuspended in 500 µl of dilution buffer at 4°C. The beads were then incubated overnight at 4°C with 10 µg of immunoprecipitating (IP) antibody (anti-PY20). Protein samples were obtained from membrane preparations as described above. BCA assays (Pierce) were performed according to the manufacturer's recommendation for each membrane preparation prior to IP to ensure equal amounts of protein were used for each assay. For each IP reaction, 500 µl of 0.8 to 1.0 µg/µl of protein solubilized in dilution buffer were incubated with antibody-conjugated beads by gentle end-over-end rotation for 4 to 6 hr at 4°C. The beads were then washed twice with washing buffer (50 mM Tris pH 7.5, 150 mM NaCl, 0.1% Triton X-100, 0.02% SDS, 10 mM EGTA pH 8 containing protease inhibitors). Proteins were eluted from the beads by addition of Laemmeli buffer and 10 min incubation at 80°C.

Immunoblotting

Samples were separated by SDS-PAGE on 12 or 15% polyacrylamide gels and transferred to nitrocellulose for Western blot analysis. Western blotting was performed using the SnapId system (Millipore). Immunoblots were probed with antibody as indicated, detected with Westfemto Chemiluminescent reagent (Pierce), and imaged

using a LI-COR Odessey® Fc imaging system. All results presented are representative of three independent repeats.

Fyn kinase assay

A fyn kinase assay was performed according to the manufacturer's recommendations (Fyn kinase assay kit, Promega). Reactions were performed in triplicate and each reaction contained 200 ng of active GST-tagged Fyn kinase, 50 µM Ultrapure ATP, 0.2 mg/mL peptide substrate, 50 µM DTT diluted in a standard kinase reaction buffer (contents of 5X buffer: 40 mM Tris pH 7.5, 20 mM MgCl2, 0.1 mg/mL BSA). β1 peptides corresponded to the intracellular domain of β1 surrounding residue Y181 (amino acids 175 to 185; β1 peptide, QENASEYLAITC; pYβ1 peptide, QENASE[pY]LAITC) and were generated by Pierce. The pYβ1 peptide was synthesized using a pre-phosphorylated tyrosine amino acid. The Poly E_4Y_1 peptide, used as a positive control, is a well-characterized substrate of fyn kinase. Kinase reactions lacking substrate were used to normalize the kinase activity in substrate containing reactions. Three independent experiments were performed. Statistical significance was determined using the Student's t-test with significance defined as $p < 0.05$.

PolyHEMA aggregate cultures

Cell culture plates were coated with polyHEMA using standard coating methods (Vinci et al. 2012) to prevent cell attachment and thus promote cellular aggregation. Cells were then harvested within 16 to 20 hr of plating.

Results

Characterization of BacMam 2.0 constructs

To assess the functional consequence of tyrosine 181 phosphomimetic β1 expression in neurons, we chose to use BacMam 2.0 viruses because they robustly transduce mammalian cells, including neurons, and result in little to no cytotoxicity within a wide range of transduction conditions. Further, unlike adenovirus or herpes viral vectors (Sato et al. 2009; Storey et al. 2002), they have little to no effect on sodium current (personal communication, Dr. James Offord). Preparations of virus were obtained that encoded wildtype (WT) β1 or β1Y181E or GFP. Expression of β1 WT or β1Y181E was initially characterized in four different mammalian cell lines, including Chinese hamster lung (not shown), Chinese hamster ovary (not shown), B35 (not shown), and MDA-MB-231 (**Figure 3.1**). Induced expression of β1 WT and β1Y181E in MDA-MB-231 cells are shown in **Figure 3.1C** and **Figure 3.1E**, respectively. Transduction efficiency increased with increasing virus concentration and it was possible to achieve 100% transduction efficiency (data not shown). While we observed generally even expression of β1 WT throughout the cell (**Figure 3.1C**), β1Y181E appeared to cluster at the leading edge of the filopodia (**Figure 3.1 E**, arrow). These results suggest that, similar to our previous data in cardiac myocytes (Malhotra et al. 2004), β1 WT and β1Y181E are differentially localized in breast cancer cells.

β1Y181E induces neurite outgrowth independent of cell-cell adhesion

We demonstrated previously that β1 subunits promote neurite extension in CGNs via *trans* homophilic cell adhesion *in vitro* between β1 subunits expressed on the substrate monolayer and β1 subunits expressed by the neuron (Davis et al. 2004; Brackenbury et al. 2008a). We have proposed that similar events occur in the cerebellum *in vivo* between β1 subunits expressed by Bergmann glia and β1 subunits expressed in

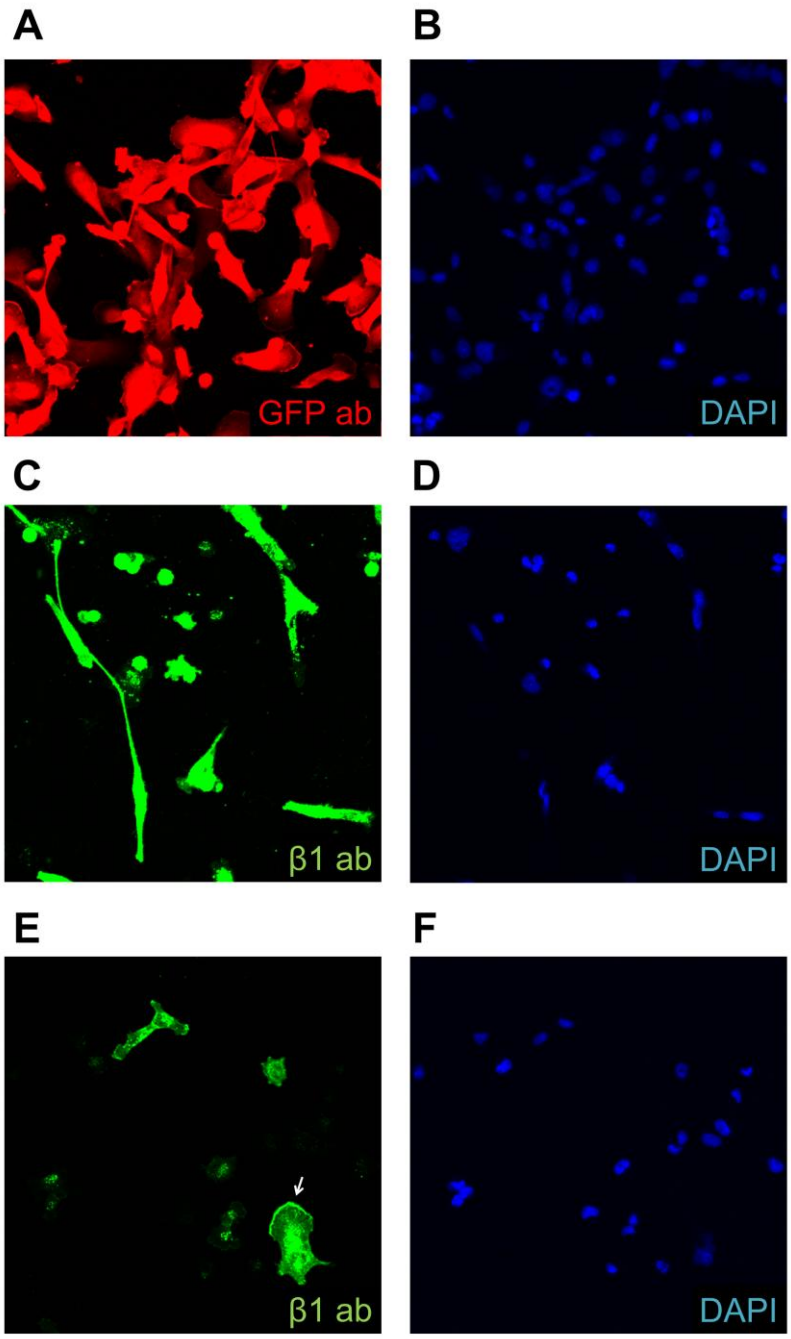

Figure 3.1. Characterization of BacMam virus. MDA-MB-231 cells were infected with 10% v/v of BacMam virus and fixed 24 hr post transduction. Cells infected with GFP BacMam virus were immunolabeled with a GFP antibody (A). Cells infected with β1 WT virus were immunolabeled with anti-β1intra antibody (C). Cells infected with β1Y181E virus were immunolabeled with anti-β1intra antibody. Preliminary results suggest that β1 expression is distributed evenly throughout the cell while β1Y181E is found at the leading edge (arrow). (E). Corresponding DAPI staining for A, C, and E are provided in B, D, and F, respectively.

CGNs (Brackenbury et al. 2008a; Brackenbury et al. 2013). Further, we have proposed that β1-β1 adhesion leads to β1 tyrosine phosphorylation and that this event serves as a key event to initiate a signaling cascade that ultimately promotes neurite extension. Here, to investigate whether tyrosine phosphorylation of β1 residue Y181 is sufficient to induce neurite outgrowth in the absence of *trans* homophilic cell-cell adhesion, we utilized BacMam2.0 baculovirus encoding β1WT or β1Y181E to transduce cultures of *Scn1b* null CGNs. We found that expression of β1Y181E resulted in increased neurite length in *Scn1b* null CGNs compared to β1 WT. Importantly, this occurred in *Scn1b* null CGNs that were plated without a substrate monolayer as a source of β1 subunits for cell-cell adhesion (**Figure 3.2**). Thus, phosphomimetic β1Y181E induces neurite extension to a greater extent than β1 WT in the absence of β1-β1 *trans* homophilic adhesion.

Aggregate culture enhances tyrosine phosphorylation of β1

To analyze levels of tyrosine phosphorylated β1 subunits biochemically, we utilized the human metastatic breast cancer cell line (MDA-MB-231) stably transfected with β1GFP (MDA-MB-231-β1GFP cells) that was described in Chapter II. In the construct used to generate this cell line, GFP was fused to the β1 C-terminus, resulting in an intracellular epitope tag. MDA-MB-231-β1GFP cells were grown as monolayers or in aggregate culture on polyHEMA-coated tissue culture plates. Cells grown on polyHEMA-coated tissue culture plates did not attach and grew in suspension, readily forming large aggregates visible by the naked eye. Membrane preparations were generated and tyrosine phosphorylated proteins were subsequently immunoprecipitated from Triton X-100 solubilized fractions using anti-PY20 antibody. The immunoprecipitated proteins were separated by SDS-PAGE, transferred to nitrocellulose, and immunoblotted with anti-GFP antibody to detect GFP-tagged pY-β1 subunits. Immunoreactive bands corresponding to the predicted MW of full-length β1 + GFP (64 kDa) were detected in the anti-PY20-immunoprecipitated fractions (**Figure 3.3A**). When

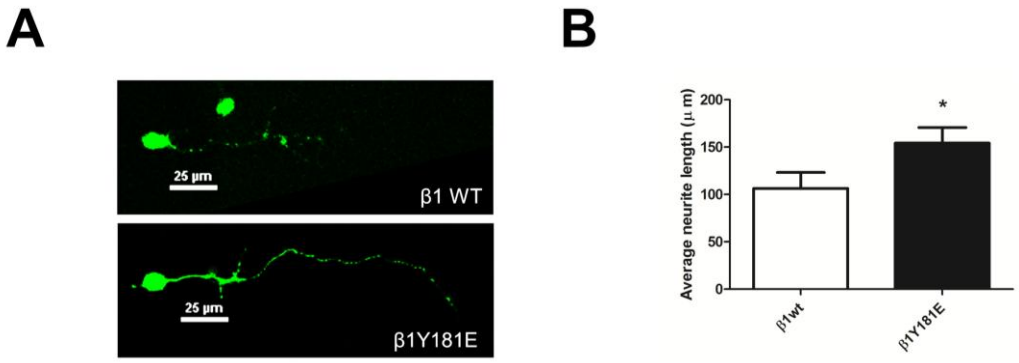

Figure 3.2. β1Y181E increases neurite length in cultured CGNs in the absence of *trans* homophilic adhesion. Acutely isolated *Scn1b* null CGNs were transduced with 3 % (v/v) of β1 WT BacMam 2.0 or β1Y181E BacMam 2.0 directly after plating onto poly-D-lysine coated coverslips. After 48 hr of culture, cells were fixed and labeled with antibodies to detect neuronal marker Tuj1 (mouse; Covance, not shown) or β1 (rabbit; kind gift of Dr. Nobuyuki Nukina). **A.** Representative images of transduced *Scn1b* null CGNs expressing β1 WT (top) or β1Y181E (bottom) labeled with anti-β1 antibody. **B.** Mean length of longest neurite measured from CGNs expressing β1 WT or β1Y181E. A minimum of 30 neurites were measured for each condition (N = 3 independent experiments). * denotes $p < 0.05$. Statistical significance was determined using the Mann-Whitney rank sum test.

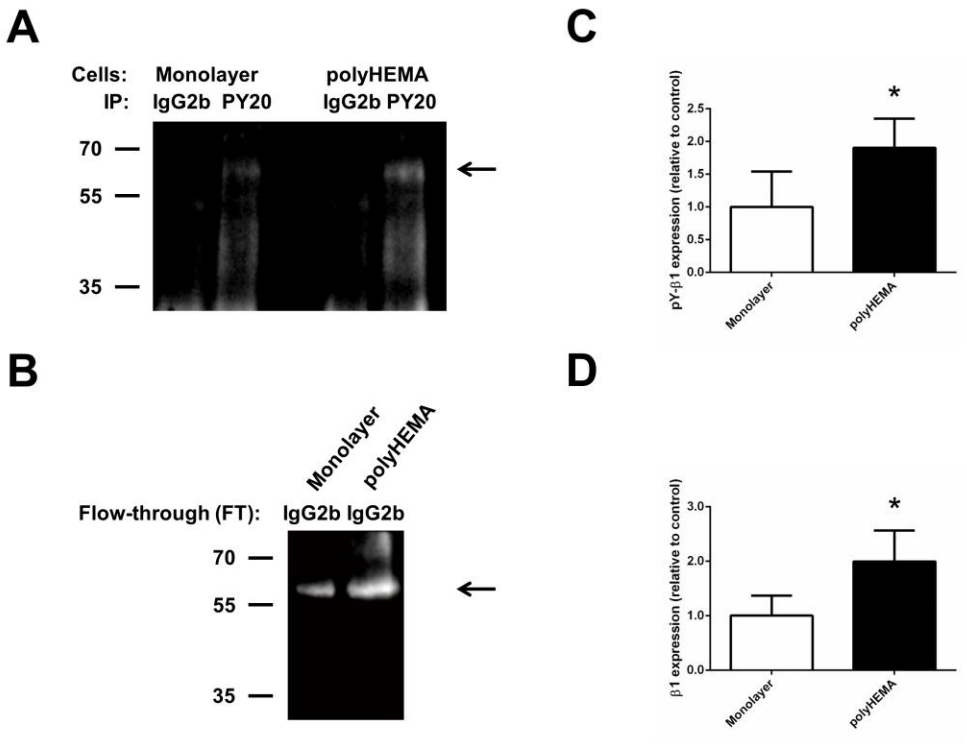

Figure 3.3. Cellular aggregation increases tyrosine phosphorylation of β1. Tyrosine phosphorylated proteins were immunoprecipitated (using anti-PY20 antibody) from equal aliquots of Triton X-100 solubilized membrane preparations collected from confluent monolayers or polyHEMA-plated aggregates of MDA-MB-231 cells stably transfected with β1GFP. As a negative control, non-immune mouse IgG2b was used as the immunoprecipitating antibody. Samples were separated by SDS-PAGE, transferred to nitrocellulose, and immunoblotted with anti-GFP antibody. (A) Tyrosine phosphorylated β1 subunits (pY-β1GFP, arrow) are detected in cells grown as confluent monolayers and in polyHEMA aggregates. Levels of pY-β1GFP are 1.9-fold higher in cells grown as polyHEMA aggregates, suggesting that cell-cell aggregation promotes β1 tyrosine phosphorylation. (B) Representative examples of β1GFP protein in control IgG2b flow-through samples following the immunoprecipation step, indicating β1 expression increases 2-fold as a result of aggregate culture in cells grown on polyHEMA-coated dishes. Quantification of data in panels A and B are provided in panels C and D, respectively. * denotes $P < 0.05$. Statistical significance was determined with Student's t-test. This figure is representative of three independent experimental repeats.

cells were grown on polyHEMA-coated dishes to prevent attachment and promote aggregation, the extent of tyrosine phosphorylation increased 1.9-fold, suggesting that β1 tyrosine phosphorylation occurs as a result of β1-β1 adhesion (**Figure 3.3A and 3.3C**). Total expression of β1 was similarly increased (2-fold) in cells grown on polyHEMA-coated dishes (**Figure 3.3B and 3.3D**).

Identification of the β1 intracellular domain as a potential substrate of fyn kinase

In silico analysis suggested that β1 residue Y181 might be a target for fyn kinase (data not shown), in agreement with our previous work (Malhotra et al. 2002). Here, we used a commercially available cell-free kinase assay to test whether a peptide representing the β1 intracellular domain and including residue Y181, could be phosphorylated by fyn (**Figure 3.4**). Robust tyrosine phosphorylation was detected when either the β1 or poly E_4Y_1 peptides were incubated in the presence of fyn kinase (**Figure 3.4**). Importantly, we did not observe tyrosine phosphorylation when the pYβ1 peptide (chemically tyrosine phosphorylated at Y181) was incubated in the presence of fyn. The signal displayed in the presence of fyn kinase but absence of substrate is likely due to a low level of autophosphorylation. We observed a significant increase in signal between reactions lacking substrate (containing fyn kinase; lacking substrate) compared to reactions lacking kinase (lacking fyn kinase; containing poly E_4Y_1 substrate) (data not shown).

Discussion

To investigate the functional relevance of tyrosine phosphorylation of β1, we used BacMam 2.0 virus to express β1 WT or the phosphomimetic β1Y181E construct in neuronal cultures that were plated on poly-D-lysine. We observed that expression of β1Y181E resulted in increased neurite length in *Scn1b* null CGNs compared to β1 WT.

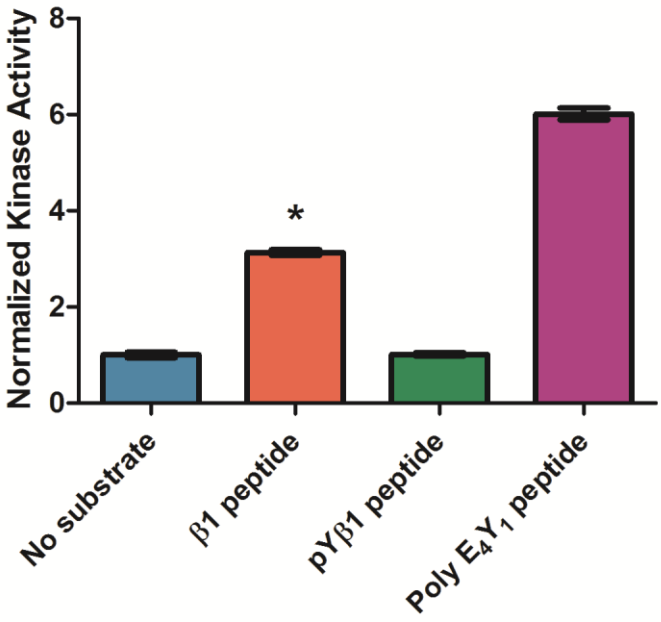

Figure 3.4. A peptide representing the intracellular domain of β1, containing residue Y181, is a substrate for fyn kinase. Fyn kinase assay was performed according to manufacturer's recommendations (Promega ADP-Glo kit). Each reaction contained 200 ng of active GST-tagged fyn kinase, 50 µM Ultrapure ATP, 0.2 mg/mL peptide substrate, 50 µM DTT diluted in a standard kinase reaction buffer (contents of 5X buffer: 40 mM Tris pH 7.5, 20 mM $MgCl_2$, 0.1 mg/mL BSA). β1 peptides corresponded to the intracellular domain of β1 surrounding Y181 (amino acids 175 to 185; β1 peptide, QENASEYLAITC; pYβ1 peptide, QENASE[pY]LAITC). The Poly E4Y1 peptide, used as a positive control and provided in the kit, is a well-characterized substrate for fyn kinase. Kinase reactions lacking substrate were used to normalize the kinase activity in substrate containing reactions. N = 3. * denotes $P < 0.05$. Statistical significance was determined with Student's t-test.

Importantly, β1Y181E-induced neurite extension occurred in the absence of a substrate that expressed β1. These results suggest that, under normal conditions, tyrosine phosphorylation of β1 in response to β1-β1 *trans* homophilic adhesion is a critical first step in the signal transduction cascade leading to β1-mediated neurite outgrowth.

We next postulated that β1-β1 *trans* homophilic adhesion might regulate the phosphorylation state of β1. To test this, we utilized MDA-MB-231-GFP cells. The parental MDA-MB-231 cell line was originally selected because it shares some qualities of electrically excitable cells including expression of $nNa_v1.5$, a neonatal splice variant of the major cardiac sodium channel (Brackenbury et al. 2007). In addition, MDA-MB-231 cells have low endogenous cell adhesive activity and we demonstrated that cellular aggregation is enhanced in this line by stable expression of β1 (Chioni et al. 2009). We utilized an immunoprecipitation method to ask whether β1 is phosphorylated in MDA-MB-231 β1GFP monolayers and in aggregates formed subsequent to plating of cells on polyHEMA-coated dishes. We detected pY-β1-GFP in membrane preparations from cells cultured under both conditions. Interestingly, we detected enhanced levels of phosphorylated β1 subunits in cells grown in aggregate culture, in agreement with the idea that β1-β1 *trans* homophilic adhesion regulates the extent of tyrosine phosphorylation of β1. The level of β1 expression similarly increased in aggregate culture, suggesting that stabilization of β1 at the cell membrane by increased points of homophilic adhesive contact results in increased total β1 expression in the cell. Taken together, these data suggest a possible molecular mechanism for the regulation of tyrosine phosphorylation of β1. The stabilization of cell surface β1 due to homophilic β1-β1 adhesion may mediate tyrosine phosphorylation of β1 by membrane-associated kinases such as fyn.

Previously, we identified fyn, a src family kinase, as a critical component of the β1-mediated neurite outgrowth signaling cascade *in vivo* (Brackenbury et al. 2008a). We hypothesized that the intracellular domain of β1, specifically residue Y181, was a

substrate for fyn-mediated phosphorylation. To test this hypothesis, we used a commercially available cell-free kinase assay. We found that a peptide representing the β1 intracellular domain is a fyn substrate *in vitro,* suggesting that fyn-mediated phosphorylation of β1 may be an important step within the β1-mediated neurite outgrowth signaling cascade *in vivo*. We propose that this event may occur directly downstream of β1-β1*trans* homophilic adhesion.

The results presented here augment the early steps of our β1-mediated neurite outgrowth model (Davis et al. 2004; Brackenbury et al. 2008a). We propose that the initiating event for this signal transduction cascade is extracellular β1-β1 *trans* homophilic adhesion or binding of soluble β1B to β1, at the growth cone plasma membrane (Davis et al. 2004; Patino et al. 2011). This initiating event is then proposed to result in two consecutive events: (1) the recruitment of ankyrin to the point of cell-cell contact (Malhotra et al. 2000) and (2) tyrosine phosphorylation of β1Y181 via fyn kinase. We showed previously that β1Y181 expression in place of β1 disrupts the interaction between β1 and ankyrin (Malhotra et al. 2002). These dueling events suggest a signaling mechanism in which ankyrin is recruited to points of contact in response to β1-β1 *trans* adhesion or β1B binding to β1 and subsequently released by β1 tyrosine phosphorylation, resulting in a dynamic cycle. We envision that β1 subunits located at the neuronal growth cone initiate points of contact with β1 subunits expressed on the plasma membranes of adjacent glia or neurons or with soluble β1B in the extracellular matrix. Following this interaction, we propose that ankyrin initially colocalizes transiently with β1 but then this association is disrupted when β1 becomes phosphorylated. This scheme would allow ankyrin to continually be recruited to new points of cell-cell contact or areas of β1B secretion as the growth cone moves and extends along a cellular substrate or through the extracellular matrix. An additional possibility is that pY-β1 can act as an activator of fyn and provide positive feedback, given that binding of a src family kinase SH2 domain to

tyrosine phosphorylated proteins can result in increased src family kinase activity (Harrison 2003).

In conclusion, we propose that tyrosine phosphorylation of β1 by fyn kinase following *trans* homophilic adhesion is a key regulatory step in neurite outgrowth. These data, taken together with the identification of other key factors regulating β1-mediated neurite outgrowth, including contactin, γ-secretase activity, Nav1.6 expression, and sodium channel activity (Brackenbury et al. 2010; Brackenbury and Isom 2011), demonstrate that a complex signaling cascade ties together disparate cell processes, including ion flux, kinase signaling, and cell-cell adhesion. Understanding how β1 acts as a channel modulator and as a CAM to modulate cell migration, axon outgrowth and pathfinding, and fasciculation is critical to understanding its contribution to brain development and *SCN1B*-linked epilepsy.

Acknowledgments

Life Technologies™ collaborated on the generation of BacMam 2.0 viral constructs.

Chapter IV: Identification of the cysteine residue responsible for disulfide linkage of sodium channel α and β2 subunits

Chapter IV was published in the Journal of Biological Chemistry (Chen et al. 2012). My primary contributions to this work include: (1) generation of all *in silico* datasets, (2) significant intellectual contributions to the experiment design and data interpretation, in particular overcoming a critical technical problem which hindered the progress of the study, and (3) generation of an immunocytochemistry dataset to assess protein expression and subcellular localization.

Abstract

Voltage-gated sodium channels in brain are composed of a single pore-forming α subunit, one non-covalently linked β subunit (β1 or β3), and one disulfide-linked β subunit (β2 or β4). The final step in sodium channel biosynthesis in central neurons is concomitant α-β2 disulfide linkage and insertion into the plasma membrane. Consistent with this, *Scn2b* (encoding β2) null mice have reduced sodium channel cell surface expression in neurons and action potential conduction is compromised. Here we generated a series of mutant β2 cDNA constructs to investigate the cysteine (C) residue(s) responsible for α-β2 subunit covalent linkage. We demonstrate that a single cysteine-to-alanine (A) substitution at extracellular residue C26, located within the immunoglobulin (Ig) domain, abolishes the covalent linkage between α and β2 subunits. Loss of α-β2 covalent complex formation disrupts the targeting of β2 to nodes of Ranvier in a myelinating co-culture system and to the axon initial segment (AIS) in primary

hippocampal neurons, suggesting that linkage with α is required for normal β2 subcellular localization *in vivo*. Wildtype (WT) β2 subunits are resistant to live cell Triton X-100 detergent extraction from the hippocampal AIS, while mutant β2 subunits, that cannot form disulfide bonds with α, are removed by detergent. Taken together, our results demonstrate that α-β2 covalent association via a single, extracellular disulfide bond, is required for β2 targeting to specialized neuronal subcellular domains and for β2 association with the neuronal cytoskeleton within those domains.

Introduction

Voltage-gated sodium channels are heterotrimeric complexes containing a single pore-forming α subunit, a non-covalently linked β1 or β3 subunit, and a covalently linked β2 or β4 subunit (Catterall 2012). While sodium channel β subunits are non-pore-forming, they play essential roles in channel targeting, regulation of channel gating and voltage-dependence, and channel-independent roles in cell adhesion (Brackenbury and Isom 2011). Sodium channel β2 subunits (encoded by *Scn2b*) are disulfide-linked to the ion-conducting α subunit and are expressed in brain, peripheral nerve, and heart (Isom et al. 1995a; Dhar Malhotra et al. 2001; Lopez-Santiago et al. 2006). Similar to the other sodium channel β subunit family members, β2 is a type 1 transmembrane protein containing an extracellular N-terminal V-set Ig domain, a single transmembrane segment, and an intracellular C-terminal domain. In *Xenopus* oocytes, β2 modulates $Na_v1.2$ channel gating and increases functional channel expression through promotion of intracellular vesicle fusion with the plasma membrane as measured by changes in cell capacitance (Isom et al. 1995a). In transfected fibroblasts, β2 increases $Na_v1.2$ cell surface expression only if β1 is also expressed (Kazarinova-Noyes et al. 2001). β2 functions as a *trans* homophilic cell adhesion molecule *in vitro*, resulting in recruitment of ankyrin to points of cell-cell contact (Malhotra et al. 2000). The extracellular β2 Ig

domain associates with the extracellular domain of β1 in an *in vitro* cell adhesion assay, suggesting that these two subunits may associate via cell adhesive interactions *in vivo* (McEwen and Isom 2004). Similar to the other sodium channel β subunits, β2 can be detected in detergent-resistant membrane preparations from primary neurons and is sequentially cleaved by β and γ secretases (Wong et al. 2005). The cleaved intracellular domain of β2 is postulated to translocate to the nucleus to modulate *Scn1a* α subunit gene transcription (Kim et al. 2007), however, the regulation of this process is not understood. A series of studies has demonstrated that β2 plays important roles *in vivo* in both neurons and cardiac myocytes. *Scn2b* null mice have significantly reduced (~50-60%) tetrodotoxin-sensitive (TTX-S) sodium current density in brain and small dorsal root ganglion (DRG) neurons, altered voltage dependence of sodium current inactivation, reduced sensitivity to pain and increased susceptibility to seizures (Chen et al. 2002; Lopez-Santiago et al. 2006). *Scn2b* has been implicated in disease: *Scn2b* expression is upregulated in a neuropathic pain model (Pertin et al. 2005) and *Scn2b* null mice have a neuroprotective phenotype in a model of demyelinating disease (O'Malley et al. 2009). The *Scn2b* null mutation has been proposed to prevent pathologic sodium channel upregulation along axons in response to demyelination, thus attenuating the extent of neuronal degeneration. While *SCN2B* has not yet been linked to human brain disease, mutations in *SCN2B* are associated with atrial fibrillation in heart (Watanabe et al. 2009).

Concomitant covalent linkage of α to β2 through disulfide bonding and insertion into the plasma membrane are the final steps in sodium channel biosynthesis in primary neurons (Schmidt and Catterall 1986). These results suggested that covalent linkage of α to β2 may occur at the extracellular face of the plasma membrane, however, the specific cysteine residue(s) involved have not been identified. Here we show, using a mutagenesis study, that a single cysteine-to-alanine substitution at the β2 extracellular residue C26 is sufficient to disrupt the formation of α-β2 covalent complexes *in vitro*. While β2WT subunits do not affect the level of sodium current expressed by $Na_v1.1$ in a heterologous

system, co-expression of $Na_v1.1$ with β2C26A results in decreased sodium current compared to α alone, suggesting that β2C26A may cause intracellular retention of a population of α subunits. Using a primary myelinating co-culture system, we demonstrate that, while β2WT traffics to nodes of Ranvier and heminodes, β2C26A is targeted to the axonal compartment but is not detectable at nodes or heminodes. In cultured hippocampal neurons, β2WT is enriched in the AIS, as defined by anti-ankyrin G staining whereas β2C26A is expressed in a non-polarized distribution in all of the neuronal processes. Thus, covalent linkage of β2 to α is essential for proper targeting of this subunit to specialized subcellular neuronal compartments. Finally, β2WT subunits are resistant to live cell detergent extraction from the hippocampal AIS, while mutant β2 subunits, that cannot form disulfide bonds with α are removed by detergent. Taken together, our results demonstrate that α-β2 covalent association via a single, extracellular disulfide bond, is required for β2 targeting to specialized neuronal subcellular domains and for β2 association with the neuronal cytoskeleton within those domains.

Methods

Antibodies

For immunoprecipitation and Western blot studies, primary antibodies used included rabbit polyclonal anti-pan-VGSC antibody obtained from Sigma (S6936; 1:200 dilution) and mouse monoclonal anti-V5 antibody obtained from AbD Serotec (MCA1360; 1:300 dilution). For immunofluorescence studies, primary antibodies used included rabbit antibody against ankyrin G (S. Lux, Yale University School of Medicine, New Haven, CT, 1:4,000 dilution), goat antibody against GFP (AbD Serotec, 1:4,000 dilution), guinea-pig antibody against Caspr/Neurexin IV (1:4000 dilution, M. Bhat, University of Texas, San Antonio, TX), and chicken antibodies against MBP (Chemicon,

Temecula, CA, 1:100 dilution) and MAP2 (Covance, 1:10,000 dilution). Secondary donkey antibodies conjugated to Rhodamine Red-X, Alexa Fluro488, AMCA, or DyLight 649 were obtained from Jackson ImmunoResearch Laboratories (West Grove, PA) and used at 1:200 dilution.

Plasmids and Cell Culture

To generate a C-terminal β2V5 epitope tagged expression plasmid, cDNA encoding rat β2 (minus the termination codon) was cloned into the multiple cloning site of pcDNA3.1/V5-His (+) using standard TA cloning. This plasmid is referred to here as β2V5. Mutagenesis of β2 cysteine residues to alanine within this vector was performed using the Quikchange II site-directed mutagenesis kit (Stratagene). A subset of β2 constructs, including β2WT, Φ (the construct with all cysteine residues mutated to alanine), and β2C26A, were subcloned into pEGFP-N1 to add a C-terminal GFP epitope tag. The integrity of all plasmids was confirmed by DNA sequencing at the University of Michigan DNA Sequencing Core. HEK-293 cells stably expressing human $Na_v1.1$ (GenBank accession number NP_008851.3; HEK$hNa_v1.1$) were obtained from Glaxo-SmithKline under a materials transfer agreement as previously described (Patino et al. 2011).

Co-immunoprecipitation

Co-immunoprecipitation was performed similar to (Rusconi et al. 2007). Briefly, HEK$hNa_v1.1$ cells cultured as described (Patino et al. 2011) were transfected with 4 μg of β2WT or mutant plasmid using Fugene 6 as recommended by the manufacturer. Protein A-Sepharose beads (Sigma) were washed with PBS and resuspended in 500 μl of dilution buffer (DB: 60 mM Tris/HCl pH 7.5, 180 mM NaCl, 1.25% Triton X-100, 6 mM EDTA pH 8 containing Complete Mini protease inhibitor tablets (Roche) at 2x the manufacturer's recommended concentration) at 4°C. The beads were then incubated overnight at 4°C with 5 μg of anti-pan sodium channel antibody. The transfected cells

were detached from the culture dishes using 50 mM Tris, 10 mM EGTA (pH 8) and centrifuged at 5,000 rpm in a microfuge for 5 min at 4°C. The cell pellet was resuspended in DB for cell lysis. After 30 min of lysis on ice, a 10 min centrifugation at 10,000 rpm in a microfuge was performed to remove insoluble material. The resulting supernatant was added to the beads and incubated by rotating end-over-end for 5 h at 4°C. The beads were then washed twice with washing buffer (50 mM Tris pH 7.5, 150 mM NaCl, 0.1% Triton X-100, 0.02% SDS, 5 mM EDTA pH 8 containing Complete Mini protease inhibitor tablets at 2x the manufacturer's recommended concentration) followed by one wash with the same buffer lacking Triton X-100. Samples were then separated by SDS-PAGE on a 5 % polyacrylamide gel and transferred to nitrocellulose for Western blot analysis. Western blotting was performed using the SnapId system (Millipore). Immunoblots were probed with anti-V5 or anti-pan-VGSC antibody as indicated, detected with Westfemto Chemiluminescent reagent (Pierce), and imaged using autoradiography film (Denville Scientific) or using the LI-COR Odessey® Fc imaging system. All results presented are representative of at least two independent repeats, as specified in the figure legends.

Surface Biotinylation

Surface biotinylation of β2WT or mutant proteins was performed as in (Patino et al. 2011). Briefly, membrane proteins were biotinylated using the Cell Surface Labeling Accessory Pack (Pierce) following the manufacturer's instructions utilizing Complete Mini (Roche) as protease inhibitor. Samples were separated on 12% SDS PAGE gels. Proteins were transferred to nitrocellulose membranes that were processed for Western blotting using the SnapId system (Millipore). Anti-V5 immunoreactive signals detecting β2 subunits were compared with the immunoreactive signal for Na^+/K^+ ATPase β1-subunit, a loading control for cell surface protein preparations (Patino et al. 2011). All results presented are representative of at least two independent repeats, as specified in the figure legends.

Immunocytochemical analysis of β2 expression in HEK cells

HEKhNa$_v$1.1 cells were transiently transfected with GFP alone, β2WT-GFP, β2C26A-GFP, or Φ-GFP using Fugene 6 following the manufacturer's recommendations. Twenty four h post-transfection, cells were replated onto 8-well glass chamber slides (BD Falcon). Twenty four h later, cells were fixed for 20 min at RT with 4% paraformaldehyde. After a 1 h blocking step (PBSTGS: dPBS containing 10% goat serum and 0.3 % Triton X-100), cells were incubated overnight at RT with rabbit anti-GFP antibody (Invitrogen; A6455; 1:1000) diluted in PBSTGS. Following 3 - 10 min washes with dPBS, cells were incubated 2 h at RT with Alexafluor568 goat anti-rabbit secondary antibody (Invitrogen; A-11011; 1:500) diluted in PBSTGS. After 3 - 10 min washes with dPBS, slides were allowed to dry for 20 min and coverslipped using mounting media (Invitrogen; ProLong Gold Antifade Reagent with DAPI; P36931). Slides were imaged using a Nikon A1R confocal microscope utilizing Nikon NIS-Elements software located in the Department of Pharmacology at the University of Michigan.

Whole-cell patch-clamp recording and analysis

HEKhNa$_v$1.1 cells were transfected with V5- or GFP-tagged β2 subunits as described above and plated for electrophysiological analysis. To detect cells that were transfected with V5-tagged plasmids, a 1:10 ratio of GFP:β2 cDNA was used such that β2-expressing cells could be detected by epifluorescence. Aliquots of each transfection were analyzed for protein expression by Western blot to confirm protein expression. Micropipettes were obtained from capillary glass tubing (Warner Instruments) using a horizontal P-97 puller (Sutter Instruments). Micropipette resistance was between 1.5 and 3.5 MΩ, when filled with intracellular solution containing the following (in mM): 10 NaCl, 10 CsCl, 105 (Cs)Aspartate, 10 EGTA, and 10 HEPES, pH 7.4 with CsOH. And the extracellular solution containing (in mM): 130 NaCl, 4 KCl, 1.5 $CaCl_2$, 1 $MgCl_2$, 5 glucose, 10 HEPES, pH 7.4 with NaOH. Voltage pulses were applied and data recorded

using Clampex 9.2 or 10, Axopatch 200B or 700B amplifier and a Digidata 1322A digitizer (Molecular Devices). Pipette and whole cell capacitance were fully compensated. When appropriated, series resistance compensation was set to approximately 40-70% with the lag set to 10 μs. Signals were low-pass filtered at 5 kHz, and data were sampled at 40 kHz online. To determine the sodium current amplitude and voltage dependence of activation, sodium currents were evoked by 250 ms depolarizing test pulses (from -110 to 40 mV at 5 and 10 mV intervals) from a holding potential of -80 mV and a hyperpolarizing -120 mV, 250 ms prepulse. Peak sodium current was normalized to cell capacitance and used to plot I–V curves; also to calculate conductance ($g=I/(V-V_{rev})$, where V is the test potential, and V_{rev} is the measured reversal potential). Voltage dependence of inactivation was determined by applying a 50 ms test pulse to 0 mV after 250 ms prepulses to the same voltages as described for the voltage dependence of activation. Peak currents were normalized to the maximum peak I_{Na} amplitude. Normalized activation and inactivation curves were fit with a Boltzmann equation $1/[1+\exp(V-V_{1/2})/\kappa]$, where $V_{1/2}$ is the membrane potential in the midpoint of the curve, and κ as the slope factor. The kinetics of inactivation was measured on the test pulse to 0 mV from the same protocol used for voltage dependence of activation. The current, from 90% of the peak amplitude to 20 ms after the test pulse was initiated, was fitted to a double exponential equation of the form $I=(F_f * \exp(-\tau/\tau_f))+(Fs*\exp(-\tau/\tau_s)+C$ using the Chebyshev method, where I is the current, τ_f and τ_s are the time constants for the fast and slow inactivation component, and C is the steady-state persistent current. Analysis of the recorded sodium current was performed using the software packages Clampfit 10 (Molecular Devices) and SigmaPlot 11.2 (Systat Software, Inc., San Jose, CA). The statistical significance of differences between mean values for β2C26A-GFP or Φ-GFP compared with β2WT-GFP was evaluated using Student's unpaired *t* test, with $p < 0.05$ considered significant. Results are presented as means ± SEM.

Myelinating Co-cultures

Co-cultures of rat Schwann cells and dorsal root ganglion (DRG) neurons were established as described previously (Zhang et al. 2012). Briefly, DRGs were removed from E15 or E16 rat spinal cords, dissociated with 0.25% trypsin, and plated onto Matrigel (BD Bioscience) coated coverslips. After cycling with antimitotics to eliminate non-neuronal cells, Schwann cells were added to the cultures and maintained in C media (containing 10% fetal bovine serum, 50 ng/ml 2.5S nerve growth factor, 0.4% glucose, and 2 mM L-glutamine in minimum essential medium) for 1-3 days before adding 50 µg/ml ascorbic acid to allow myelination to ensue.

Primary hippocampal neuron cultures

Primary cultures of hippocampal neurons were established essentially as described previously (Dzhashiashvili et al. 2007). Briefly, hippocampi from E18 rat were treated with 0.05% trypsin (Invitrogen) in dissecting solution (0.6% glucose, 10 mM HEPES in PBS) for 30 min at 37°C and cells were dissociated by repeated passage through a fire-polished constricted Pasteur pipette and then plated onto 12 mm coverslips coated with poly-L-lysine (0.1 mg/ml in PBS) in MEM containing Earles' salts and glutamine with 10% FBS, 0.45% glucose, 1 mM pyruvate, and penicillin and streptomycin. After 2 hours, the medium was replaced by Neurobasal medium (Invitrogen) with 2% B-27, and 0.5 mM L-glutamine. Cultures were maintained at 37°C in a humidified 5% CO2 atmosphere until used.

Nucelofection

Nucleofector™ Technology was used to introduce β2-GFP constructs into DRG neurons prior to co-culture with Schwann cells or into hippocampal neurons. Nucleofection was performed with Amaxa Rat Neuron Nucleofector Kit (Lonza) by using Nucleofector II (Lonza).

Immunofluorescence and Imaging

Hippocampal neurons or myelinating co-cultures were fixed in 4% paraformaldehyde for 10 min, permeabilized and blocked with buffer containing 1% donkey serum, 5% BSA, and 0.2% Triton X-100 in 1X PBS for 30 min, then stained with primary and secondary antibodies diluted in blocking buffer. Immunofluorescence images of cultures were taken with a Zeiss LSM 510 Meta confocal microscope.

Triton extraction

Live hippocampal cultures were incubated in extraction buffer (30 mM PIPES, 1 mM MgCl2, 5 mM EDTA, 0.5% Triton X-100) for 20 min at 37 ºC, and then rinsed in PBS, fixed in 4% PFA and processed for immunofluorescence.

Protein structure modeling

The extracellular domain of β2 was modeled based on the reported crystal structure for rat myelin P_0ex (Shapiro et al. 1996) using PyMOL (PyMOL Molecular Graphics System, Version 1.5.0.4 Schrödinger, LLC.).

Multiple alignments of sodium channel sequences

Multiple alignments of sodium channel polypeptide sequences were performed using MEGA version 5 (Tamura et al. 2011) utilizing the ClustalW methodology (Thompson et al. 1994).

Results

Sodium channel β2 subunits contain five extracellular cysteine residues (C21, C26, C43, C46, C98) and one intracellular cysteine residue (C143) (Isom et al. 1995a). Two of the extracellular cysteine residues form an intramolecular disulfide-bridge as part of the Ig-fold structure (Isom et al. 1995a). Aligning the amino acid sequence of β2 with β1 and

β4, we found that β2C21 and β2C98 were conserved among the three β subunits, suggesting that these residues are responsible for formation of the Ig loop intramolecular disulfide bridge that is common to all three (**Figure 4.1A**). β3 was not included in this alignment because evidence suggests that it does not participate in homophilic cell-cell adhesion and thus may have a slightly different Ig domain structure (McEwen et al. 2009). β2C98 aligns with β1C121, which is proposed to be critical to formation of the disulfide bridge in the Ig loop domain. β1C121 is mutated to tryptophan in human epilepsy, resulting in disruption of β1-mediated cell-cell adhesion (Meadows et al. 2002b). These data support the idea that β2C21 and β2C98 participate in intramolecular disulfide bond formation in the Ig domain. Comparing β2 with β4 (Yu et al. 2003), the β subunits that are disulfide-linked to α, we found that β2C26 is conserved between subunits, whereas β2C43 and β2C46 are not conserved, suggesting that C26 may be involved in disulfide linkage to α. In previous studies we used the crystal structure of the myelin P_0 extracellular domain to model the sodium channel β1 Ig loop (McCormick et al. 1998). Employing a similar strategy here for the related β2 extracellular domain, we show that β2C21 and β2C98 are optimally aligned to form an intramolecular disulfide bond (**Figure 4.1B,** left and right panels). In contrast, β2C26 is located in the linker region between the B and C faces of the Ig loop (McCormick et al. 1998), in a position that is more accessible for association with sodium channel α subunits (**Figure 4.1B,** left panel). Thus, we hypothesized that β2C26 was the most logical candidate to form an intermolecular disulfide bridge between β2 and α.

β2C26 mediates the disulfide-linkage between β2 and α

To identify the β2 cysteine residue(s) responsible for α-β2 linkage, β2 mutant expression constructs were generated substituting each single cysteine to alanine. In addition, every possible combination of multiple cysteine to alanine substitutions was

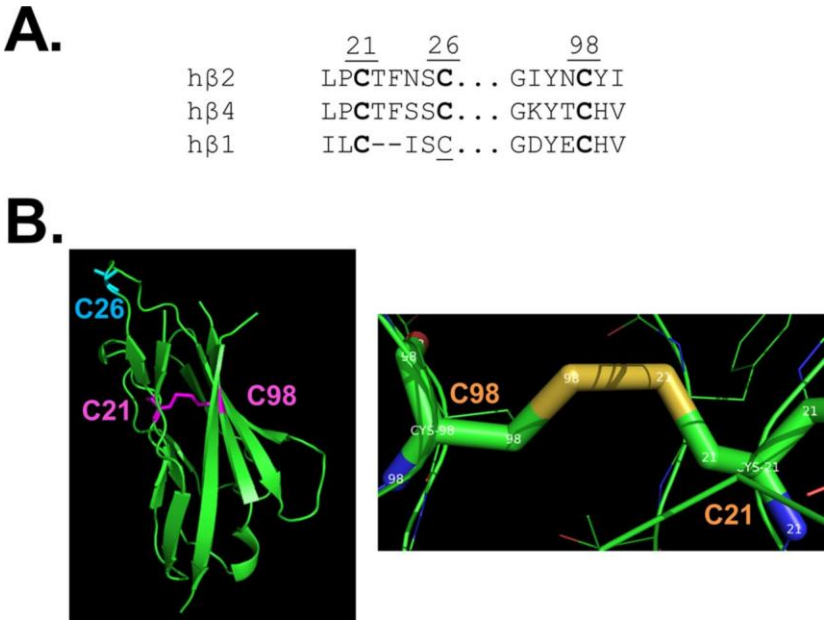

Figure 4.1. Structural predictions for β2. **A.** Alignment of the N-terminal regions of human β2, β4, and β1 with conserved cysteine residues highlighted in bold. Residue numbering corresponds to β2. **B.** Left: The crystal structure of the Ig loop of human myelin P_0 (Liu et al. 2012) was used as a template to show the predicted position of β2C26 (cyan), β2C21 (magenta), and β2C98 (magenta). Right: The crystal structure of the Ig loop of human myelin P_0 (Liu et al. 2012), was used as a template to show the predicted intramolecular disulfide bond between β2C21 and β2C98.

generated, in the event that multiple cysteine residues were involved in α-β2 linkage. Each construct was engineered to contain carboxyl-terminal V5 epitope tag to facilitate biochemical identification. β2WT or cysteine-to-alanine β2 mutant constructs were then expressed separately in HEKhNa$_v$1.1 cells. Na$_v$1.1 was immunoprecipitated with anti-pan-VGSC α subunit antibody and α-β2 protein complexes (MW > 250 kDa) were detected by non-reducing SDS-PAGE followed by immunoblotting with a mouse monoclonal anti-V5 antibody to label V5-tagged β2 subunits. As expected (Schmidt and Catterall 1986), co-expression of β2WT with Na$_v$1.1 resulted in detection of a high MW α-β2 channel complex (**Figure 4.2A and B**). Mutation of all 6 cysteine residues within β2 (Φ) completely disrupted α-β2 association (**Figure 4.2A**). A single alanine substitution, C26A, was sufficient to disrupt the α-β2 linkage (**Figure 4.2A**). Of all of the possible β2 cysteine-to-alanine mutant constructs, only those with the β2C26A mutation abolished β2-Na$_v$1.1 association under non-reducing conditions (**Figure 4.2B, Table 4.1**). Importantly, mutation of β2C21 or β2C98, the residues proposed to form the intramolecular Ig loop disulfide bond, to alanine did not disrupt intermolecular α-β2 subunit association. All of the cysteine-to-alanine mutant β2 constructs displayed robust expression levels in cell lysates collected post-transfection (β2WT, Φ, and β2C26A shown in **Figure 4.2C**, others not shown). These data suggest that a single extracellular cysteine residue, β2C26, mediates the disulfide linkage between β2 and α.

Cell surface expression and modulation of sodium currents

The β2 mutant polypeptides Φ and β2C26A do not form disulfide bonds with Na$_v$1.1. Nevertheless, these subunits traffic to the cell surface where they may be available to modulate sodium currents through non-covalent association with α. Surface biotinylation analyses, shown in **Figure 4.3A and B**, demonstrated that β2WT, Φ, and β2-C26A are expressed at the cell surface. Fluorescence immunocytochemical data (**Figure 4.3C**), confirmed cell surface expression of all three subunits. To test for the

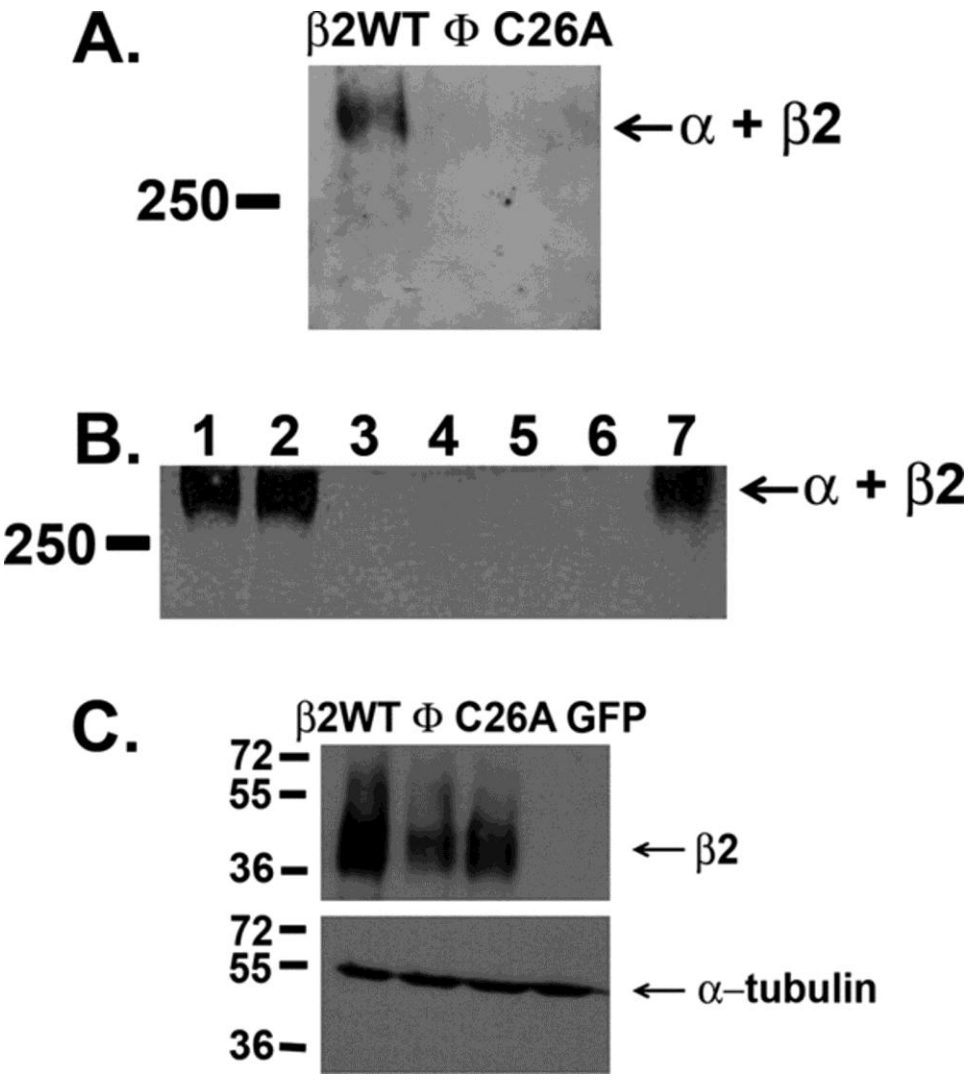

Figure 4.2. Na^+ channel β2 and α subunits are disulfide linked at β2 residue C26. Coimmunoprecipitation was performed with HEKhNa_v1.1 cells transiently transfected with V5-tagged β2WT or various β2 cysteine-to-alanine mutants, as indicated. Solubilized Na_v1.1 complexes were immunoprecipitated with anti-pan-Na^+ channel antibody and separated on non-reducing SDS-PAGE gels as described in Experimental Procedures. Western blots were detected with anti-V5 antibody to visualize high α-β2 protein complexes (arrows). **A.** Disulfide-linked α-β2WT complexes are detected, whereas α-ϕ and α-β2C26A are not detectable, indicating that disulfide linkage between subunits was lost. **B.** (Lane 1) α-β2WT, (Lane 2) α-β2C43A, and (Lane 7) α-β2C43AC46AC143A complexes are detected. In contrast, (Lane 4) α-β2C26AC43A and (Lane 5) α-β2C26AC43AC46AC143A complexes are not detectable, indicating that disulfide linkage between subunits was lost. Lanes 3 and 6 were left empty. Results of similar experiments for the remaining β2 constructs are summarized in **Table 4.1**. **C.** Western blot analysis shows robust expression of β2WT and mutant constructs: Top panel: HEKhNa_v1.1 cells were transfected with V5-tagged β2WT, Φ, or β2C26A or with

GFP alone, as indicated. Cells were then were solubilized and analyzed by Western blot with anti-V5 antibody to confirm subunit expression. Lower panel: The blot was stripped and reprobed with anti-α-tubulin as a loading control. Results presented in this figure are representative of 5 independent experiments.

Construct	Detection of immunoreactive Nav1.1-β2 protein complex by SDS PAGE
β2WT	Yes
Φ	No
β2C21A	Yes
β2C26A	No
β2C43A	Yes
β2C46A	Yes
β2C98A	Yes
β2C143A	Yes
β2C26AC43A	No
β2C43AC46AC143A	Yes
β2C26AC43AC46AC143A	No
β2C26AC43AC46AC98AC143A	No
β2C21AC43AC46AC98AC143A	Yes
β2C21AC26AC46AC98AC143A	No
β2C21AC26AC43AC46AC143A	No

Table 4.1. Detection of β2-Na_v1.1 disulfide-linkage by coimmunoprecipitation. Coimmunoprecipitation was performed with HEKhNa_v1.1 cells transiently transfected with V5-tagged β2WT or various β2 cysteine-to-alanine mutants, as indicated. Solubilized Na_v1.1 complexes were immunoprecipitated with anti-pan-Na^+ channel antibody and separated on non-reducing SDS-PAGE gels as described in Experimental Procedures. Western blots were detected with anti-V5 antibody to visualize high α-β2 protein complexes, as demonstrated in Figure 4.2. Results presented in this table are representative of 2 independent experiments, except for β2WT ϕ, β2C26A, β2C43A, β2C43AC46AC143A, β2C26AC43A, and β2C26AC43AC46AC143A, which were performed 5 times each.

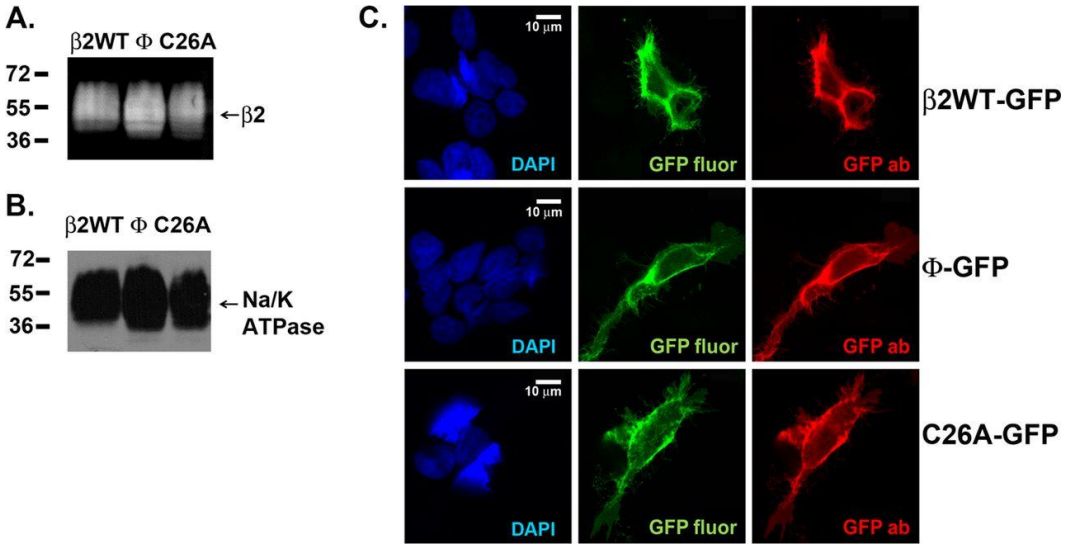

Figure 4.3. β2WT, Φ, and β2C26A subunits are expressed at the cell surface. **A.** Cell surface biotinylation was performed on HEKhNa$_v$1.1 cells transfected with β2WT, Φ, or β2C26A as described in Experimental Procedures. Immunoreactive bands were detected with anti-V5 antibody. The position of β2 subunit migration on the gel is indicated by the arrow. Similar to previous experiments to assess β1 subunit cell surface expression using this method (Patino et al. 2009), we observed multiple V5 immunoreactive bands, likely representing various levels of avidin attachment to β2. **B.** Na/K ATPase β1 subunit immunoreactivity of samples from A as a loading control for cell surface proteins (arrows). **C.** HEKhNa$_v$1.1 cells expressing β2WT-GFP (top), Φ-GFP (center), or β2C26A-GFP (lower) were processed for immunocytochemistry as described in Experimental Procedures. Cells were visualized for GFP epifluorescence (green) or with an anti-GFP antibody (red; Alexa568) by confocal microscopy. DAPI (blue) indicates cell nuclei. Scale bar = 10 μm. Results presented in this figure are representative of 5 independent experiments.

possibility of non-covalent association of these mutant subunits with α, we co-immunoprecipitated HEKhNa$_v$1.1 cells transfected with α or β2C26A with anti-pan-VGSC α subunit antibody (as in Figure 2) and probed the Western blot for non-disulfide linked β2 subunits (migrating in the 33 kDa range), but were unable to detect any bands (not shown). In spite of these results, we could not rule out the possibility that non-disulfide linked β2 subunits, especially β2C26A in which the Ig loop domain is predicted to remain intact, may associate transiently with α subunits. To test this possibility, we investigated the effects of β2WT, β2C26A, or Φ on sodium currents in transfected HEKhNa$_v$1.1 cells under whole cell voltage clamp (**Table 4.2**). The V5- and GFP-tagged plasmids for each construct yielded similar results and thus values were pooled. Similar to previous work with other sodium channel α subunits co-expressed with β2 in heterologous cells (Kazarinova-Noyes et al. 2001; Watanabe et al. 2009), we observed that co-expression of β2WT with Na$_v$1.1 did not change the level of sodium current density compared that observed for α alone. Co-expression of Φ with Na$_v$1.1 also had no effect on sodium current density compared to α alone (**Figure 4.4**). In contrast, we observed that co-expression of β2C26A with Na$_v$1.1 resulted in a significant decrease in transient sodium current compared to WT (**Figure 4.4**). Interestingly, these data are analogous to results reported for the *SCN2B* atrial fibrillation mutations R28Q and R28W, located in a similar region of the β2 Ig domain, which decreased the amplitude of Na$_v$1.5-expressed currents compared to β2WT (Watanabe et al. 2009). Also similar to (Watanabe et al. 2009) and to our results with Na$_v$1.5 expressed in a heterologous system (Dhar Malhotra et al. 2001), β2WT did not increase Na$_v$1.5-generated currents compared to α alone (Watanabe et al. 2009). In addition to the effect of β2C26A on current density, we observed a small but significant depolarizing shift in the voltage-dependence of sodium current inactivation in the presence of Φ compared to α alone. Thus, even though we were unable to detect non-covalent association of β2C26A or Φ with Na$_v$1.1 biochemically, our electrophysiological results suggest that these subunits may associate

	GFP	β2WT	Φ	β2C26A
I_{Na} peak (pA/pF)	-147.7 ± 30.7	-149.8 ± 20.7	-144.3 ± 35.1	-95.8 ± 11.5[a]
I_{Na} persistent (pA/pF)	-14.0 ± 5.9	-24.1 ± 8.2	-9.8 ± 2.7	-7.8 ± 1.9
τ_{inac} fast (ms)	0.78 ± 0.16	0.74 ± 0.12	0.62 ± 0.05	0.62 ± 0.03
τ_{inac} slow (ms)	5.55 ± 1.2	6.17 ± 0.77	4.81 ± 0.79	4.25 ± 0.45
n	10	13	9	12
V_{rev} (mV)	67.2 ± 5.6	68.6 ± 4.5	73.8 ± 7.4	59.7 ± 6.3
n	7	10	8	10
Voltage-dependence of activation				
G_{max} (nS)	35.5 ± 5.9	32.0 ± 4.0	31.7 ± 13.9	31.5 ± 7.5
K	4.6 ± 0.7	5.0 ± 0.6	5.0 ± 0.9	5.1 ± 0.5
$V_{1/2}$ (mV)	-19.6 ± 1.6	-19.4 ± 1.3	-14.8 ± 2.4	-19.4 ± 2.2
Voltage-dependence of inactivation				
K	-5.2 ± 0.3	-6.7 ± 0.6	-5.0 ± 0.2	-5.2 ± 0.3
$V_{1/2}$ (mV)	-44.1 ± 2.7	-44.4 ± 2.1	-38.9 ± 1.0[b]	-44.6 ± 2.2
C	0.04 ± 0.01	0.06 ± 0.01	0.05 ± 0.01	0.06 ± 0.01

[a] P = 0.036 with WT

[b] P = 0.044 compared with WT

Table 4.2. Modulation of Na^+ current properties by β2 subunits.

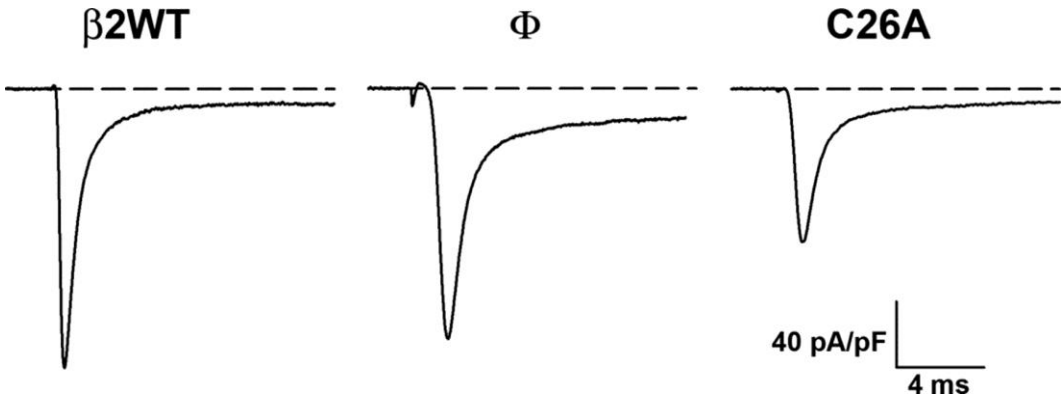

Figure 4.4. Representative Na^+ current traces. Representative Na^+ currents evoked by a depolarizing pulse to 0 mV obtained from HEKhNa$_v$1.1 cells transfected with β2WT-GFP, Φ-GFP, or β2C26A-GFP, as indicated.

with α through low affinity interactions.

Disulfide-linkage of β2 with α is critical for β2 targeting to nodes of Ranvier and the AIS

Sodium channel clustering at nodes of Ranvier is critical for action potential conduction in myelinated axons. Localization of β2 to nodes of Ranvier (Kaplan et al. 2001) suggests a functional role for this non-pore-forming subunit in these highly organized structures. Sodium channel α subunits traffic normally to nodes of Ranvier in *Scn2b* null mice, demonstrating that β2 is not necessary for proper nodal localization and clustering of the ion channel pore. However, action potential conduction is significantly decreased in *Scn2b* null optic nerve, indicating that the density of sodium channel α subunits at the node is reduced compared to WT.

To test whether α-β2 subunit disulfide linkage affects β2 targeting to nodes, we generated myelinating co-cultures consisting of DRG neurons and Schwann cells. Prior to co-culture, neurons were transfected with β2WT-GFP, β2C26A-GFP, or Φ-GFP. C-terminal GFP epitope tags were added to the constructs to facilitate imaging of β2 localization. We examined the targeting of these constructs to heminodes, i.e. the initial nodal clusters that form at the ends of individual myelin segments, and to mature nodes, which are flanked on both sides by myelin segments. β2WT-GFP was targeted specifically to nodes of Ranvier as well as to the heminodes (**Figure 4.5A, upper panels**). Thus, all nodes (20 out of 20) and all heminodes (44 out of 44) scored in a representative experiment were labeled by the β2WT-GFP construct. These results also indicate that the C-terminal GFP tag does not interfere with normal β2 trafficking in neurons. In contrast to β2WT-GFP, Φ-GFP (**Figure 4.5A, middle panels**) and β2C26A-GFP (**Figure 4.5A, lower panels**) were diffusely expressed in the neurites of the sensory neurons but absent from the nodes and heminodes. In the case of Φ-GFP, 0 out of 52 heminodes and 0 out of 21 nodes were positive; β2C26A-GFP was present in 0 out of 48

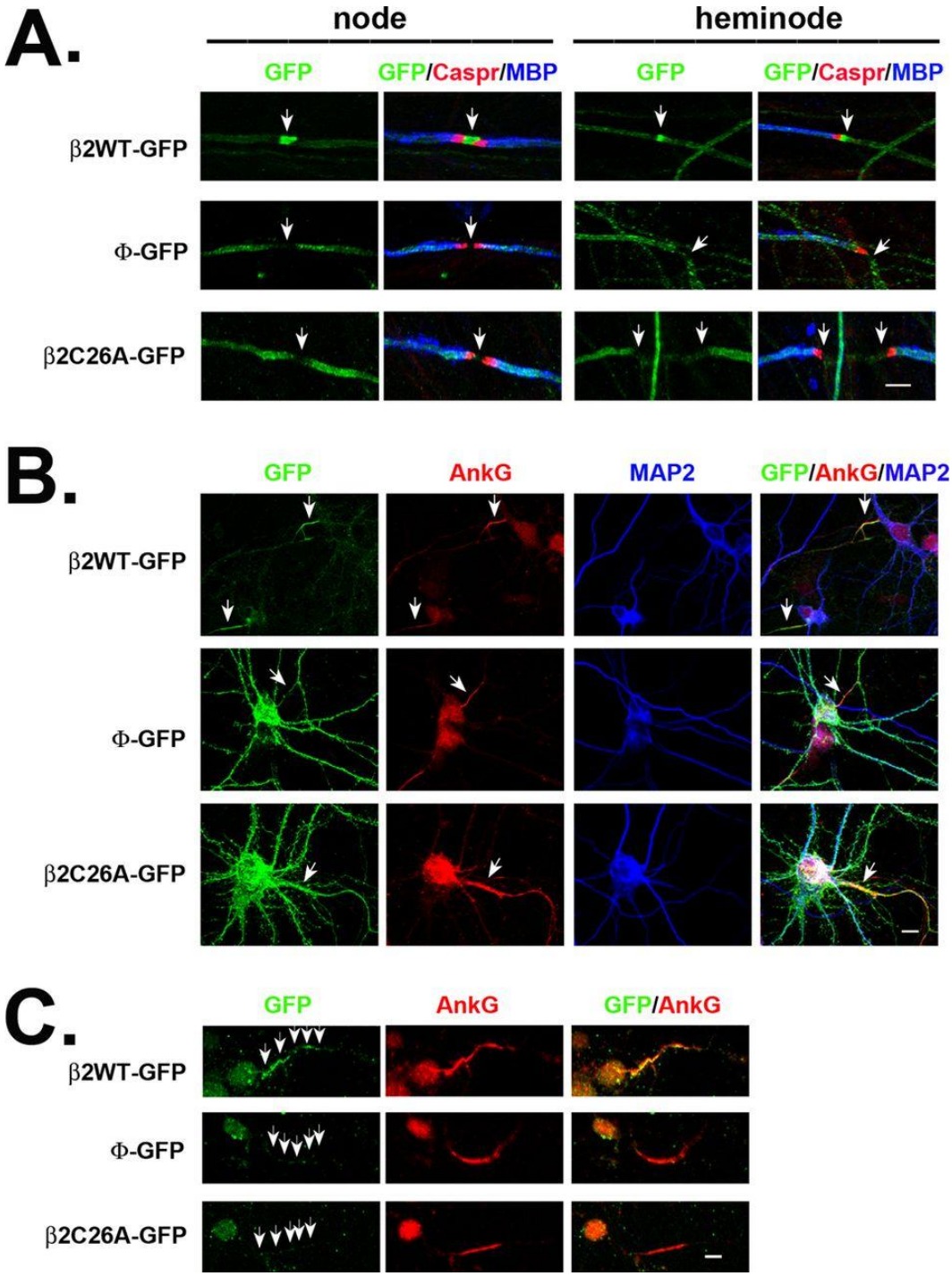

Figure 4.5. Covalent α-β2 linkage is critical for targeting of β2 to nodes of Ranvier and the AIS. **A.** Targeting of β2 constructs to nodes of Ranvier. DRG neurons were nucleofected with WT or mutant β2-GFP constructs, as indicted, then co-cultured with Schwann cells under myelinating conditions for ~2 weeks. Cultures were fixed and analyzed by immunofluorescence staining. β2WT-GFP (green) accumulated at nodes and heminodes (arrows), whereas the mutant constructs failed to accumulate at these sites.

Paranodes were stained with Caspr (red) and myelin segments were stained with MBP (blue). Scale bar = 5 μm. **B.** Targeting of β2 constructs in hippocampal neurons. β2-GFP constructs were nucleofected into hippocampal neurons and analyzed at 18 DIV. β2WT-GFP (green) was enriched in the AIS, labeled by ankyrin G staining (red) (arrows). In contrast, Φ-GFP and β2C26A-GFP mutants (green) were equally distributed in axons and dendrites, or preferentially concentrated in dendrites, and were not enriched in the AIS. Dendrites were stained with MAP2 (blue). Scale bar = 10 μm. **C.** Triton X-100 extracts mutant β2 constructs from hippocampal neuron cultures. β2WT-GFP nucleofected hippocampal neuron cultures were extracted with Triton X-100 prior to fixation, then fixed and stained. The β2WT-GFP construct was retained at the AIS despite detergent treatment and was extracted from other sites. Both Φ-GFP and β2C26A-GFP were largely extracted from the neurons, including from the AIS, by detergent treatment. Arrows in the GFP staining panels delineate the positions of AIS; neuronal somata are located on the left. Scale bar = 5 μm.

heminodes and 0 out of 12 nodes. Thus, while β2 subunits that are not covalently linked to α still traffic to the neurites, they fail to cluster at nodes or heminodes.

Sodium channel clustering at the AIS is critical for action potential initiation. We tested the targeting of β2WT-GFP, Φ-GFP, and β2C26A-GFP to the AIS using primary hippocampal neuronal cultures. Similar to our results in myelinating co-cultures, we found that disruption of α-β2 covalent linkage disrupted β2 targeting. β2WT-GFP was enriched at the AIS, defined by ankyrin-G expression, in 59 out of 60 neurons scored. (It was exclusively expressed in the AIS in 5 of 60 neurons and faintly expressed in the remainder of the axon in 22 out of 60 neurons and in all processes in 32 out of 60 neurons) (**Figure 4.5B, upper panels**). In contrast, the Φ-GFP (**Figure 4.5B, middle panel)** and β2C26A-GFP (**Figure 4.5B**, **lower panel**) constructs failed to concentrate at the AIS in any neurons scored, i.e. 0 out of 54 and 60 neurons, respectively. Rather, expression of both constructs was either non-polarized or confined to the dendrites. Finally, we used the live cell detergent extraction technique (Zhang et al. 2012) to investigate the association of β2 subunits with cytoskeletal elements at the AIS. As shown in **Figure 4.5C**, β2WT subunits are resistant to Triton X-100 extraction from the hippocampal AIS (**Figure 4.5C, upper panel**). In contrast, Φ-GFP (**Figure 4.5C**, **middle panel**) and β2C26A-GFP (**Figure 4.5C**, **lower panel**), subunits that cannot form disulfide bonds with α are removed completely by detergent treatment. Taken together, these results demonstrate that α-β2 covalent association is required for β2 targeting to specialized neuronal subcellular domains and for β2 association with the neuronal cytoskeleton within those domains.

Discussion

Voltage-gated sodium channels are essential regulators of neuronal excitability in mammals (Catterall 2012). Concomitant covalent association of sodium channel α with

β2 subunits and insertion into the plasma membrane are the final steps in channel biosynthesis in central neurons (Schmidt and Catterall 1986). Thus, α-β2 association is considered to be a critical rate-limiting step in the formation of functional sodium channels and consequently the development of excitability, playing an essential role in the regulation of channel density and channel targeting to specialized locations in the neuron (Schmidt and Catterall 1986). Studies with *Scn2b* null mice have demonstrated that β2 subunits are critical regulators of central and peripheral neuronal excitability *in vivo* via modulation of channel cell surface expression (Chen et al. 2002; Lopez-Santiago et al. 2006). Here we set out to close a critical gap in the sodium channel literature: the molecular identification of the site of covalent α-β2 association.

Via a combination of molecular biological, biochemical, and electrophysiological techniques, we show that the β2 residue C26 is necessary and sufficient to mediate α-β2 covalent association through disulfide bonding. We also expressed these constructs in primary hippocampal neurons and in myelinating co-cultures to investigate the role of covalent α subunit association in β2 targeting to the AIS and nodes of Ranvier, respectively. Mutation of β2 extracellular residue C26 to alanine resulted in disruption of α-β2 covalent association. In spite of the disruption of covalent α-β2 association by this amino acid substitution, co-expression of β2C26A with $Na_v1.1$ decreased the level of transient sodium current density compared to expression of α alone, suggesting that β2C26A and α may associate through transient, non-covalent interactions that we were unable to detect using biochemical techniques. The β2WT subunit is enriched in the AIS of hippocampal neurons and selectively expressed at nodes and heminodes in myelinating DRG-Schwann cell co-cultures. In contrast, β2C26A was not enriched in the AIS of hippocampal neurons but rather, was diffusely expressed in both axons and dendrites or just in dendrites indicating that its targeting was dramatically altered. Similarly, in myelinating co-cultures, β2C26A was never expressed at nodes but rather remained diffusely distributed along the neurites. Triton X-100 extraction of hippocampal neurons

removed β2C26A from the AIS but left β2WT undisturbed, suggesting that β2 subunits are normally associated with the neuronal cytoskeleton and that disruption of α-β2 covalent association eliminates β2 cytoskeletal interactions. These data suggest that α-β2 subunit covalent association is essential for proper β2 clustering at specialized neuronal subcellular domains. In other words, β2 follows α. Further, β2 interactions with the cytoskeleton at the AIS may be mediated exclusively through sodium channel α subunits rather than through other CAMs or via direct association with cytoskeletal proteins. We demonstrated previously, using a heterologous system, that β2 binds to the cytoskeletal protein ankyrin in response to cellular aggregation (Malhotra et al. 2000). Based on these results, we predict that β2-β2 *trans* homophilic adhesion, e.g. through axonal fasciculation, may be required to transduce an outside-in signal to stimulate β2 association with ankyrin in neurons. In the absence of β2-β2 *trans* adhesion, as is the case in the neuronal cultures used here, β2 does not associate with other β2 subunits on adjacent cells, and thus does not bind ankyrin. In this case, β2 must depend on covalent linkage with α for the cytoskeletal association.

Previous work proposed that the A/A' face of the extracellular β1 Ig loop domain is critical for $Na_v1.2$ modulation (McCormick et al. 1998). In addition, the extracellular segment IVSS2-S6 of $Na_v1.2$ was shown to play a dominant role in α-β1 subunit association (Qu et al. 1999). These critical regions of β1 association may be conserved in multiple sodium channel α subunits. Our results here, identifying β2C26 as the critical residue responsible for covalent α-β2 linkage, raise the question of which cysteine residue on the α subunit forms the corresponding disulfide-bridge with β2. While experiments to address this question are beyond the scope of the current study, we took an *in silico* approach to identify potential extracellular α subunit cysteine residues based on evolutionary conservation. Analysis of a multiple alignment of a set of sodium channel α subunit amino acid sequences including mammalian (human, mouse, and rat) $Na_v1.1$, $Na_v1.2$, $Na_v1.6$, and $Na_v1.7$ identified a set of 12 conserved, candidate cysteine residues

within the extracellular portions of domain I-IV S5-6 loops (**Figure 4.6**). Further analysis of a multiple alignment containing the same mammalian protein sequences as well as two additional non-mammalian sodium channel coding sequences (*Electrophorus electricus* Nav and *Drosophila* paralytic) demonstrated that 9 of the 12 cysteine residues are conserved in all of the sequences. Interestingly, 3 of the cysteine residues within the domain II S5-6 loop are less conserved. Two of these residues are conserved in *Electrophorus electricus* Nav but not in the *Drosophila paralytic*, whereas a single cysteine residue was conserved only in mammalian channels but not in *Electrophorus electricus* Nav nor in *Drosophila* paralytic. Given that neither *Drosophila* nor *Electrophorus electricus* contain genes orthologous to the mammalian sodium channel β subunits, these 3, less conserved cysteine residues are attractive candidates for the formation of a disulfide bond with β2C26 in mammals. While the *in silico* analysis suggests a subset of 3 candidate cysteine residues, it is impossible to determine the exact cysteine residue(s) involved based on evolutionary conservation alone. Future mutagenesis studies will allow for the elucidation of the exact cysteine residue on α subunits that fulfills this role.

Acknowledgments

The work in Chapter IV was performed in collaboration with Chunling Chen, Senior Research Associate in the Isom laboratory, and Dr. Luis Lopez-Santiago, Assistant Research Scientist in the Isom laboratory. Dr. Yanqing Zhang, a collaborator in the lab of Dr. James Salzer, was a key contributor to Chapter IV. Chunling Chen generated wildtype and mutant β2 cDNA constructs and performed critical experimentation including immunoprecipitation, SDS-PAGE, immunoblotting, and surface biotinylation. Dr. Luis Lopez-Santiago performed the electrophysiological experiments described in

Chapter IV. Dr. Yanqing Zhang used confocal imaging to test subcellular localization of wildtype and mutant β2 cDNA constructs in myelinating co-culture.

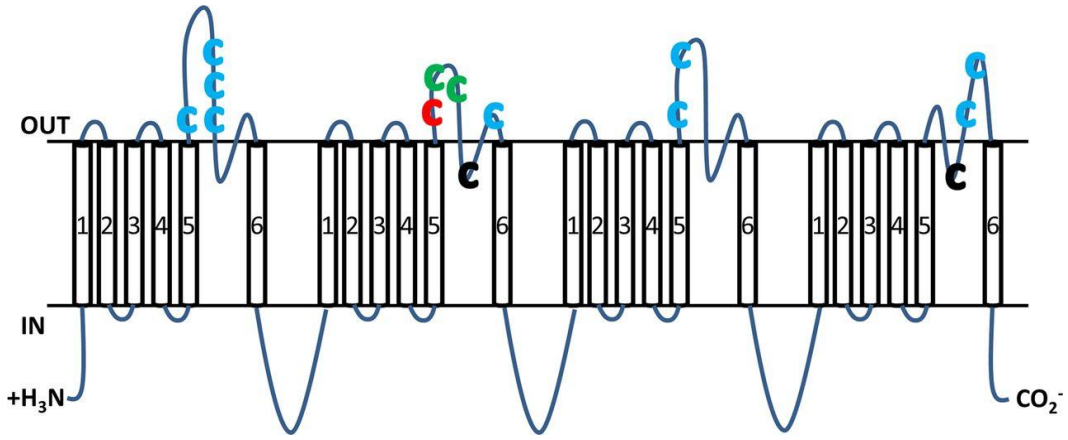

Figure 4.6. Map of conserved extracellular C residues within Na^+ channel α subunits. Locations of cysteine residues within the topology of the α subunit are denoted by 'C'. All extracellular cysteine residues map to S5-6 loop regions. 12 candidate residues are extracellular, while 2 residues are embedded in the membrane as part of a P loop region, and are indicated in black. The color of the 'C' symbol denotes the amount of evolutionary conservation: Conservation in all sequences tested is denoted by blue; conservation in mammalian and *Electrophorus electricus* Nav is denoted by green, and conservation in mammalian channels only is denoted by red.

Chapter V: Discussion and Future Directions

This chapter will serve two purposes. First, I will provide a brief summary of what has been described in the previous chapters of this dissertation. The remainder of the chapter will be devoted to a discussion of important future directions based primarily on continuation of the projects discussed herein. Near the end of the chapter, I will provide a brief discussion of some potential future directions for the VGSC β subunit field in general.

Objectives of Study

The overall goal of my thesis work was to better understand how VGSC β subunits regulate important cell processes such as cell motility. Furthermore, I wanted to improve our knowledge regarding how β subunits in turn are regulated by other proteins. Specifically, for the cancer project outlined in Chapter II, the goal was to determine whether VGSC β subunits, in particular β1, might be involved in human breast cancer cell motility and metastatic potential *in vitro*. For the study described in Chapter III, our objective was to examine the potential role for tyrosine phosphorylation of β1 as a key regulatory step in β1-mediated signaling events. For the project depicted in Chapter IV, the goal was to determine the cysteine residue(s) of β2 involved in covalent linkage with α subunits and ask whether this linkage affected protein trafficking.

Summary

Chapter I

VGSC β subunits are multifunctional proteins that play important roles in modulating cellular excitability and in signal transduction. In addition to being ion channel regulatory subunits and forming a protein complex with the pore-forming VGSC α subunit, β subunits are unique among ion channel accessory subunits in that they contain an extracellular immunoglobulin (Ig) domain, thus placing them in the Ig superfamily of cell adhesion molecules (CAMs) (Isom et al. 1992; Isom et al. 1995a). β subunits function in traditional ion channel accessory subunit roles by modulating α subunit gating and cell surface expression (Isom et al. 1992; Isom et al. 1995a). Importantly, β subunits also function as CAMs during brain development and are involved in both extracellular and intracellular signaling pathways to help guide neuronal patterning (Davis et al. 2004; Brackenbury et al. 2008a; Brackenbury et al. 2013). β subunits, in particular those encoded by *SCN1B*, act as regulators of cell proliferation and migration, axon outgrowth, pathfinding, and fasciculation in many central nervous system (CNS) areas including the hippocampus, cerebellum, and corticospinal tract (Davis et al. 2004; Brackenbury et al. 2008a; Brackenbury et al. 2013).

β subunits are involved in pathophysiological processes, including but not limited to, epilepsy, cardiac arrhythmia, neuropathic and inflammatory pain, neurodegeneration, and cancer (Wallace et al. 1998; Patino et al. 2009; Medeiros-Domingo et al. 2007; Watanabe et al. 2008; Pertin et al. 2005; Lopez-Santiago et al. 2006; O'Malley et al. 2009; Chioni et al. 2009). Mutations in the genes encoding β subunits result in human disease. Mutation of *SCN1B*, encoding the β1/β1B subunits, is linked to diseases on the Genetic Epilepsy with Febrile Seizures plus (GEFS+) spectrum (Wallace et al. 1998; Wallace et al. 2002; Patino et al. 2009). Patients who lack both functional copies of the *SCN1B* gene have Dravet syndrome (DS), a severe pediatric epileptic encephalopathy,

while patients who inherit a single mutant copy of *SCN1B* present with the milder GEFS+ or may not exhibit seizures (Wallace et al. 1998; Wallace et al. 2002; Patino et al. 2009; Ogiwara et al. 2012). Importantly, knockout mice which do not express β1/β1B subunits encoded by *Scn1b* (*Scn1b* null mice) recapitulate the hallmark phenotypes associated with DS, suggesting *Scn1b* null mice are a DS model (Chen et al. 2004; Patino et al. 2009). The roles of β subunits in normal physiology and in disease processes suggest these molecules are potential targets for novel therapeutics.

Chapter II

Ion channels, including VGSCs, appear to be involved in carcinogenesis (Prevarskaya et al. 2010). Increasing evidence suggests that VGSC α subunits may promote metastatic potential, the ability of a cancer cell to release from the primary tumor and form secondary tumors (Brackenbury 2012). Therefore, it is proposed that VGSCs may be novel targets for treating metastatic cancer (Brackenbury et al. 2007; Yang et al. 2012). Prior to the work described in this dissertation and in Chioni et al. (Chioni et al. 2009), little work had been done to address the potential role of VGSC β subunits in cancer. We hypothesized that β subunits might be involved in other cancer subtypes.

Expression datasets from cultured cancer cell lines suggests that *SCN1B* mRNAs are observed in prostate cancer and may correlate with high metastatic potential (Diss et al. 2008). Interestingly, the expression level of *SCN1B* mRNA may correlate with increasing metastatic potential in prostate cancer cell lines (Diss et al. 2008). We observed the opposite trend in human breast cancer cell lines: β1 expression is high in weakly metastatic cells (MCF-7) and low in strongly metastatic cells (MDA-MB-231) (Chioni et al. 2009). In MCF-7 and MDA-MB-231 cells, *SCN1B*, *SCN4B*, and *SCN2B* mRNAs were detected while *SCN3B* mRNA was not detected. We observed elevated levels of β subunit mRNAs in MCF-7 cells relative to MDA-MB-231 cells. Importantly,

SCN1B mRNA was found to be the most abundant β subunit mRNA in both cell lines and MCF-7 cells were enriched in β1 mRNA and protein compared to MDA-MB-231 cells. siRNA-mediated reduction of β1 expression in MCF-7 cells reduced cell-substrate adhesion and increased migration. The change in migration was reversed by tetrodotoxin (TTX), suggesting that changes in VGSC α subunit expression might be induced following β1 knockdown. We observed that the amount of nNav1.5 mRNA and protein were elevated following β1 down-regulation. Stable expression of β1 in MDA-MB-231 cells promoted cell-cell adhesion and decreased lateral motility and proliferation. Importantly, this reduction in cell migration occurred in the presence of increased functional VGSC activity. Taken together, these observations suggest that β1 subunits are novel cell adhesion molecules in human breast cancer cell lines and β1 functions both in the modulation of VGSC α subunits and the regulation of cellular migration.

Chapter III

SCN1B, encoding the β1 subunit, encodes both an accessory subunit of the VGSC as well as an Ig-CAM (Isom et al. 1992). β1 is expressed in neurons and glia during postnatal development and plays important roles in brain development (**Table 1.2**). Disruption of β1 function or expression can result in pathogenesis in human patients and transgenic mice including epilepsy and ataxia (Wallace et al. 1998; Chen et al. 2004; Patino et al. 2009). Defects in hippocampal, cerebellar, and corticospinal tract microorganization in *Scn1b* null mice lacking β1 subunit expression suggests a role for β1 in neuronal migration, axon outgrowth, and axonal pathfinding (Davis et al. 2004; Brackenbury et al. 2008a; Brackenbury et al. 2013). β1-β1 *trans* homophilic adhesion promotes neurite outgrowth of cerebellar granule neurons (CGNs) via a mechanism that requires fyn kinase (Davis et al. 2004; Brackenbury et al. 2008a). β1 is known to be subject to post-translational modification, including tyrosine phosphorylation (Malhotra

et al. 2002). We hypothesized that post-translational modifications are essential to the β1-mediated neurite outgrowth signaling cascade.

β1-β1 *trans* homophilic adhesion recruits ankyrin to points of cell-cell contact and increases neurite outgrowth in cultured neurons (Malhotra et al. 2000; Davis et al. 2004). We postulated these two processes might be linked. Further, β1 phosphomimetic mutant, β1Y181E, is adhesion-competent, but does not recruit ankyrin to points of cell-cell contact (Malhotra et al. 2002). We predicted that β1 tyrosine phosphorylation functions as a regulatory switch in the pathway leading to neurite outgrowth. We virally expressed β1 and phosphomimetic β1Y181E in *Scn1b* null CGNs to examine a possible effect of pY- β1 on neurite outgrowth. We observed elevated neurite outgrowth in CGNs expressing β1Y181E. This result suggested that tyrosine phosphorylation of β1 occurs downstream of the initiating event, β1-β1 *trans* homophilic adhesion, and is an important downstream step in β1-mediated neurite outgrowth. Further, the level of phosphorylation of β1 increases in aggregate culture. This result provides additional evidence that β1 adhesive contacts affect the extent of phosphorylation of β1. A kinase assay suggested β1 as a putative substrate of fyn kinase, a member of the src kinase family. Our results suggest a model where tyrosine phosphorylation of β1 occurs downstream of adhesion, possibly by fyn kinase, and this phosphorylation event is important for propagating the signal to second messengers.

Chapter IV

VGSC are heterotrimeric complexes containing a single pore-forming α subunit, a non-covalently linked β1 or β3 subunit, and a covalently linked β2 or β4 subunit (Catterall 2012). β2 subunits (encoded by *Scn2b*) are linked to the ion-conducting α subunit via disulfide bond and are present in brain, peripheral nerve, and heart (Isom et al. 1995a; Dhar Malhotra et al. 2001; Lopez-Santiago et al. 2006). Covalent linkage of α to β2 and insertion into the plasma membrane occur simultaneously and are the final

steps in sodium channel biosynthesis in primary neurons (Schmidt and Catterall 1986). *Scn2b* null mice lacking β2 subunits display reduced tetrodotoxin-sensitive (TTX-S) sodium current density in brain and small dorsal root ganglion (DRG) neurons, altered voltage dependence of sodium current inactivation, reduced sensitivity to pain, increased susceptibility to seizures, and compromised action potential conduction (Lopez-Santiago et al. 2006; Chen et al. 2002).

The specific cysteine residue(s) involved in α/β2 covalent linkage had not been identified prior to this study. Given that disulfide bonds are generally unstable in the reducing environment of the cytosol, we predicted that covalent linkage of α to β2 may occur at the extracellular face of the plasma membrane. Using mutagenesis, we determined that a single cysteine-to-alanine substitution at the β2 extracellular residue C26 is sufficient to disrupt the formation of α-β2 covalent complexes *in vitro*. Disruption of the α/β2 covalent linkage *in vitro* by co-expression of Nav1.1 with β2C26A decreased sodium current density, possibly as a result of intracellular retention of a population of α subunits. We observed that β2, but not β2C26A, traffics to nodes of Ranvier and heminodes in a primary myelinating co-culture system. In cultured hippocampal neurons, β2, but not β2C26A, is enriched in the AIS and resistant to live cell detergent extraction. Thus, covalent linkage of β2 to α is essential for proper targeting of this subunit to specialized subcellular neuronal compartments.

Future Directions

Role of VGSCs in Cancer

There are many remaining questions regarding the role of β1 in cancer. The first step will be to establish a comprehensive dataset on the expression of *SCN1B* in breast cancer to address the following questions: (1) is *SCN1B* mRNA expressed in primary

tissue from human breast cancer?; (2) is β1 protein expressed in primary tissue from human breast cancer?; (3) is expression of *SCN1B* in breast cancer common or rare?; and (4) does expression of *SCN1B* in human breast cancer correlate with any clinical traits? To address these concerns, we will need to utilize public microarray datasets such as those found in Oncomine to examine *SCN1B* mRNA expression in cell lines and primary tissues. In addition, we will need to gain access to primary tissue through collaboration with colleagues at the University of Michigan Comprehensive Cancer Center. Using IHC to survey β1 expression in a tissue microarray would provide a useful dataset for expression in patient samples. We anticipate expression of *SCN1B* in a proportion of human breast cancer samples, and that expression levels may inversely correlate with metastatic potential.

As described above, *in vitro* data suggest that β1 increases adhesion and reduces cell migration in human breast cancer cells. However, a possible role for β1 in the regulation of cancer cell invasion has not been directly tested. It will be critical to use a matrigel invasion assay, a modified version of a classic Boyden chamber assay. Cells are plated onto a filter pre-coated with matrigel and induced to invade through the matrigel via a chemotactic gradient. The number of invaded cells 24 hours post plating provides a measure of *in vitro* invasiveness. I would predict that, due to its effects on adhesion and migration, β1 expressing cells will display reduced invasion. It is conceivable that β1 may interact with ECM components of matrigel, which may enhance or impede the invasive behavior of β1 expressing cells.

It will be important to test the *in vivo* effect of β1 on tumorigenesis and metastatic potential. One model to study these processes *in vivo* is to use a xenograft, an insertion of cultured cancer cells into immune-compromised mice (NOD-SCID mice). To do this, the MDA-MB-231 cell lines stably expressing GFP (negative control) and β1-GFP would be grown in 3D culture in matrigel and injected into the mammary fat pad of NOD-SCID mice. The effect of β1 on tumor growth would be evaluated by measuring tumor volume

and by histological analysis. The effect of β1 on metastasis would be evaluated by counting the number of secondary tumors, measuring the tumor volume of secondary tumors, and by monitoring the levels of circulating tumor cells in the bloodstream. As β1 expression reduced cell cycle progression in MDA-MB-231 cells, I would predict that β1 expressing xenografts are reduced in size relative to control xenografts and that β1 expressing xenografts would display reduced metastatic potential. These results would support the proposal that β1 expression is dynamically regulated in the transition to metastatic disease.

One significant caveat with xenograft based experiments is the disrupted immune system in NOD-SCID mice. Also, xenografts do not replicate the entire tumorigenesis process as the cancers do not arise spontaneously in the host. Use of a genetic driver of breast cancer allows for investigation of tumorigenesis and metastasis in host-derived cancer in mice with normal immune systems (Khanna and Hunter 2005). An example of such a driver (MMTV-PyMT) uses the mouse mammary tumor virus promoter to drive expression of the polyomavirus middle T oncogene (Guy et al. 1992). To assay the effect of β1 subunits on cancer tumorigenesis and metastasis in such a model, cancers would need to be generated in mice containing and lacking *Scn1b* alleles. Conditional knockout of *Scn1b* in this experiment design is necessary; global knockout of *Scn1b* results in postnatal lethality at approximately P20, before the formation of metastatic disease with the MMTV-PyMT driver. In order to conditionally ablate β1 expression, a conditional *Scn1b* null allele (Chen et al. 2007) would need to be combined with an allele which drives Cre recombinase expression in mammary tissue. One possible system, WAP-Cre, utilizes the promoter of the whey acidic protein promoter to drive expression of Cre recombinase specifically in mammary tissue (Wagner et al. 1997). The effect of β1 on tumor growth and metastasis would be evaluated similarly to that described above for the xenograft model, namely histological analysis, measurements of tumor volume, counting the number of secondary tumors, and monitoring of cancer cells circulating in the

bloodstream. Our hypothesis is that *Scn1b* null mice would harbor more secondary tumors and elevated levels of circulating tumor cells due to elevated metastatic potential. Further, because β1 expression reduced cell cycle progression in MDA-MB-231 cells, *Scn1b* null tumors might display increased tumor volume.

Previous experiments testing the metastatic potential of β1 expressing cells were performed in 2D culture. It is possible that β1 CAM interactions in 3D and in the complex *in vivo* microenvironment will change how it functions in breast cancer cells. We may find that β1 expressing tumors have unchanged or increased metastatic potential relative to tumors lacking β1 expression. It could be that β1 adhesive events in 3D *in vivo* result in signaling cascades reminiscent of that for β1-mediated neurite outgrowth which are not fully recapitulated in standard 2D culture. In an *in vivo* model of breast cancer, β1 appears to promote tumor growth and metastasis (personal communication, Dr. William Brackenbury). This suggests a potential role for β1 as a CAM and signaling molecule in breast cancer akin to β1-mediated neurite outgrowth in CGNs. Importantly, this observation suggests β1as a novel target for therapeutic intervention.

β1-β1 trans homophilic adhesion initiates a neurite outgrowth signaling cascade

β1 signaling is abrogated in *Scn1b* null mice which results in neuronal patterning defects that precede the onset of seizures. β1 signaling as a cell adhesion molecule is proposed to contribute to postnatal brain development. There are significant gaps in knowledge regarding β1-mediated neurite outgrowth.

It will be important to investigate the role of tyrosine phosphorylation of β1 in postnatal brain development. BAC transgenes could be generated which express phosphomimetic β1 (β1Y181E) or phosphodead β1 (β1Y181A or β1Y181F). Transgenic mice could then be bred with *Scn1b* null mice to replace the endogenous transcripts encoding β1 with the phosphomimetic or phosphodead β1 mutants. The animals may display overt phenotypes, including spontaneous seizures, ataxia, or prenatal lethality,

though it is quite possible that the phenotypes may be more subtle in nature than the DS phenotype observed in *Scn1b* null mice. Of most interest will be to perform immunohistochemical analysis of cell migration and axonal outgrowth and pathfinding to ask whether tyrosine phosphorylation of β1 plays a role in β1 CAM signaling *in vivo*. Based on previous data informing our model, I would expect phosphomimetic β1 expressing transgenic mice to display neuronal patterning defects due to overactive signaling. While I would also predict to observe neuronal patterning defects in phosphodead β1 expressing mice, in this case the defects would likely be due to reduced signaling. In other words, locking β1 into an 'on' or 'off' conformation is predicted to result in developmental defects due to the inability of the mutant β1 protein to naturally cycle between conformations in response to β1-β1 *trans* homophilic adhesion.

We observed that a β1 peptide is a fyn kinase substrate *in vitro* (Chapter III). In addition, we previously showed that fyn is required for β1-mediated neurite outgrowth (Brackenbury et al. 2008a). Taken together, these data suggest the potential for a protein-protein interaction between β1 and fyn. Furthermore, fyn, like other members of the src kinase family, contains an SH2 domain which binds intracellularly to tyrosine phosphorylated proteins and this is important in the regulation of fyn kinase activity (Harrison 2003). I hypothesize that β1 associates with fyn, and that the interaction may be modulated by tyrosine phosphorylation of β1. These hypotheses could first be tested by co-immunoprecipitation experiments in transfected 1610 cells which endogenously express fyn and can be transfected or virally transduced to express phosphomimetic (β1Y181E) or phosphodead (β1Y181A or β1Y181F) mutants of β1. It will be important to test for co-immunoprecipitation in both raft and non-raft fractions, as both β1 and fyn are reported to partition to both raft and non-raft membrane fractions (Brackenbury et al. 2008a). Preliminary data from our laboratory (T. Davis, E. Slat, and L. Isom, unpublished results) suggested that β1 and fyn can be co-immunoprecipitated from transfected 1610 cell Triton X-100-solubilized lysates. However, these investigators found that the

association was difficult to capture biochemically and these proteins may interact only transiently. I would predict that the association of phosphomimetic β1Y181E with fyn will be robust while the association of wildtype β1 and fyn is likely to be transient and difficult to capture. Phosphodead mutant constructs (β1Y181A and β1Y181F) may not associate with fyn kinase or may associate only transiently with fyn. Future experiments using co-immunoprecipitation from rodent brain membranes will be important to ask whether or not it is possible to capture the association between β1 and fyn *in vivo*. If transgenic mice expressing phosphomutant β1 proteins are generated as discussed above, it would be useful to assess whether phosphomimetic β1 or phosphodead β1 associates with fyn kinase *in vivo*. The investigation of association between β1 and fyn will be an important avenue of investigation in the future.

Based on our evidence that fyn kinase is an essential member of the β1-mediated neurite outgrowth signaling cascade and that the β1 intracellular domain peptide is a fyn kinase substrate, it would be important to further explore the placement of fyn in the signaling cascade. One possibility is that fyn signals upstream of β1 and phosphorylates β1. Another possibility is that fyn lies both upstream and downstream of β1. As mentioned above, the intracellular binding of fyn's SH2 domain to tyrosine phosphorylated proteins is important in the regulation of fyn kinase activity. Therefore, fyn phosphorylation of β1 may feed back and result in increased fyn activity. To test this hypothesis, it would be important to ask whether inhibition of fyn kinase activity blocks neurite outgrowth induced by expression of phosphomimetic β1Y181E in *Scn1b* null cerebellar granule neurons and in the absence of β1-β1 *trans* homophilic adhesion. Inhibition of fyn kinase activity can be achieved in a number of ways, some of which include using *Fyn* null mice (Brackenbury et al. 2008a) or src family kinase inhibitors PP2 and SU6656.

While characterization of β1 as a cell adhesion signaling molecule has been primarily performed in cultured cerebellar granule neurons, *in vivo* evidence suggests it

may function similarly in other types of neurons, including hippocampal neurons. It will be important to perform neurite outgrowth experiments using different neuronal subtypes, including neurons isolated from hippocampus, cortex, and DRG, plated onto β1 expressing or control fibroblast monolayers to ask whether β1 signaling is broadly similar or cell type specific in these different lineages.

The discovery of a noncanonical signaling pathway for β1 as a CAM continues to offer new questions to address. Considering that the loss of this signaling pathway likely contributes to the severe phenotype in *SCN1B*-linked DS and in *Scn1b* null mice, it is important to characterize this signaling pathway as it may yield targets for the development of novel therapeutic strategies for *SCN1B*-linked DS.

Post-translational modification of VGSC β1 is a key regulatory step in cellular signaling

We observed that β1Y181E drives neurite outgrowth in cerebellar granule neurons in the absence of β1-β1 *trans* homophilic adhesion. This suggests a role for post-translational modification, especially tyrosine phosphorylation, of β1 in the β1-mediated neurite outgrowth signaling cascade. There are significant gaps in knowledge regarding the post-translational modification of β1.

It would be of interest to investigate the developmental timing of tyrosine phosphorylation of β1. If, in neurons, tyrosine phosphorylation of β1 mainly functions in neurite outgrowth, one might expect that tyrosine phosphorylation of β1 to occur during the critical postnatal period of brain development. But does tyrosine phosphorylation of β1 persist or wane after this important developmental window? If it persists, does it play important roles in signaling, perhaps in neuronal migration or axonal pathfinding of newly born neurons?

Tyrosine phosphorylation of β1 may also be related to lipid rafts. β1 is present in both raft and non-raft fractions of brain membrane preparations (Brackenbury et al.

2008a). However, the partitioning of pY-β1 has not been investigated. Immunoprecipitation of β1 from raft and non-raft fractions of brain membranes would allow for analysis of pY-β1. pY-β1 may favor lipid raft compartments, as lipid rafts have been proposed as signaling centers in neurite outgrowth (Taylor and Hooper 2006). An important follow-up to this line of inquiry would be to ascertain whether tyrosine phosphorylation of β1 affects the partitioning of β1 into lipid raft microenvironments, or whether phosphorylation is simply favored in one microenvironment due to the expression of kinases and phosphatases in each compartment. The use of mutants mimicking tyrosine phosphorylation (β1Y181E) or lacking sites for phosphorylation (β1Y181A or β1Y181F) would be useful for this approach. One potential caveat here is that the abundance of pY-β1 may be limiting and thus may require a more sensitive technique, such as mass spectrometry.

pY-β1 colocalizes with Nav1.5 at intercalated disks within cardiac myocytes, while non-phosphorylated β1 colocalizes with TTX-S channels at the T-tubules (Malhotra et al. 2004). These data suggest that tyrosine phosphorylation of β1Y181 regulates its cellular targeting, at least in ventricular myocytes. Alternatively, the colocalization of kinases, such as fyn, for which β1 is a substrate, with β1 may fully or partially determine the cellular compartments containing pY-β1. In either case, the presence of pY-β1 in subcellular compartments may suggest active involvement of β1 in cellular signaling in these particular compartments. What cellular compartment(s) contain pY-β1 in cultured neurons and in neurons *in vivo*? β1 is reported to partition to the cell soma, the AIS, nodes of Ranvier, and the growth cone, but the subcellular localization of pY-β1 in neurons is not known. ICC and IHC using an antibody which selectively binds pY-β1 will allow insight into this question. Of particular importance is the growth cone, as we would predict enrichment of pY-β1 within the growth cone of neurites in which active β1 adhesive contacts are being made. While a high-quality anti-pY-β1 antibody is

not currently available, we have precedence that generation of this tool is possible, albeit difficult (Malhotra et al. 2002).

Tyrosine phosphorylation and proteolytic cleavage of β1 are two post-translational modifications with the potential to regulate β1 expression, localization, and function. β1 is cleaved sequentially in a model where first the ectodomain is shed by BACE activity, which results in a transmembrane segment-containing C-terminal fragment (β1CTF) (Wong et al. 2005). This is followed by γ-secretase activity, which converts the β1CTF into a soluble protein containing only the intracellular domain of β1 (β1ICD) (Wong et al. 2005). This sequential cleavage paradigm is similar to what has been described for amyloid precursor protein (APP) (O'Brien and Wong 2011). To confirm proteolytic cleavage of β1, we examined the different species of GFP immunoreactive bands using immunoblotting of total cell lysates and membrane preparations from MDA-MB-231 cells stably expressing β1GFP. In preliminary experiments, we observed three GFP immunoreactive bands in total cell lysates (**Figure 5.1**). In agreement with the current model, the Mr of the cleavage products reported here match those reported for β1CTF and β1ICD. Importantly, β1CTF is present in both total cell lysates and membrane preparations, whereas β1ICD is present in total cell lysates but not membrane preparations, suggesting that β1CTF has an intact transmembrane domain and β1ICD contains only residues corresponding to the intracellular domain of β1.

Is it possible that proteolytic processing and tyrosine phosphorylation might be linked? To test this hypothesis, MDA-MB-231 cells stably expressing β1-GFP were grown in the presence of low-dose trypsin and EDTA to artificially enhance proteolytic cleavage of the extracellular domain of β1 (**Figure 5.2**). Importantly, but preliminarily, robust tyrosine phosphorylation of β1GFP-CTF (containing the transmembrane domain and intracellular domain of β1 fused to eGFP) was observed under these conditions (**Figure 5.2**). β1CTF appears to be a robust kinase substrate, suggesting it may be a kinase substrate in neurons or myoyctes. Given that β1CTF and β1ICD share the same C-

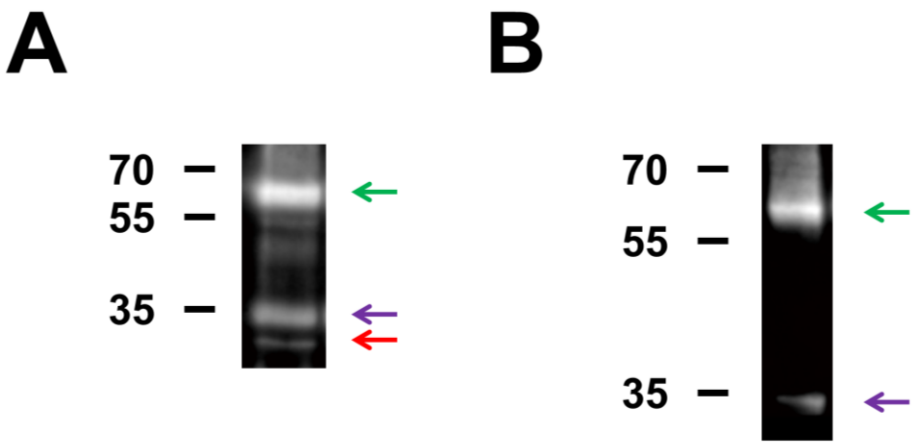

Figure 5.1. Proteolytic cleavage of β1 in MDA-MB-231 cells. In addition to full-length β1, total lysates prepared from MDA-MB-231 cells stably expressing β1GFP contain two cleavage products corresponding to β1CTF (purple arrow) and β1ICD (red arrow) in addition to full-length β1GFP (green arrow) (A). Membrane preparations prepared from MDA-MB-231 cells stably expressing β1GFP contain a single cleavage product corresponding to β1CTF (purple arrow) in addition to full-length β1GFP (green arrow) (B). These results are in agreement with the sequential cleavage model (Wong et al. 2005). β1CTF is the result of ectodomain shedding and contains the transmembrane domain and intracellular domain of β1. β1ICD is the result of cleavage of β1CTF at the membrane which releases the intracellular domain of β1 as a soluble protein.

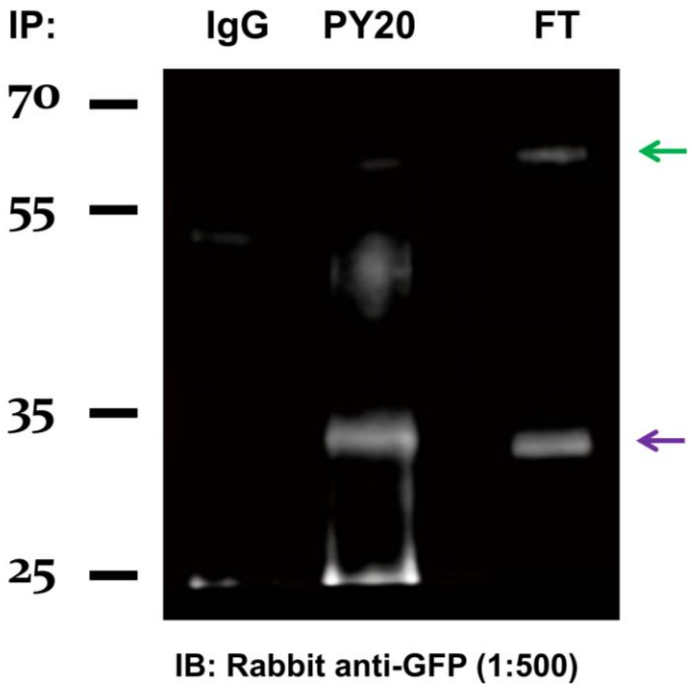

Figure 5.2. β1CTF is tyrosine phosphorylated. Tyrosine phosphorylated proteins were immunoprecipitated (anti-PY20 antibody) from protein samples collected from confluent monolayers of MDA-MB-231 cells stably transfected with β1GFP and treated with low dose trypsin-EDTA to enhance proteolytic cleavage. Protein samples used were membrane preparations using standard centrifugation following homogenization. As a control, non-immune mouse IgG was used in the immunoprecipitation. A cleavage fragment, β1CTF-GFP (purple arrow; ~35 kDa), is detected in both the tyrosine phosphorylation immunoprecipitation (middle lane) as well as the flowthrough from the control IgG IP (right lane). Full-length β1GFP (green arrow; ~64kDa) is also detected in the flowthrough from the control IP (right lane). This figure is representative of five independent experimental repeats.

terminal domain, β1ICD may also be a kinase substrate. Future work will be necessary to address whether β1CTF and β1ICD are physiological kinase substrates and what roles they play in cellular signaling.

Currently, the potential role for proteolytic cleavage of β1 in cellular signaling is unclear. Inhibition of γ-secretase, responsible for the cleavage of transmembrane β1CTF into β1ICD, is sufficient to abrogate β1-mediated neurite outgrowth (Brackenbury and Isom 2011). This observation suggests proteolytic cleavage of β1 may be important in signaling downstream of β1-β1 *trans* homophilic adhesion. However, γ-secretase has substrates other than β1, including APP (De Strooper et al. 1998), Notch (De Strooper et al. 1999), ErbB4 (Ni et al. 2001), E-cadherin (Marambaud et al. 2002), and EphrinB2 (Georgakopoulos et al. 2006), so we cannot rule out the possibility that γ-secretase cleavage of substrates other than β1 are necessary for β1-mediated neurite outgrowth. Further experiments will be required to tease out the importance of proteolytic cleavage of β1. The generation of mutant β1 cDNA constructs that prevent proteolytic processing would provide useful tools to interrogate the role of proteolytic cleavage of β1.

Recently, the potential for threonine phosphorylation of β1 was reported in a large proteomic screen of mouse brain membranes (Trinidad et al. 2012). While threonine phosphorylation of β1 will need to be validated to ensure the validity of the modification, it is certainly intriguing. It will be interesting to ask whether the threonine phosphorylation of β1 is dynamically regulated and whether it serves a significant role in regulating the expression, localization, or function of β1.

We have provided evidence herein that tyrosine phosphorylation of β1 plays an important role in a noncanonical signaling pathway initiated by β1-β1 *trans* homophilic adhesion. Furthermore, β subunits, including β1, are cleaved sequentially and the cleavage products may play roles in signaling and gene expression. The investigation of post-translational modification of β1 is an important area for future investigation.

Role of β subunits in trafficking of VGSCs

Evidence from multiple model systems suggests a role for VGSC β subunits at regulating cell surface expression and subcellular targeting of VGSC α subunits (Isom et al. 1992; Isom et al. 1995a; Chen et al. 2002). The covalent α-β2 linkage plays important roles in VGSC biosynthesis and trafficking (Schmidt and Catterall 1986). We report herein the identification of the cysteine residue on β2 which forms a disulfide bond with α subunits, an important step in better understanding the covalent α-β2 linkage. However, the cysteine residue(s) on the α subunit which forms a disulfide bond with β2 has not been identified. Identification of this crucial cysteine residue(s) on the α subunit will improve our understanding of VGSC biosynthesis and trafficking. By employing a similar strategy to that used in Chapter Four, mutagenesis of cysteine residues on the α subunit is likely the simplest approach to identifying the exact residue(s) that bind the β2 subunit. It is worth noting that, while certainly feasible to accomplish, the cDNA encoding α subunits is large and extremely prone to rearrangement, which makes the cloning of mutant cDNAs challenging. *In silico* analysis suggests that of the twelve candidate residues, three are more likely based on evolutionary conservation (see Chapter IV and **Figure 4.6**).

Transgenic mice and gene transfer techniques open the door to further expand our understanding of VGSC α and β subunit protein trafficking within primary cells including neurons and myocytes. However, primary cells express endogenous α and β subunits, complicating both experimental design and data interpretation. Additionally, there may be functional redundancy in the β subunit family, which complicates data interpretation.

Does β subunit CAM activity vary by cell type and by cellular compartment?

VGSC β subunits are expressed in a variety of cell types, including neurons, myocytes, and glia (**Table 1.2**). Additionally, β subunits target to specific subcellular compartments, including the AIS, nodes of Ranvier, growth cones, intercalated disks, and

T-tubules (reviewed in **Chapter I**). We propose that expression levels of homophilic and heterophilic binding partners, as well as their cellular compartmentalization, may be important influences on the binding of β subunit CAM domains.

In order to test this, it will be necessary to generate and purify recombinant proteins of the β subunit extracellular (βex) loop, containing the Ig loop CAM domain. To generate recombinant βex molecules, cDNAs encoding the extracellular domains of β subunits can be cloned upstream and in-frame with the Fc region of human IgG1. The resulting molecules will be soluble CAMs that can be generated in mammalian cell lines and used to study CAM interactions. After generation of these β subunit CAMs, binding assays can be performed to assess binding to various cell types and to subcellular compartments. Importantly, cells can be isolated from *Scnxb* null mice lacking homophilic β subunits to separate homophilic and heterophilic binding events. The present lack of *Scn4b* null mice will complicate the analysis of β4 as a CAM. Utilization of 129P2/OlaHsd mice may partially alleviate the lack of *Scn4b* null mice. 129P2/OlaHsd mice are cardiac β4 hypomorphs, potentially allowing us to differentiate homophilic and heterophilic binding of β4 to cardiac myocytes (Remme et al. 2009). 129P2/OlaHsd mice express β4 subunits in brain, complicating the analysis of homophilic β4 CAM activity in neurons and glia (**Figure 5.3**).

Is proteolytic processing of β4 important for the generation of resurgent sodium current?

Multiple observations suggest that the β4 subunit is important for the generation of resurgent sodium current, or sodium influx mediated by VGSCs during repolarization, a phase of the action potential in which VGSCs are generally inactivated (Bean 2005). Resurgent sodium current is particularly important for high-frequency firing and is an adaptation in neurons such as cerebellar Purkinje neurons (Burgess et al. 1995; Raman and Bean 1997). The molecular mechanism underlying resurgent current proposes that an

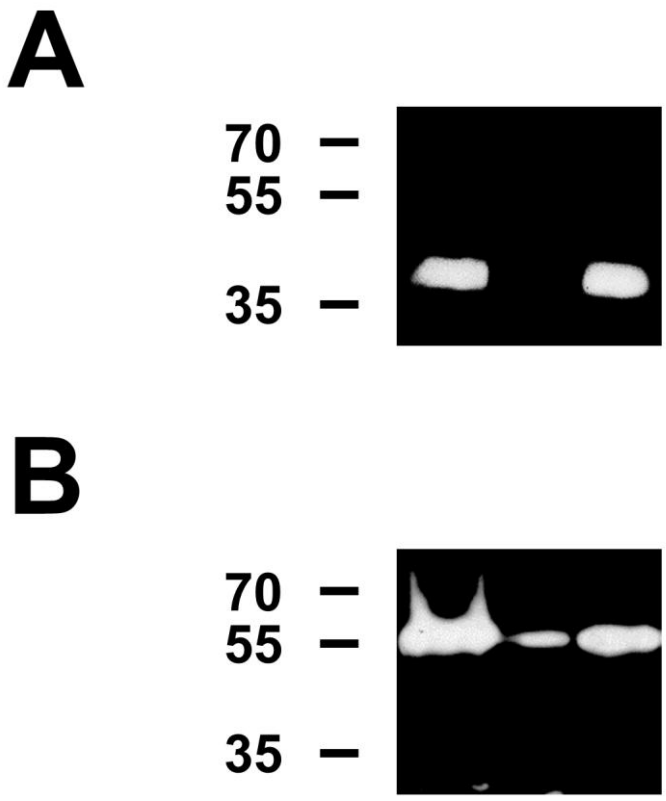

Figure 5.3. 129P2/OlaHsd mice are cardiac hypomorphs for β4. Membrane preparations from C57BL/6 brain (left lane), 129P2/OlaHsd heart (middle lane), and 129P2/OlaHsd brain (right lane) were immunoblotted with a rabbit polyclonal anti-β4 antibody to assay for β4 protein expression (A). The blot was stripped and reprobed for α-tubulin as a loading control (B). β4 expression is not detectable in 129P2/OlaHsd heart, in general agreement with (Remme et al. 2009). However, β4 protein is abundant in 129P2/OlaHsd brain.

endogenous blocking particle prevents classical channel inactivation, allowing for rapid channel recovery. A β4 C-terminal peptide is sufficient to rescue resurgent sodium current after protease treatment is performed to remove the activity of the endogenous blocking particle (Grieco et al. 2005). A C-terminal β4 peptide induces resurgent sodium current in a heterologous expression system lacking the endogenous blocking particle (Theile and Cummins 2011). siRNA-mediated knockdown of β4 expression in cultured CGNs results in diminished resurgent sodium current and decreased repetitive firing (Bant and Raman 2010). However, co-expression of full-length β4 and Nav1.6 subunits in a heterologous expression system is not sufficient to generate resurgent current (Chen et al. 2008).

We hypothesize that post-translational proteolytic processing of β4 in neurons is necessary to convert β4 into the endogenous open-channel blocking particle. To test this, it would be necessary to co-express β4 cleavage products with Nav1.6 in HEK cells. β4CTF, the product of ectodomain shedding which contains the transmembrane and intracellular domains of β4, and β4ICD, the product of γ-secretase cleavage, which contains only the intracellular domain of β4, should be tested to see if they generate resurgent sodium current when co-expressed with Nav1.6. In addition, co-expression of BACE or BACE and γ-secretase along with full-length β4 and Nav1.6 can be used to generate β4 cleavage products to ask whether they induce resurgent sodium current. It would be important to also test this hypothesis in neurons. Inhibitors of ectodomain sheddase activity and γ-secretase activity can be used to test if blockade of proteolytic activity affects resurgent sodium current in cultured CGNs or Purkinje neurons. I predict that blockade of proteolytic cleavage will reduce or completely block resurgent sodium current in HEK cells or cultured neurons. Furthermore, expression of β4 cleavage products alone will be sufficient to induce resurgent current when co-expressed with Nav1.6 in HEK cells.

Null mouse models have been generated for *Scn1b*, *Scn2b*, and *Scn3b*, and these mice have proven to be incredibly valuable tools for understanding the roles of β subunits *in vivo* (Chen et al. 2002; Chen et al. 2004; Hakim et al. 2008). However, generation of a *Scn4b* null mouse has remained elusive for the field. Generation of this transgenic animal would be incredibly useful for understanding the role of β4 *in vivo*.

Identification of genes that modify the *Scn1b* null DS phenotype

Scn1b null mice exhibit spontaneous seizures, ataxia, and postnatal lethality (Chen et al. 2004). *Scn1b* null mice are a model of DS (Chen et al. 2004; Patino et al. 2009), a catastrophic pediatric epileptic encephalopathy, and represent the opportunity to screen for modifier genes that modify *SCN1B*-linked DS. These modifier genes may represent novel therapeutic targets for treatment of DS.

To accomplish this, test crosses with $Scn1b^{+/-}$ mice congenic on C57BL/6 with mice from a small selection of other mouse strains would be performed to generate F1 $Scn1b^{+/-}$ mice with genomes derived from equivalent contributions of the C57BL/6 strain and the test strain. Mice from the F1 generation would then be crossed to generate F2 *Scn1b* null mice on a background that derives equally from C57BL/6 and the test strain. *Scn1b* null mice from the F2 cross would be compared to *Scn1b* null mice congenic on C57BL/6. Spontaneous seizure occurrence, seizure severity, postnatal survival, and gait analysis would then be measured. Test strains that affect the severity of the phenotype of *Scn1b* null mice would be selected for mapping of candidate modifier loci.

Identification of novel β subunit protein-protein interactions

VGSCs are heterotrimeric complexes composed of a single pore-forming α subunit, a non-covalently associated β subunit (β1 or β3), and a covalently associated β subunit (β2 or β4). In addition to forming a complex with VGSC α subunits, β1 interacts with a number of other proteins. As a CAM, β1 participates in both homophilic (with itself) and heterophilic (with other CAMs) interactions (Malhotra et al. 2000; McEwen

and Isom 2004). Heterophilic β1 CAM interactions include contactin, VGSC β2, N-cadherin, neurofascin-155 (NF155), neurofascin-186 (NF186), and NrCAM (McEwen and Isom 2004; Malhotra et al. 2004; Ratcliffe et al. 2001). β1-β1 *trans* homophilic adhesion is sufficient to induce both cellular aggregation and ankyrin recruitment (Malhotra et al. 2000). β1 also binds ECM protein tenascin-R, suggesting a role for β1 in cell-matrix adhesion (Xiao et al. 1999). Recently, a proteomics approach identified a novel interaction between β1 and voltage-gated potassium channels (Marionneau et al. 2012). Thus, identification of novel protein-protein interactions for β1 has the possibility of helping us understand its unique role as both an ion channel modulator and a CAM.

An intriguing option to identify novel protein-protein interactions with VGSC β1 subunits is affinity chromatography using recombinant β1 proteins tethered to a solid support. Two proteins would be used: (1) β1Fc, a soluble CAM and fusion of the β1 extracellular domain to the Fc domain of human IgG1, and (2) GST-β1ICD, a fusion of the β1 intracellular domain to the widely used glutathione-S-transferase (GST) epitope tag. The resulting β1Fc and GST-β1ICD molecules could be generated in mammalian cells and bacteria, respectively. Potential β1Fc and GST-β1ICD interacting partners would be identified from rodent brain and heart lysates. Importantly, mutant constructs of these recombinant molecules could be utilized. Of particular interest is the phosphomimetic mutation β1Y181E, which may bind a different subset of proteins than β1.

Another approach to identifying novel protein-protein interaction partners is immunoprecipitation of β1 subunits followed by mass spectrometry to identify proteins which are also pulled down. Currently, the availability of high-quality anti-β1 antibodies is limiting which hinders such an approach. The Isom Lab has formed a collaboration with Cell Signaling Technologies™ to generate monoclonal rabbit β1 antibodies directed toward extracellular and intracellular epitopes. To date, we have identified one rabbit producing potentially suitable antibodies for the extracellular antigen and another for the

intracellular antigen (**Figure 5.4**). Hybridomas are currently being generated to screen for candidate monoclonal anti-β1 antibodies. If, as a result of this collaboration, β1 antibodies are available for this study, we would immunoprecipitate β1 from rodent brain and rodent heart and identify potential novel protein interaction partners using a strategy similar to the recent successful coimmunoprecipitation of β1 and voltage-gated potassium channels (Marionneau et al. 2012).

The use of *Scn1b* null lysates as a negative control would be incredibly valuable for both of these purification strategies. Additionally, Fc, GST, and nonimmune rabbit IgG tethered to a solid support would be used to control for proteins which bind specifically to the epitope tags or nonspecifically to rabbit IgG or the solid support. While the above experiments focus on the β1 subunit which is of the most immediate interest, the same basic strategy is applicable to identification of protein-protein interactions of other VGSC β subunits.

Conclusions

Our work on the role of β1 subunits in breast cancer has identified β1 as a novel CAM. Our results suggest *SCN1B* has roles in the regulation of cellular migration and the functional expression of VGSC α subunits in breast cancer cells. β1 may be a target for novel therapeutics and is a potential biomarker for metastatic potential.

Our work on post-translational modification of β1 has implicated tyrosine phosphorylation as a key step in β1-mediated neurite outgrowth. Our data suggest β1 is phosphorylated downstream of adhesion, possibly by fyn kinase, in order to disseminate the signal to second messengers.

We were successful in identifying the cysteine residue on VGSC β2 which forms disulfide bonds with α subunits. Further, we demonstrated that covalent linkage of α and β2 is essential for protein trafficking of β2 to the AIS and to nodes of Ranvier.

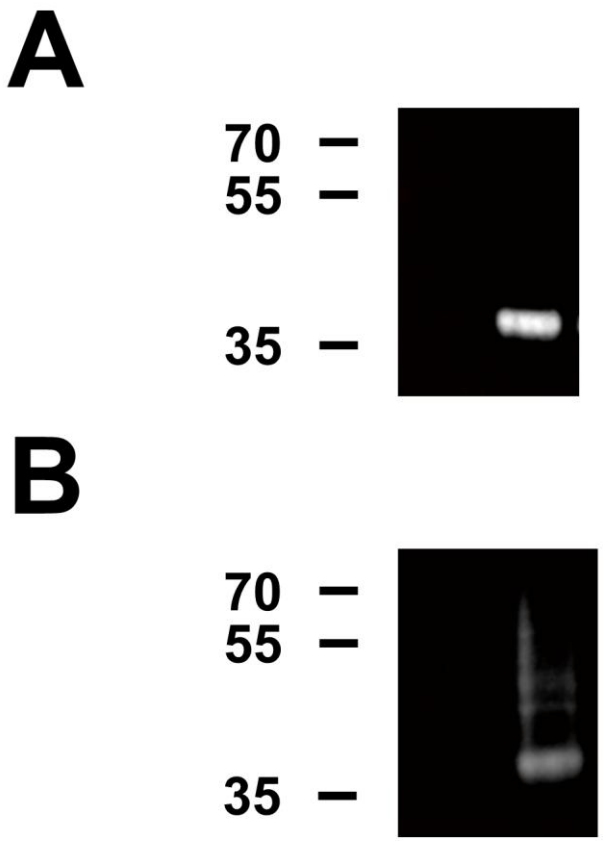

Figure 5.4. Characterization of novel anti-β1 antibodies. Rabbit anti-β1intra (A) and anti-β1ex (B) antibodies directed towards intracellular and extracellular epitopes, respectively, were tested by immunoblot on membrane preparations from 1610 cells lacking β1 expression (left lane) and 1610 cells stably expressing β1 (right lane). Of 6 rabbits tested, only two rabbits were found to produce selective anti-β1 antibodies (data above; data for negative rabbits not shown).

Bibliography

Abriel H, Kass RS (2005) Regulation of the voltage-gated cardiac sodium channel Nav1.5 by interacting proteins. Trends in cardiovascular medicine 15 (1):35-40.

Adachi K, Toyota M, Sasaki Y, Yamashita T, Ishida S, Ohe-Toyota M, Maruyama R, Hinoda Y, Saito T, Imai K, Kudo R, Tokino T (2004) Identification of SCN3B as a novel p53-inducible proapoptotic gene. Oncogene 23 (47):7791-7798.

Allen DH, Lepple-Wienhues A, Cahalan MD (1997) Ion channel phenotype of melanoma cell lines. The Journal of membrane biology 155 (1):27-34.

Aman TK, Grieco-Calub TM, Chen C, Rusconi R, Slat EA, Isom LL, Raman IM (2009) Regulation of persistent Na current by interactions between beta subunits of voltage-gated Na channels. The Journal of neuroscience : the official journal of the Society for Neuroscience 29 (7):2027-2042.

An RH, Wang XL, Kerem B, Benhorin J, Medina A, Goldmit M, Kass RS (1998) Novel LQT-3 mutation affects Na+ channel activity through interactions between alpha- and beta1-subunits. Circulation research 83 (2):141-146.

Arnestad M, Crotti L, Rognum TO, Insolia R, Pedrazzini M, Ferrandi C, Vege A, Wang DW, Rhodes TE, George AL, Jr., Schwartz PJ (2007) Prevalence of long-QT syndrome gene variants in sudden infant death syndrome. Circulation 115 (3):361-367.

Aronica E, Troost D, Rozemuller AJ, Yankaya B, Jansen GH, Isom LL, Gorter JA (2003) Expression and regulation of voltage-gated sodium channel beta1 subunit protein in human gliosis-associated pathologies. Acta neuropathologica 105 (5):515-523.

Audenaert D, Claes L, Ceulemans B, Lofgren A, Van Broeckhoven C, De Jonghe P (2003) A deletion in SCN1B is associated with febrile seizures and early-onset absence epilepsy. Neurology 61 (6):854-856.

Auld VJ, Goldin AL, Krafte DS, Marshall J, Dunn JM, Catterall WA, Lester HA, Davidson N, Dunn RJ (1988) A rat brain Na+ channel alpha subunit with novel gating properties. Neuron 1 (6):449-461.

Bant JS, Raman IM (2010) Control of transient, resurgent, and persistent current by open-channel block by Na channel beta4 in cultured cerebellar granule neurons. Proceedings of the National Academy of Sciences of the United States of America 107 (27):12357-12362.

Bean BP (2005) The molecular machinery of resurgent sodium current revealed. Neuron 45 (2):185-187.

Bennett ES, Smith BA, Harper JM (2004) Voltage-gated Na+ channels confer invasive properties on human prostate cancer cells. Pflugers Archiv : European journal of physiology 447 (6):908-914.

Brackenbury WJ (2012) Voltage-gated sodium channels and metastatic disease. Channels 6 (5):352-361.
Brackenbury WJ, Calhoun JD, Chen C, Miyazaki H, Nukina N, Oyama F, Ranscht B, Isom LL (2010) Functional reciprocity between Na+ channel Nav1.6 and beta1 subunits in the coordinated regulation of excitability and neurite outgrowth. Proceedings of the National Academy of Sciences of the United States of America 107 (5):2283-2288.
Brackenbury WJ, Chioni AM, Diss JK, Djamgoz MB (2007) The neonatal splice variant of Nav1.5 potentiates in vitro invasive behaviour of MDA-MB-231 human breast cancer cells. Breast cancer research and treatment 101 (2):149-160.
Brackenbury WJ, Davis TH, Chen C, Slat EA, Detrow MJ, Dickendesher TL, Ranscht B, Isom LL (2008a) Voltage-gated Na+ channel beta1 subunit-mediated neurite outgrowth requires Fyn kinase and contributes to postnatal CNS development in vivo. The Journal of neuroscience : the official journal of the Society for Neuroscience 28 (12):3246-3256.
Brackenbury WJ, Djamgoz MB (2006) Activity-dependent regulation of voltage-gated Na+ channel expression in Mat-LyLu rat prostate cancer cell line. The Journal of physiology 573 (Pt 2):343-356.
Brackenbury WJ, Djamgoz MB (2007) Nerve growth factor enhances voltage-gated Na+ channel activity and Transwell migration in Mat-LyLu rat prostate cancer cell line. Journal of cellular physiology 210 (3):602-608.
Brackenbury WJ, Djamgoz MB, Isom LL (2008b) An emerging role for voltage-gated Na+ channels in cellular migration: regulation of central nervous system development and potentiation of invasive cancers. The Neuroscientist : a review journal bringing neurobiology, neurology and psychiatry 14 (6):571-583.
Brackenbury WJ, Isom LL (2008) Voltage-gated Na+ channels: potential for beta subunits as therapeutic targets. Expert opinion on therapeutic targets 12 (9):1191-1203.
Brackenbury WJ, Isom LL (2011) Na Channel beta Subunits: Overachievers of the Ion Channel Family. Frontiers in pharmacology 2:53.
Brackenbury WJ, Yuan Y, O'Malley HA, Parent JM, Isom LL (2013) Abnormal neuronal patterning occurs during early postnatal brain development of Scn1b-null mice and precedes hyperexcitability. Proceedings of the National Academy of Sciences of the United States of America 110 (3):1089-1094.
Brette F, Orchard C (2003) T-tubule function in mammalian cardiac myocytes. Circulation research 92 (11):1182-1192.
Buffington SA, Rasband MN (2013) Na+ channel-dependent recruitment of navbeta4 to axon initial segments and nodes of ranvier. The Journal of neuroscience : the official journal of the Society for Neuroscience 33 (14):6191-6202.
Burgess DL, Kohrman DC, Galt J, Plummer NW, Jones JM, Spear B, Meisler MH (1995) Mutation of a new sodium channel gene, Scn8a, in the mouse mutant 'motor endplate disease'. Nature genetics 10 (4):461-465.
Calhoun JD, Isom LL (2013) The role of non-pore-forming beta subunits in physiology and pathophysiology of voltage-gated sodium channels. Handbook of Experimental Pharmacology.

Casula MA, Facer P, Powell AJ, Kinghorn IJ, Plumpton C, Tate SN, Bountra C, Birch R, Anand P (2004) Expression of the sodium channel beta3 subunit in injured human sensory neurons. Neuroreport 15 (10):1629-1632.
Catterall WA (1992) Cellular and molecular biology of voltage-gated sodium channels. Physiological reviews 72 (4 Suppl):S15-48.
Catterall WA (2000) From ionic currents to molecular mechanisms: the structure and function of voltage-gated sodium channels. Neuron 26 (1):13-25.
Catterall WA (2012) Voltage-gated sodium channels at 60: structure, function and pathophysiology. The Journal of physiology 590 (Pt 11):2577-2589.
Charalambous K, Wallace BA (2011) NaChBac: the long lost sodium channel ancestor. Biochemistry 50 (32):6742-6752.
Chen C, Bharucha V, Chen Y, Westenbroek RE, Brown A, Malhotra JD, Jones D, Avery C, Gillespie PJ, 3rd, Kazen-Gillespie KA, Kazarinova-Noyes K, Shrager P, Saunders TL, Macdonald RL, Ransom BR, Scheuer T, Catterall WA, Isom LL (2002) Reduced sodium channel density, altered voltage dependence of inactivation, and increased susceptibility to seizures in mice lacking sodium channel beta 2-subunits. Proceedings of the National Academy of Sciences of the United States of America 99 (26):17072-17077.
Chen C, Calhoun JD, Zhang Y, Lopez-Santiago L, Zhou N, Davis TH, Salzer JL, Isom LL (2012) Identification of the Cysteine Residue Responsible for Disulfide Linkage of Na+ Channel alpha and beta2 Subunits. The Journal of biological chemistry 287 (46):39061-39069.
Chen C, Dickendesher TL, Oyama F, Miyazaki H, Nukina N, Isom LL (2007) Floxed allele for conditional inactivation of the voltage-gated sodium channel beta1 subunit Scn1b. Genesis 45 (9):547-553.
Chen C, Westenbroek RE, Xu X, Edwards CA, Sorenson DR, Chen Y, McEwen DP, O'Malley HA, Bharucha V, Meadows LS, Knudsen GA, Vilaythong A, Noebels JL, Saunders TL, Scheuer T, Shrager P, Catterall WA, Isom LL (2004) Mice lacking sodium channel beta1 subunits display defects in neuronal excitability, sodium channel expression, and nodal architecture. The Journal of neuroscience : the official journal of the Society for Neuroscience 24 (16):4030-4042.
Chen Y, Yu FH, Sharp EM, Beacham D, Scheuer T, Catterall WA (2008) Functional properties and differential neuromodulation of Na(v)1.6 channels. Molecular and cellular neurosciences 38 (4):607-615.
Chioni AM, Brackenbury WJ, Calhoun JD, Isom LL, Djamgoz MB (2009) A novel adhesion molecule in human breast cancer cells: voltage-gated Na+ channel beta1 subunit. The international journal of biochemistry & cell biology 41 (5):1216-1227.
Chioni AM, Fraser SP, Pani F, Foran P, Wilkin GP, Diss JK, Djamgoz MB (2005) A novel polyclonal antibody specific for the Na(v)1.5 voltage-gated Na(+) channel 'neonatal' splice form. Journal of neuroscience methods 147 (2):88-98.
Chopra SS, Watanabe H, Zhong TP, Roden DM (2007) Molecular cloning and analysis of zebrafish voltage-gated sodium channel beta subunit genes: implications for the evolution of electrical signaling in vertebrates. BMC evolutionary biology 7:113.
Cirak S, Arechavala-Gomeza V, Guglieri M, Feng L, Torelli S, Anthony K, Abbs S, Garralda ME, Bourke J, Wells DJ, Dickson G, Wood MJ, Wilton SD, Straub V,

Kole R, Shrewsbury SB, Sewry C, Morgan JE, Bushby K, Muntoni F (2011) Exon skipping and dystrophin restoration in patients with Duchenne muscular dystrophy after systemic phosphorodiamidate morpholino oligomer treatment: an open-label, phase 2, dose-escalation study. Lancet 378 (9791):595-605.

Claes L, Del-Favero J, Ceulemans B, Lagae L, Van Broeckhoven C, De Jonghe P (2001) De novo mutations in the sodium-channel gene SCN1A cause severe myoclonic epilepsy of infancy. American journal of human genetics 68 (6):1327-1332.

Davis TH, Chen C, Isom LL (2004) Sodium channel beta1 subunits promote neurite outgrowth in cerebellar granule neurons. The Journal of biological chemistry 279 (49):51424-51432.

De Strooper B, Annaert W, Cupers P, Saftig P, Craessaerts K, Mumm JS, Schroeter EH, Schrijvers V, Wolfe MS, Ray WJ, Goate A, Kopan R (1999) A presenilin-1-dependent gamma-secretase-like protease mediates release of Notch intracellular domain. Nature 398 (6727):518-522.

De Strooper B, Saftig P, Craessaerts K, Vanderstichele H, Guhde G, Annaert W, Von Figura K, Van Leuven F (1998) Deficiency of presenilin-1 inhibits the normal cleavage of amyloid precursor protein. Nature 391 (6665):387-390.

Delmar M (2004) The intercalated disk as a single functional unit. Heart rhythm : the official journal of the Heart Rhythm Society 1 (1):12-13.

Deschenes I, Armoundas AA, Jones SP, Tomaselli GF (2008) Post-transcriptional gene silencing of KChIP2 and Navbeta1 in neonatal rat cardiac myocytes reveals a functional association between Na and Ito currents. Journal of molecular and cellular cardiology 45 (3):336-346.

Deschenes I, Tomaselli GF (2002) Modulation of Kv4.3 current by accessory subunits. FEBS letters 528 (1-3):183-188.

Dhar Malhotra J, Chen C, Rivolta I, Abriel H, Malhotra R, Mattei LN, Brosius FC, Kass RS, Isom LL (2001) Characterization of sodium channel alpha- and beta-subunits in rat and mouse cardiac myocytes. Circulation 103 (9):1303-1310.

Diaz D, Delgadillo DM, Hernandez-Gallegos E, Ramirez-Dominguez ME, Hinojosa LM, Ortiz CS, Berumen J, Camacho J, Gomora JC (2007) Functional expression of voltage-gated sodium channels in primary cultures of human cervical cancer. Journal of cellular physiology 210 (2):469-478.

Dib-Hajj SD, Waxman SG (2010) Isoform-specific and pan-channel partners regulate trafficking and plasma membrane stability; and alter sodium channel gating properties. Neuroscience letters 486 (2):84-91.

Ding Y, Brackenbury WJ, Onganer PU, Montano X, Porter LM, Bates LF, Djamgoz MB (2008) Epidermal growth factor upregulates motility of Mat-LyLu rat prostate cancer cells partially via voltage-gated Na+ channel activity. Journal of cellular physiology 215 (1):77-81.

Ding Y, Djamgoz MB (2004) Serum concentration modifies amplitude and kinetics of voltage-gated Na+ current in the Mat-LyLu cell line of rat prostate cancer. The international journal of biochemistry & cell biology 36 (7):1249-1260.

Diss JK, Archer SN, Hirano J, Fraser SP, Djamgoz MB (2001) Expression profiles of voltage-gated Na(+) channel alpha-subunit genes in rat and human prostate cancer cell lines. The Prostate 48 (3):165-178.

Diss JK, Fraser SP, Walker MM, Patel A, Latchman DS, Djamgoz MB (2008) Beta-subunits of voltage-gated sodium channels in human prostate cancer: quantitative in vitro and in vivo analyses of mRNA expression. Prostate cancer and prostatic diseases 11 (4):325-333.

Diss JK, Stewart D, Pani F, Foster CS, Walker MM, Patel A, Djamgoz MB (2005) A potential novel marker for human prostate cancer: voltage-gated sodium channel expression in vivo. Prostate cancer and prostatic diseases 8 (3):266-273.

Djamgoz MBA, Mycielska M, Madeja Z, Fraser SP, Korohoda W (2001) Directional movement of rat prostate cancer cells in direct-current electric field: involvement of voltagegated Na+ channel activity. Journal of cell science 114 (Pt 14):2697-2705.

Dzhashiashvili Y, Zhang Y, Galinska J, Lam I, Grumet M, Salzer JL (2007) Nodes of Ranvier and axon initial segments are ankyrin G-dependent domains that assemble by distinct mechanisms. The Journal of cell biology 177 (5):857-870.

Eckford PD, Li C, Ramjeesingh M, Bear CE (2012) Cystic fibrosis transmembrane conductance regulator (CFTR) potentiator VX-770 (ivacaftor) opens the defective channel gate of mutant CFTR in a phosphorylation-dependent but ATP-independent manner. The Journal of biological chemistry 287 (44):36639-36649.

Ellerkmann RK, Remy S, Chen J, Sochivko D, Elger CE, Urban BW, Becker A, Beck H (2003) Molecular and functional changes in voltage-dependent Na(+) channels following pilocarpine-induced status epilepticus in rat dentate granule cells. Neuroscience 119 (2):323-333.

Escayg A, Goldin AL (2010) Sodium channel SCN1A and epilepsy: mutations and mechanisms. Epilepsia 51 (9):1650-1658.

Escayg A, MacDonald BT, Meisler MH, Baulac S, Huberfeld G, An-Gourfinkel I, Brice A, LeGuern E, Moulard B, Chaigne D, Buresi C, Malafosse A (2000) Mutations of SCN1A, encoding a neuronal sodium channel, in two families with GEFS+2. Nature genetics 24 (4):343-345.

Fahmi AI, Patel M, Stevens EB, Fowden AL, John JE, 3rd, Lee K, Pinnock R, Morgan K, Jackson AP, Vandenberg JI (2001) The sodium channel beta-subunit SCN3b modulates the kinetics of SCN5a and is expressed heterogeneously in sheep heart. The Journal of physiology 537 (Pt 3):693-700.

Fein AJ, Meadows LS, Chen C, Slat EA, Isom LL (2007) Cloning and expression of a zebrafish SCN1B ortholog and identification of a species-specific splice variant. BMC genomics 8:226.

Fein AJ, Wright MA, Slat EA, Ribera AB, Isom LL (2008) scn1bb, a zebrafish ortholog of SCN1B expressed in excitable and nonexcitable cells, affects motor neuron axon morphology and touch sensitivity. The Journal of neuroscience : the official journal of the Society for Neuroscience 28 (47):12510-12522.

Fendri-Kriaa N, Kammoun F, Salem IH, Kifagi C, Mkaouar-Rebai E, Hsairi I, Rebai A, Triki C, Fakhfakh F (2011) New mutation c.374C>T and a putative disease-associated haplotype within SCN1B gene in Tunisian families with febrile seizures. European journal of neurology : the official journal of the European Federation of Neurological Societies 18 (5):695-702.

Filbin MT, Tennekoon GI (1993) Homophilic adhesion of the myelin P0 protein requires glycosylation of both molecules in the homophilic pair. The Journal of cell biology 122 (2):451-459.

Fraser SP, Ding Y, Liu A, Foster CS, Djamgoz MB (1999) Tetrodotoxin suppresses morphological enhancement of the metastatic MAT-LyLu rat prostate cancer cell line. Cell and tissue research 295 (3):505-512.

Fraser SP, Diss JK, Chioni AM, Mycielska ME, Pan H, Yamaci RF, Pani F, Siwy Z, Krasowska M, Grzywna Z, Brackenbury WJ, Theodorou D, Koyuturk M, Kaya H, Battaloglu E, De Bella MT, Slade MJ, Tolhurst R, Palmieri C, Jiang J, Latchman DS, Coombes RC, Djamgoz MB (2005) Voltage-gated sodium channel expression and potentiation of human breast cancer metastasis. Clinical cancer research : an official journal of the American Association for Cancer Research 11 (15):5381-5389.

Fraser SP, Diss JK, Lloyd LJ, Pani F, Chioni AM, George AJ, Djamgoz MB (2004) T-lymphocyte invasiveness: control by voltage-gated Na+ channel activity. FEBS letters 569 (1-3):191-194.

Fraser SP, Salvador V, Manning EA, Mizal J, Altun S, Raza M, Berridge RJ, Djamgoz MB (2003) Contribution of functional voltage-gated Na+ channel expression to cell behaviors involved in the metastatic cascade in rat prostate cancer: I. Lateral motility. Journal of cellular physiology 195 (3):479-487.

Fulgenzi G, Graciotti L, Faronato M, Soldovieri MV, Miceli F, Amoroso S, Annunziato L, Procopio A, Taglialatela M (2006) Human neoplastic mesothelial cells express voltage-gated sodium channels involved in cell motility. The international journal of biochemistry & cell biology 38 (7):1146-1159.

Georgakopoulos A, Litterst C, Ghersi E, Baki L, Xu C, Serban G, Robakis NK (2006) Metalloproteinase/Presenilin1 processing of ephrinB regulates EphB-induced Src phosphorylation and signaling. The EMBO journal 25 (6):1242-1252.

Goldin AL (2002) Evolution of voltage-gated Na(+) channels. The Journal of experimental biology 205 (Pt 5):575-584.

Goldin AL, Snutch T, Lubbert H, Dowsett A, Marshall J, Auld V, Downey W, Fritz LC, Lester HA, Dunn R, et al. (1986) Messenger RNA coding for only the alpha subunit of the rat brain Na channel is sufficient for expression of functional channels in Xenopus oocytes. Proceedings of the National Academy of Sciences of the United States of America 83 (19):7503-7507.

Grieco TM, Malhotra JD, Chen C, Isom LL, Raman IM (2005) Open-channel block by the cytoplasmic tail of sodium channel beta4 as a mechanism for resurgent sodium current. Neuron 45 (2):233-244.

Grimes JA, Fraser SP, Stephens GJ, Downing JE, Laniado ME, Foster CS, Abel PD, Djamgoz MB (1995) Differential expression of voltage-activated Na+ currents in two prostatic tumour cell lines: contribution to invasiveness in vitro. FEBS letters 369 (2-3):290-294.

Guy CT, Cardiff RD, Muller WJ (1992) Induction of mammary tumors by expression of polyomavirus middle T oncogene: a transgenic mouse model for metastatic disease. Molecular and cellular biology 12 (3):954-961.

Hakim P, Brice N, Thresher R, Lawrence J, Zhang Y, Jackson AP, Grace AA, Huang CL (2010) Scn3b knockout mice exhibit abnormal sino-atrial and cardiac conduction properties. Acta physiologica 198 (1):47-59.
Hakim P, Gurung IS, Pedersen TH, Thresher R, Brice N, Lawrence J, Grace AA, Huang CL (2008) Scn3b knockout mice exhibit abnormal ventricular electrophysiological properties. Progress in biophysics and molecular biology 98 (2-3):251-266.
Harrison SC (2003) Variation on an Src-like theme. Cell 112 (6):737-740.
Hartshorne RP, Catterall WA (1984) The sodium channel from rat brain. Purification and subunit composition. The Journal of biological chemistry 259 (3):1667-1675.
Hartshorne RP, Messner DJ, Coppersmith JC, Catterall WA (1982) The saxitoxin receptor of the sodium channel from rat brain. Evidence for two nonidentical beta subunits. The Journal of biological chemistry 257 (23):13888-13891.
Irie K, Kitagawa K, Nagura H, Imai T, Shimomura T, Fujiyoshi Y (2010) Comparative study of the gating motif and C-type inactivation in prokaryotic voltage-gated sodium channels. The Journal of biological chemistry 285 (6):3685-3694.
Ishikawa T, Takahashi N, Ohno S, Sakurada H, Nakamura K, On YK, Park JE, Makiyama T, Horie M, Arimura T, Makita N, Kimura A (2013) Novel SCN3B Mutation Associated With Brugada Syndrome Affects Intracellular Trafficking and Function of Nav1.5. Circulation journal : official journal of the Japanese Circulation Society 77 (4):959-967.
Isom LL (2001) Sodium channel beta subunits: anything but auxiliary. The Neuroscientist : a review journal bringing neurobiology, neurology and psychiatry 7 (1):42-54.
Isom LL, De Jongh KS, Catterall WA (1994) Auxiliary subunits of voltage-gated ion channels. Neuron 12 (6):1183-1194.
Isom LL, De Jongh KS, Patton DE, Reber BF, Offord J, Charbonneau H, Walsh K, Goldin AL, Catterall WA (1992) Primary structure and functional expression of the beta 1 subunit of the rat brain sodium channel. Science 256 (5058):839-842.
Isom LL, Ragsdale DS, De Jongh KS, Westenbroek RE, Reber BF, Scheuer T, Catterall WA (1995a) Structure and function of the beta 2 subunit of brain sodium channels, a transmembrane glycoprotein with a CAM motif. Cell 83 (3):433-442.
Isom LL, Scheuer T, Brownstein AB, Ragsdale DS, Murphy BJ, Catterall WA (1995b) Functional co-expression of the beta 1 and type IIA alpha subunits of sodium channels in a mammalian cell line. The Journal of biological chemistry 270 (7):3306-3312.
Ito M, Xu H, Guffanti AA, Wei Y, Zvi L, Clapham DE, Krulwich TA (2004) The voltage-gated Na+ channel NaVBP has a role in motility, chemotaxis, and pH homeostasis of an alkaliphilic Bacillus. Proceedings of the National Academy of Sciences of the United States of America 101 (29):10566-10571.
Itoh K, Stevens B, Schachner M, Fields RD (1995) Regulated expression of the neural cell adhesion molecule L1 by specific patterns of neural impulses. Science 270 (5240):1369-1372.
Jackson AL, Bartz SR, Schelter J, Kobayashi SV, Burchard J, Mao M, Li B, Cavet G, Linsley PS (2003) Expression profiling reveals off-target gene regulation by RNAi. Nature biotechnology 21 (6):635-637.

Johnson D, Bennett ES (2006) Isoform-specific effects of the beta2 subunit on voltage-gated sodium channel gating. The Journal of biological chemistry 281 (36):25875-25881.
Johnson D, Montpetit ML, Stocker PJ, Bennett ES (2004) The sialic acid component of the beta1 subunit modulates voltage-gated sodium channel function. The Journal of biological chemistry 279 (43):44303-44310.
Joho RH, Moorman JR, VanDongen AM, Kirsch GE, Silberberg H, Schuster G, Brown AM (1990) Toxin and kinetic profile of rat brain type III sodium channels expressed in Xenopus oocytes. Brain research Molecular brain research 7 (2):105-113.
Kaplan MR, Cho MH, Ullian EM, Isom LL, Levinson SR, Barres BA (2001) Differential control of clustering of the sodium channels Na(v)1.2 and Na(v)1.6 at developing CNS nodes of Ranvier. Neuron 30 (1):105-119.
Kaufmann SG, Westenbroek RE, Maass AH, Lange V, Renner A, Wischmeyer E, Bonz A, Muck J, Ertl G, Catterall WA, Scheuer T, Maier SK (2013) Distribution and Function of Sodium Channel Subtypes in Human Atrial Myocardium. Journal of molecular and cellular cardiology.
Kazarinova-Noyes K, Malhotra JD, McEwen DP, Mattei LN, Berglund EO, Ranscht B, Levinson SR, Schachner M, Shrager P, Isom LL, Xiao ZC (2001) Contactin associates with Na+ channels and increases their functional expression. The Journal of neuroscience : the official journal of the Society for Neuroscience 21 (19):7517-7525.
Kazen-Gillespie KA, Ragsdale DS, D'Andrea MR, Mattei LN, Rogers KE, Isom LL (2000) Cloning, localization, and functional expression of sodium channel beta1A subunits. The Journal of biological chemistry 275 (2):1079-1088.
Khanna C, Hunter K (2005) Modeling metastasis in vivo. Carcinogenesis 26 (3):513-523.
Kim DY, Carey BW, Wang H, Ingano LA, Binshtok AM, Wertz MH, Pettingell WH, He P, Lee VM, Woolf CJ, Kovacs DM (2007) BACE1 regulates voltage-gated sodium channels and neuronal activity. Nature cell biology 9 (7):755-764.
Kim DY, Ingano LA, Carey BW, Pettingell WH, Kovacs DM (2005) Presenilin/gamma-secretase-mediated cleavage of the voltage-gated sodium channel beta2-subunit regulates cell adhesion and migration. The Journal of biological chemistry 280 (24):23251-23261.
Ko SH, Lenkowski PW, Lee HC, Mounsey JP, Patel MK (2005) Modulation of Na(v)1.5 by beta1-- and beta3-subunit co-expression in mammalian cells. Pflugers Archiv : European journal of physiology 449 (4):403-412.
Koishi R, Xu H, Ren D, Navarro B, Spiller BW, Shi Q, Clapham DE (2004) A superfamily of voltage-gated sodium channels in bacteria. The Journal of biological chemistry 279 (10):9532-9538.
Krafte DS, Goldin AL, Auld VJ, Dunn RJ, Davidson N, Lester HA (1990) Inactivation of cloned Na channels expressed in Xenopus oocytes. The Journal of general physiology 96 (4):689-706.
Kramer EM, Klein C, Koch T, Boytinck M, Trotter J (1999) Compartmentation of Fyn kinase with glycosylphosphatidylinositol-anchored molecules in oligodendrocytes facilitates kinase activation during myelination. The Journal of biological chemistry 274 (41):29042-29049.

Laniado ME, Lalani EN, Fraser SP, Grimes JA, Bhangal G, Djamgoz MB, Abel PD (1997) Expression and functional analysis of voltage-activated Na+ channels in human prostate cancer cell lines and their contribution to invasion in vitro. The American journal of pathology 150 (4):1213-1221.

Lenkowski PW, Shah BS, Dinn AE, Lee K, Patel MK (2003) Lidocaine block of neonatal Nav1.3 is differentially modulated by co-expression of beta1 and beta3 subunits. European journal of pharmacology 467 (1-3):23-30.

Li J, Waterhouse RM, Zdobnov EM (2011) A remarkably stable TipE gene cluster: evolution of insect Para sodium channel auxiliary subunits. BMC evolutionary biology 11:337.

Li RG, Wang Q, Xu YJ, Zhang M, Qu XK, Liu X, Fang WY, Yang YQ (2013) Mutations of the SCN4B-encoded sodium channel beta4 subunit in familial atrial fibrillation. International journal of molecular medicine.

Li T, Chang CY, Jin DY, Lin PJ, Khvorova A, Stafford DW (2004) Identification of the gene for vitamin K epoxide reductase. Nature 427 (6974):541-544.

Liu Z, Wang Y, Yedidi RS, Brunzelle JS, Kovari IA, Sohi J, Kamholz J, Kovari LC (2012) Crystal structure of the extracellular domain of human myelin protein zero. Proteins 80 (1):307-313.

Livak KJ, Schmittgen TD (2001) Analysis of relative gene expression data using real-time quantitative PCR and the 2(-Delta Delta C(T)) Method. Methods 25 (4):402-408.

Lo AC, Black JA, Waxman SG (2002) Neuroprotection of axons with phenytoin in experimental allergic encephalomyelitis. Neuroreport 13 (15):1909-1912.

Lo AC, Saab CY, Black JA, Waxman SG (2003) Phenytoin protects spinal cord axons and preserves axonal conduction and neurological function in a model of neuroinflammation in vivo. Journal of neurophysiology 90 (5):3566-3571.

Lopez-Santiago LF, Brackenbury WJ, Chen C, Isom LL (2011) Na+ channel Scn1b gene regulates dorsal root ganglion nociceptor excitability in vivo. The Journal of biological chemistry 286 (26):22913-22923.

Lopez-Santiago LF, Meadows LS, Ernst SJ, Chen C, Malhotra JD, McEwen DP, Speelman A, Noebels JL, Maier SK, Lopatin AN, Isom LL (2007) Sodium channel Scn1b null mice exhibit prolonged QT and RR intervals. Journal of molecular and cellular cardiology 43 (5):636-647.

Lopez-Santiago LF, Pertin M, Morisod X, Chen C, Hong S, Wiley J, Decosterd I, Isom LL (2006) Sodium channel beta2 subunits regulate tetrodotoxin-sensitive sodium channels in small dorsal root ganglion neurons and modulate the response to pain. The Journal of neuroscience : the official journal of the Society for Neuroscience 26 (30):7984-7994.

Lowery LA, Van Vactor D (2009) The trip of the tip: understanding the growth cone machinery. Nature reviews Molecular cell biology 10 (5):332-343.

Lucas PT, Meadows LS, Nicholls J, Ragsdale DS (2005) An epilepsy mutation in the beta1 subunit of the voltage-gated sodium channel results in reduced channel sensitivity to phenytoin. Epilepsy research 64 (3):77-84.

Maier SK, Westenbroek RE, McCormick KA, Curtis R, Scheuer T, Catterall WA (2004) Distinct subcellular localization of different sodium channel alpha and beta

subunits in single ventricular myocytes from mouse heart. Circulation 109 (11):1421-1427.
Makita N, Bennett PB, Jr., George AL, Jr. (1994) Voltage-gated Na+ channel beta 1 subunit mRNA expressed in adult human skeletal muscle, heart, and brain is encoded by a single gene. The Journal of biological chemistry 269 (10):7571-7578.
Malhotra JD, Kazen-Gillespie K, Hortsch M, Isom LL (2000) Sodium channel beta subunits mediate homophilic cell adhesion and recruit ankyrin to points of cell-cell contact. The Journal of biological chemistry 275 (15):11383-11388.
Malhotra JD, Koopmann MC, Kazen-Gillespie KA, Fettman N, Hortsch M, Isom LL (2002) Structural requirements for interaction of sodium channel beta 1 subunits with ankyrin. The Journal of biological chemistry 277 (29):26681-26688.
Malhotra JD, Thyagarajan V, Chen C, Isom LL (2004) Tyrosine-phosphorylated and nonphosphorylated sodium channel beta1 subunits are differentially localized in cardiac myocytes. The Journal of biological chemistry 279 (39):40748-40754.
Marambaud P, Shioi J, Serban G, Georgakopoulos A, Sarner S, Nagy V, Baki L, Wen P, Efthimiopoulos S, Shao Z, Wisniewski T, Robakis NK (2002) A presenilin-1/gamma-secretase cleavage releases the E-cadherin intracellular domain and regulates disassembly of adherens junctions. The EMBO journal 21 (8):1948-1956.
Marionneau C, Carrasquillo Y, Norris AJ, Townsend RR, Isom LL, Link AJ, Nerbonne JM (2012) The sodium channel accessory subunit Navbeta1 regulates neuronal excitability through modulation of repolarizing voltage-gated K(+) channels. The Journal of neuroscience : the official journal of the Society for Neuroscience 32 (17):5716-5727.
McCormick KA, Isom LL, Ragsdale D, Smith D, Scheuer T, Catterall WA (1998) Molecular determinants of Na+ channel function in the extracellular domain of the beta1 subunit. The Journal of biological chemistry 273 (7):3954-3962.
McEwen DP, Chen C, Meadows LS, Lopez-Santiago L, Isom LL (2009) The voltage-gated Na+ channel beta3 subunit does not mediate trans homophilic cell adhesion or associate with the cell adhesion molecule contactin. Neuroscience letters 462 (3):272-275.
McEwen DP, Isom LL (2004) Heterophilic interactions of sodium channel beta1 subunits with axonal and glial cell adhesion molecules. The Journal of biological chemistry 279 (50):52744-52752.
McEwen DP, Meadows LS, Chen C, Thyagarajan V, Isom LL (2004) Sodium channel beta1 subunit-mediated modulation of Nav1.2 currents and cell surface density is dependent on interactions with contactin and ankyrin. The Journal of biological chemistry 279 (16):16044-16049.
Meadows L, Malhotra JD, Stetzer A, Isom LL, Ragsdale DS (2001) The intracellular segment of the sodium channel beta 1 subunit is required for its efficient association with the channel alpha subunit. Journal of neurochemistry 76 (6):1871-1878.
Meadows LS, Chen YH, Powell AJ, Clare JJ, Ragsdale DS (2002a) Functional modulation of human brain Nav1.3 sodium channels, expressed in mammalian

cells, by auxiliary beta 1, beta 2 and beta 3 subunits. Neuroscience 114 (3):745-753.
Meadows LS, Malhotra J, Loukas A, Thyagarajan V, Kazen-Gillespie KA, Koopman MC, Kriegler S, Isom LL, Ragsdale DS (2002b) Functional and biochemical analysis of a sodium channel beta1 subunit mutation responsible for generalized epilepsy with febrile seizures plus type 1. The Journal of neuroscience : the official journal of the Society for Neuroscience 22 (24):10699-10709.
Medeiros-Domingo A, Kaku T, Tester DJ, Iturralde-Torres P, Itty A, Ye B, Valdivia C, Ueda K, Canizales-Quinteros S, Tusie-Luna MT, Makielski JC, Ackerman MJ (2007) SCN4B-encoded sodium channel beta4 subunit in congenital long-QT syndrome. Circulation 116 (2):134-142.
Meisler MH, Kearney JA (2005) Sodium channel mutations in epilepsy and other neurological disorders. The Journal of clinical investigation 115 (8):2010-2017.
Messner DJ, Catterall WA (1985) The sodium channel from rat brain. Separation and characterization of subunits. The Journal of biological chemistry 260 (19):10597-10604.
Miller JA, Agnew WS, Levinson SR (1983) Principal glycopeptide of the tetrodotoxin/saxitoxin binding protein from Electrophorus electricus: isolation and partial chemical and physical characterization. Biochemistry 22 (2):462-470.
Miyazaki H, Oyama F, Wong HK, Kaneko K, Sakurai T, Tamaoka A, Nukina N (2007) BACE1 modulates filopodia-like protrusions induced by sodium channel beta4 subunit. Biochemical and biophysical research communications 361 (1):43-48.
Morgan K, Stevens EB, Shah B, Cox PJ, Dixon AK, Lee K, Pinnock RD, Hughes J, Richardson PJ, Mizuguchi K, Jackson AP (2000) beta 3: an additional auxiliary subunit of the voltage-sensitive sodium channel that modulates channel gating with distinct kinetics. Proceedings of the National Academy of Sciences of the United States of America 97 (5):2308-2313.
Nguyen HM, Miyazaki H, Hoshi N, Smith BJ, Nukina N, Goldin AL, Chandy KG (2012) Modulation of voltage-gated K+ channels by the sodium channel beta1 subunit. Proceedings of the National Academy of Sciences of the United States of America 109 (45):18577-18582.
Ni CY, Murphy MP, Golde TE, Carpenter G (2001) gamma -Secretase cleavage and nuclear localization of ErbB-4 receptor tyrosine kinase. Science 294 (5549):2179-2181.
Noda M, Ikeda T, Suzuki H, Takeshima H, Takahashi T, Kuno M, Numa S (1986) Expression of functional sodium channels from cloned cDNA. Nature 322 (6082):826-828.
Nuss HB, Chiamvimonvat N, Perez-Garcia MT, Tomaselli GF, Marban E (1995) Functional association of the beta 1 subunit with human cardiac (hH1) and rat skeletal muscle (mu 1) sodium channel alpha subunits expressed in Xenopus oocytes. The Journal of general physiology 106 (6):1171-1191.
O'Brien RJ, Wong PC (2011) Amyloid precursor protein processing and Alzheimer's disease. Annual review of neuroscience 34:185-204.
O'Malley HA, Shreiner AB, Chen GH, Huffnagle GB, Isom LL (2009) Loss of Na+ channel beta2 subunits is neuroprotective in a mouse model of multiple sclerosis. Molecular and cellular neurosciences 40 (2):143-155.

Ogiwara I, Nakayama T, Yamagata T, Ohtani H, Mazaki E, Tsuchiya S, Inoue Y, Yamakawa K (2012) A homozygous mutation of voltage-gated sodium channel beta(I) gene SCN1B in a patient with Dravet syndrome. Epilepsia 53 (12):e200-203.
Oh Y, Lee YJ, Waxman SG (1997) Regulation of Na+ channel beta 1 and beta 2 subunit mRNA levels in cultured rat astrocytes. Neuroscience letters 234 (2-3):107-110.
Oh Y, Waxman SG (1995) Differential Na+ channel beta 1 subunit mRNA expression in stellate and flat astrocytes cultured from rat cortex and cerebellum: a combined in situ hybridization and immunocytochemistry study. Glia 13 (3):166-173.
Olesen MS, Jespersen T, Nielsen JB, Liang B, Moller DV, Hedley P, Christiansen M, Varro A, Olesen SP, Haunso S, Schmitt N, Svendsen JH (2011) Mutations in sodium channel beta-subunit SCN3B are associated with early-onset lone atrial fibrillation. Cardiovascular research 89 (4):786-793.
Onganer PU, Djamgoz MB (2005) Small-cell lung cancer (human): potentiation of endocytic membrane activity by voltage-gated Na(+) channel expression in vitro. The Journal of membrane biology 204 (2):67-75.
Onganer PU, Seckl MJ, Djamgoz MB (2005) Neuronal characteristics of small-cell lung cancer. British journal of cancer 93 (11):1197-1201.
Onkal R, Mattis JH, Fraser SP, Diss JK, Shao D, Okuse K, Djamgoz MB (2008) Alternative splicing of Nav1.5: an electrophysiological comparison of 'neonatal' and 'adult' isoforms and critical involvement of a lysine residue. Journal of cellular physiology 216 (3):716-726.
Ou SW, Kameyama A, Hao LY, Horiuchi M, Minobe E, Wang WY, Makita N, Kameyama M (2005) Tetrodotoxin-resistant Na+ channels in human neuroblastoma cells are encoded by new variants of Nav1.5/SCN5A. The European journal of neuroscience 22 (4):793-801.
Oyama F, Miyazaki H, Sakamoto N, Becquet C, Machida Y, Kaneko K, Uchikawa C, Suzuki T, Kurosawa M, Ikeda T, Tamaoka A, Sakurai T, Nukina N (2006) Sodium channel beta4 subunit: down-regulation and possible involvement in neuritic degeneration in Huntington's disease transgenic mice. Journal of neurochemistry 98 (2):518-529.
Palmer CP, Mycielska ME, Burcu H, Osman K, Collins T, Beckerman R, Perrett R, Johnson H, Aydar E, Djamgoz MB (2008) Single cell adhesion measuring apparatus (SCAMA): application to cancer cell lines of different metastatic potential and voltage-gated Na+ channel expression. European biophysics journal : EBJ 37 (4):359-368.
Pan H, Djamgoz MB (2008) Biochemical constitution of extracellular medium is critical for control of human breast cancer MDA-MB-231 cell motility. The Journal of membrane biology 223 (1):27-36.
Patino GA, Brackenbury WJ, Bao Y, Lopez-Santiago LF, O'Malley HA, Chen C, Calhoun JD, Lafreniere RG, Cossette P, Rouleau GA, Isom LL (2011) Voltage-gated Na+ channel beta1B: a secreted cell adhesion molecule involved in human epilepsy. The Journal of neuroscience : the official journal of the Society for Neuroscience 31 (41):14577-14591.
Patino GA, Claes LR, Lopez-Santiago LF, Slat EA, Dondeti RS, Chen C, O'Malley HA, Gray CB, Miyazaki H, Nukina N, Oyama F, De Jonghe P, Isom LL (2009) A

functional null mutation of SCN1B in a patient with Dravet syndrome. The Journal of neuroscience : the official journal of the Society for Neuroscience 29 (34):10764-10778.
Patino GA, Isom LL (2010) Electrophysiology and beyond: multiple roles of Na+ channel beta subunits in development and disease. Neuroscience letters 486 (2):53-59.
Payandeh J, Scheuer T, Zheng N, Catterall WA (2011) The crystal structure of a voltage-gated sodium channel. Nature 475 (7356):353-358.
Pertin M, Ji RR, Berta T, Powell AJ, Karchewski L, Tate SN, Isom LL, Woolf CJ, Gilliard N, Spahn DR, Decosterd I (2005) Upregulation of the voltage-gated sodium channel beta2 subunit in neuropathic pain models: characterization of expression in injured and non-injured primary sensory neurons. The Journal of neuroscience : the official journal of the Society for Neuroscience 25 (47):10970-10980.
Poliak S, Peles E (2003) The local differentiation of myelinated axons at nodes of Ranvier. Nature reviews Neuroscience 4 (12):968-980.
Prevarskaya N, Skryma R, Shuba Y (2010) Ion channels and the hallmarks of cancer. Trends in molecular medicine 16 (3):107-121.
Qin N, D'Andrea MR, Lubin ML, Shafaee N, Codd EE, Correa AM (2003) Molecular cloning and functional expression of the human sodium channel beta1B subunit, a novel splicing variant of the beta1 subunit. European journal of biochemistry / FEBS 270 (23):4762-4770.
Qu Y, Isom LL, Westenbroek RE, Rogers JC, Tanada TN, McCormick KA, Scheuer T, Catterall WA (1995) Modulation of cardiac Na+ channel expression in Xenopus oocytes by beta 1 subunits. The Journal of biological chemistry 270 (43):25696-25701.
Qu Y, Rogers JC, Chen SF, McCormick KA, Scheuer T, Catterall WA (1999) Functional roles of the extracellular segments of the sodium channel alpha subunit in voltage-dependent gating and modulation by beta1 subunits. The Journal of biological chemistry 274 (46):32647-32654.
Ragsdale DS (2008) How do mutant Nav1.1 sodium channels cause epilepsy? Brain research reviews 58 (1):149-159.
Raman IM, Bean BP (1997) Resurgent sodium current and action potential formation in dissociated cerebellar Purkinje neurons. The Journal of neuroscience : the official journal of the Society for Neuroscience 17 (12):4517-4526.
Raman IM, Sprunger LK, Meisler MH, Bean BP (1997) Altered subthreshold sodium currents and disrupted firing patterns in Purkinje neurons of Scn8a mutant mice. Neuron 19 (4):881-891.
Rasband MN (2010) The axon initial segment and the maintenance of neuronal polarity. Nature reviews Neuroscience 11 (8):552-562.
Ratcliffe CF, Qu Y, McCormick KA, Tibbs VC, Dixon JE, Scheuer T, Catterall WA (2000) A sodium channel signaling complex: modulation by associated receptor protein tyrosine phosphatase beta. Nature neuroscience 3 (5):437-444.
Ratcliffe CF, Westenbroek RE, Curtis R, Catterall WA (2001) Sodium channel beta1 and beta3 subunits associate with neurofascin through their extracellular immunoglobulin-like domain. The Journal of cell biology 154 (2):427-434.

Remme CA, Bezzina CR (2010) Sodium channel (dys)function and cardiac arrhythmias. Cardiovascular therapeutics 28 (5):287-294.
Remme CA, Scicluna BP, Verkerk AO, Amin AS, van Brunschot S, Beekman L, Deneer VH, Chevalier C, Oyama F, Miyazaki H, Nukina N, Wilders R, Escande D, Houlgatte R, Wilde AA, Tan HL, Veldkamp MW, de Bakker JM, Bezzina CR (2009) Genetically determined differences in sodium current characteristics modulate conduction disease severity in mice with cardiac sodium channelopathy. Circulation research 104 (11):1283-1292.
Ren D, Navarro B, Xu H, Yue L, Shi Q, Clapham DE (2001) A prokaryotic voltage-gated sodium channel. Science 294 (5550):2372-2375.
Riuro H, Beltran-Alvarez P, Tarradas A, Selga E, Campuzano O, Verges M, Pagans S, Iglesias A, Brugada J, Brugada P, Vazquez FM, Perez GJ, Scornik FS, Brugada R (2013) A Missense Mutation in the Sodium Channel beta2 Subunit Reveals SCN2B as a New Candidate Gene for Brugada Syndrome. Human mutation.
Roger S, Besson P, Le Guennec JY (2003) Involvement of a novel fast inward sodium current in the invasion capacity of a breast cancer cell line. Biochimica et biophysica acta 1616 (2):107-111.
Roger S, Rollin J, Barascu A, Besson P, Raynal PI, Iochmann S, Lei M, Bougnoux P, Gruel Y, Le Guennec JY (2007) Voltage-gated sodium channels potentiate the invasive capacities of human non-small-cell lung cancer cell lines. The international journal of biochemistry & cell biology 39 (4):774-786.
Rusconi R, Combi R, Cestele S, Grioni D, Franceschetti S, Dalpra L, Mantegazza M (2009) A rescuable folding defective Nav1.1 (SCN1A) sodium channel mutant causes GEFS+: common mechanism in Nav1.1 related epilepsies? Human mutation 30 (7):E747-760.
Rusconi R, Scalmani P, Cassulini RR, Giunti G, Gambardella A, Franceschetti S, Annesi G, Wanke E, Mantegazza M (2007) Modulatory proteins can rescue a trafficking defective epileptogenic Nav1.1 Na+ channel mutant. The Journal of neuroscience : the official journal of the Society for Neuroscience 27 (41):11037-11046.
Sato PY, Musa H, Coombs W, Guerrero-Serna G, Patino GA, Taffet SM, Isom LL, Delmar M (2009) Loss of plakophilin-2 expression leads to decreased sodium current and slower conduction velocity in cultured cardiac myocytes. Circulation research 105 (6):523-526.
Scheffer IE, Harkin LA, Grinton BE, Dibbens LM, Turner SJ, Zielinski MA, Xu R, Jackson G, Adams J, Connellan M, Petrou S, Wellard RM, Briellmann RS, Wallace RH, Mulley JC, Berkovic SF (2007) Temporal lobe epilepsy and GEFS+ phenotypes associated with SCN1B mutations. Brain : a journal of neurology 130 (Pt 1):100-109.
Scheuer T, Auld VJ, Boyd S, Offord J, Dunn R, Catterall WA (1990) Functional properties of rat brain sodium channels expressed in a somatic cell line. Science 247 (4944):854-858.
Schmidt J, Rossie S, Catterall WA (1985) A large intracellular pool of inactive Na channel alpha subunits in developing rat brain. Proceedings of the National Academy of Sciences of the United States of America 82 (14):4847-4851.
Schmidt JW, Catterall WA (1986) Biosynthesis and processing of the alpha subunit of the voltage-sensitive sodium channel in rat brain neurons. Cell 46 (3):437-444.

Shah BS, Stevens EB, Gonzalez MI, Bramwell S, Pinnock RD, Lee K, Dixon AK (2000) beta3, a novel auxiliary subunit for the voltage-gated sodium channel, is expressed preferentially in sensory neurons and is upregulated in the chronic constriction injury model of neuropathic pain. The European journal of neuroscience 12 (11):3985-3990.

Shah BS, Stevens EB, Pinnock RD, Dixon AK, Lee K (2001) Developmental expression of the novel voltage-gated sodium channel auxiliary subunit beta3, in rat CNS. The Journal of physiology 534 (Pt 3):763-776.

Shapiro L, Doyle JP, Hensley P, Colman DR, Hendrickson WA (1996) Crystal structure of the extracellular domain from P0, the major structural protein of peripheral nerve myelin. Neuron 17 (3):435-449.

Shi X, Yasumoto S, Nakagawa E, Fukasawa T, Uchiya S, Hirose S (2009) Missense mutation of the sodium channel gene SCN2A causes Dravet syndrome. Brain & development 31 (10):758-762.

Spampanato J, Kearney JA, de Haan G, McEwen DP, Escayg A, Aradi I, MacDonald BT, Levin SI, Soltesz I, Benna P, Montalenti E, Isom LL, Goldin AL, Meisler MH (2004) A novel epilepsy mutation in the sodium channel SCN1A identifies a cytoplasmic domain for beta subunit interaction. The Journal of neuroscience : the official journal of the Society for Neuroscience 24 (44):10022-10034.

Srinivasan J, Schachner M, Catterall WA (1998) Interaction of voltage-gated sodium channels with the extracellular matrix molecules tenascin-C and tenascin-R. Proceedings of the National Academy of Sciences of the United States of America 95 (26):15753-15757.

Storey N, Latchman D, Bevan S (2002) Selective internalization of sodium channels in rat dorsal root ganglion neurons infected with herpes simplex virus-1. The Journal of cell biology 158 (7):1251-1262.

Su JL, Yang CY, Shih JY, Wei LH, Hsieh CY, Jeng YM, Wang MY, Yang PC, Kuo ML (2006) Knockdown of contactin-1 expression suppresses invasion and metastasis of lung adenocarcinoma. Cancer research 66 (5):2553-2561.

Sugawara T, Tsurubuchi Y, Agarwala KL, Ito M, Fukuma G, Mazaki-Miyazaki E, Nagafuji H, Noda M, Imoto K, Wada K, Mitsudome A, Kaneko S, Montal M, Nagata K, Hirose S, Yamakawa K (2001) A missense mutation of the Na+ channel alpha II subunit gene Na(v)1.2 in a patient with febrile and afebrile seizures causes channel dysfunction. Proceedings of the National Academy of Sciences of the United States of America 98 (11):6384-6389.

Surges R, Sander JW (2012) Sudden unexpected death in epilepsy: mechanisms, prevalence, and prevention. Current opinion in neurology 25 (2):201-207.

Sutkowski EM, Catterall WA (1990) Beta 1 subunits of sodium channels. Studies with subunit-specific antibodies. The Journal of biological chemistry 265 (21):12393-12399.

Takahashi N, Kikuchi S, Dai Y, Kobayashi K, Fukuoka T, Noguchi K (2003) Expression of auxiliary beta subunits of sodium channels in primary afferent neurons and the effect of nerve injury. Neuroscience 121 (2):441-450.

Tamura K, Peterson D, Peterson N, Stecher G, Nei M, Kumar S (2011) MEGA5: molecular evolutionary genetics analysis using maximum likelihood, evolutionary

distance, and maximum parsimony methods. Molecular biology and evolution 28 (10):2731-2739.
Tan BH, Pundi KN, Van Norstrand DW, Valdivia CR, Tester DJ, Medeiros-Domingo A, Makielski JC, Ackerman MJ (2010) Sudden infant death syndrome-associated mutations in the sodium channel beta subunits. Heart rhythm : the official journal of the Heart Rhythm Society 7 (6):771-778.
Taylor DR, Hooper NM (2006) The prion protein and lipid rafts. Molecular membrane biology 23 (1):89-99.
Theile JW, Cummins TR (2011) Inhibition of Navbeta4 peptide-mediated resurgent sodium currents in Nav1.7 channels by carbamazepine, riluzole, and anandamide. Molecular pharmacology 80 (4):724-734.
Thompson CH, Porter JC, Kahlig KM, Daniels MA, George AL, Jr. (2012) Nontruncating SCN1A mutations associated with severe myoclonic epilepsy of infancy impair cell surface expression. The Journal of biological chemistry 287 (50):42001-42008.
Thompson JD, Higgins DG, Gibson TJ (1994) CLUSTAL W: improving the sensitivity of progressive multiple sequence alignment through sequence weighting, position-specific gap penalties and weight matrix choice. Nucleic acids research 22 (22):4673-4680.
Towbin JA (2010) The A, B, Cs of sudden infant death syndrome: an electrical disorder? Heart rhythm : the official journal of the Heart Rhythm Society 7 (6):779-780.
Trinidad JC, Barkan DT, Gulledge BF, Thalhammer A, Sali A, Schoepfer R, Burlingame AL (2012) Global identification and characterization of both O-GlcNAcylation and phosphorylation at the murine synapse. Molecular & cellular proteomics : MCP 11 (8):215-229.
Uebachs M, Albus C, Opitz T, Isom L, Niespodziany I, Wolff C, Beck H (2012) Loss of beta1 accessory Na+ channel subunits causes failure of carbamazepine, but not of lacosamide, in blocking high-frequency firing via differential effects on persistent Na+ currents. Epilepsia 53 (11):1959-1967.
Uebachs M, Opitz T, Royeck M, Dickhof G, Horstmann MT, Isom LL, Beck H (2010) Efficacy loss of the anticonvulsant carbamazepine in mice lacking sodium channel beta subunits via paradoxical effects on persistent sodium currents. The Journal of neuroscience : the official journal of the Society for Neuroscience 30 (25):8489-8501.
Uysal-Onganer P, Djamgoz MB (2007) Epidermal growth factor potentiates in vitro metastatic behaviour of human prostate cancer PC-3M cells: involvement of voltage-gated sodium channel. Molecular cancer 6:76.
Van Wart A, Matthews G (2006) Impaired firing and cell-specific compensation in neurons lacking nav1.6 sodium channels. The Journal of neuroscience : the official journal of the Society for Neuroscience 26 (27):7172-7180.
Van Wart A, Trimmer JS, Matthews G (2007) Polarized distribution of ion channels within microdomains of the axon initial segment. The Journal of comparative neurology 500 (2):339-352.
Vinci M, Gowan S, Boxall F, Patterson L, Zimmermann M, Court W, Lomas C, Mendiola M, Hardisson D, Eccles SA (2012) Advances in establishment and

analysis of three-dimensional tumor spheroid-based functional assays for target validation and drug evaluation. BMC biology 10:29.
Waechter CJ, Schmidt JW, Catterall WA (1983) Glycosylation is required for maintenance of functional sodium channels in neuroblastoma cells. The Journal of biological chemistry 258 (8):5117-5123.
Wagner KU, Wall RJ, St-Onge L, Gruss P, Wynshaw-Boris A, Garrett L, Li M, Furth PA, Hennighausen L (1997) Cre-mediated gene deletion in the mammary gland. Nucleic acids research 25 (21):4323-4330.
Wallace RH, Scheffer IE, Parasivam G, Barnett S, Wallace GB, Sutherland GR, Berkovic SF, Mulley JC (2002) Generalized epilepsy with febrile seizures plus: mutation of the sodium channel subunit SCN1B. Neurology 58 (9):1426-1429.
Wallace RH, Wang DW, Singh R, Scheffer IE, George AL, Jr., Phillips HA, Saar K, Reis A, Johnson EW, Sutherland GR, Berkovic SF, Mulley JC (1998) Febrile seizures and generalized epilepsy associated with a mutation in the Na+-channel beta1 subunit gene SCN1B. Nature genetics 19 (4):366-370.
Wang DW, Desai RR, Crotti L, Arnestad M, Insolia R, Pedrazzini M, Ferrandi C, Vege A, Rognum T, Schwartz PJ, George AL, Jr. (2007) Cardiac sodium channel dysfunction in sudden infant death syndrome. Circulation 115 (3):368-376.
Watanabe H, Darbar D, Kaiser DW, Jiramongkolchai K, Chopra S, Donahue BS, Kannankeril PJ, Roden DM (2009) Mutations in sodium channel beta1- and beta2-subunits associated with atrial fibrillation. Circulation Arrhythmia and electrophysiology 2 (3):268-275.
Watanabe H, Koopmann TT, Le Scouarnec S, Yang T, Ingram CR, Schott JJ, Demolombe S, Probst V, Anselme F, Escande D, Wiesfeld AC, Pfeufer A, Kaab S, Wichmann HE, Hasdemir C, Aizawa Y, Wilde AA, Roden DM, Bezzina CR (2008) Sodium channel beta1 subunit mutations associated with Brugada syndrome and cardiac conduction disease in humans. The Journal of clinical investigation 118 (6):2260-2268.
Waxman SG (2006) Axonal conduction and injury in multiple sclerosis: the role of sodium channels. Nature reviews Neuroscience 7 (12):932-941.
Westenbroek RE, Bischoff S, Fu Y, Maier SK, Catterall WA, Scheuer T (2013) Localization of sodium channel subtypes in mouse ventricular myocytes using quantitative immunocytochemistry. Journal of molecular and cellular cardiology.
Wimmer VC, Reid CA, Mitchell S, Richards KL, Scaf BB, Leaw BT, Hill EL, Royeck M, Horstmann MT, Cromer BA, Davies PJ, Xu R, Lerche H, Berkovic SF, Beck H, Petrou S (2010) Axon initial segment dysfunction in a mouse model of genetic epilepsy with febrile seizures plus. The Journal of clinical investigation 120 (8):2661-2671.
Wong HK, Sakurai T, Oyama F, Kaneko K, Wada K, Miyazaki H, Kurosawa M, De Strooper B, Saftig P, Nukina N (2005) beta Subunits of voltage-gated sodium channels are novel substrates of beta-site amyloid precursor protein-cleaving enzyme (BACE1) and gamma-secretase. The Journal of biological chemistry 280 (24):23009-23017.
Wong MH, Filbin MT (1996) Dominant-negative effect on adhesion by myelin Po protein truncated in its cytoplasmic domain. The Journal of cell biology 134 (6):1531-1541.

Xiao ZC, Ragsdale DS, Malhotra JD, Mattei LN, Braun PE, Schachner M, Isom LL (1999) Tenascin-R is a functional modulator of sodium channel beta subunits. The Journal of biological chemistry 274 (37):26511-26517.

Xu R, Thomas EA, Gazina EV, Richards KL, Quick M, Wallace RH, Harkin LA, Heron SE, Berkovic SF, Scheffer IE, Mulley JC, Petrou S (2007) Generalized epilepsy with febrile seizures plus-associated sodium channel beta1 subunit mutations severely reduce beta subunit-mediated modulation of sodium channel function. Neuroscience 148 (1):164-174.

Yang JS, Bennett PB, Makita N, George AL, Barchi RL (1993) Expression of the sodium channel beta 1 subunit in rat skeletal muscle is selectively associated with the tetrodotoxin-sensitive alpha subunit isoform. Neuron 11 (5):915-922.

Yang M, Kozminski DJ, Wold LA, Modak R, Calhoun JD, Isom LL, Brackenbury WJ (2012) Therapeutic potential for phenytoin: targeting Na(v)1.5 sodium channels to reduce migration and invasion in metastatic breast cancer. Breast cancer research and treatment 134 (2):603-615.

Yereddi NR, Cusdin FS, Namadurai S, Packman LC, Monie TP, Slavny P, Clare JJ, Powell AJ, Jackson AP (2013) The immunoglobulin domain of the sodium channel beta3 subunit contains a surface-localized disulfide bond that is required for homophilic binding. FASEB journal : official publication of the Federation of American Societies for Experimental Biology 27 (2):568-580.

Yu FH, Westenbroek RE, Silos-Santiago I, McCormick KA, Lawson D, Ge P, Ferriera H, Lilly J, DiStefano PS, Catterall WA, Scheuer T, Curtis R (2003) Sodium channel beta4, a new disulfide-linked auxiliary subunit with similarity to beta2. The Journal of neuroscience : the official journal of the Society for Neuroscience 23 (20):7577-7585.

Zhang Y, Bekku Y, Dzhashiashvili Y, Armenti S, Meng X, Sasaki Y, Milbrandt J, Salzer JL (2012) Assembly and maintenance of nodes of ranvier rely on distinct sources of proteins and targeting mechanisms. Neuron 73 (1):92-107.

Zhou TT, Zhang ZW, Liu J, Zhang JP, Jiao BH (2012) Glycosylation of the sodium channel beta4 subunit is developmentally regulated and involves in neuritic degeneration. International journal of biological sciences 8 (5):630-639.